Supplementary Information（SI）

Scaling green hydrogen and CCUS via cement-methanol co-production in China

Yuezhang He[1,2,3], Hongxi Luo[2], Yuancheng Lin[1], Carl J. Talsma[4], Anna Li[3], Zhenqian Wang[1,5], Yujuan Fang[6], Pei Liu[1,*], Jesse D. Jenkins[2,3,*], Eric Larson[2,*], Zheng Li[1,6,*]

1. State Key Lab of Power Systems, Department of Energy and Power Engineering, Tsinghua University, Beijing, China
2. Andlinger Center for Energy and the Environment, Princeton University, Princeton, NJ, USA
3. Department of Mechanical and Aerospace Engineering, Princeton University, Princeton, NJ, USA
4. Carbon Solutions LLC, Bloomington, IN 47401
5. Research Institute of Petroleum Processing, Sinopec Corporation, Beijing, China
6. Laboratory of Low Carbon Energy, Tsinghua University, Beijing, China

1. Plant-level detailed results

For the case plant in Inner Mongolia, the magnitude and duration of temporal mismatches vary across commodities on an annual scale. Approximately 6% of electricity generation undergoes battery storage, with an energy-to-power ratio of 7 hours. H_2, gaseous O_2, and gaseous CO_2 exhibit energy-to-discharge ratios of 16–18 hours. Annually, 40% of H_2 passes through storage tanks before consumption, while 28.7% of O_2 is stored in gaseous form, and only 1.1% of captured CO_2 utilizes gaseous storage. A fully charged liquid O_2 tank can sustain oxy-fuel combustion for 114 hours, while liquid CO_2 storage supports methanol synthesis at full capacity for 435 hours. In total, 5.5% of CO_2 and 2.7% of O_2 are stored in liquid form. Due to the potential increase in O_2 storage requirements induced by mismatch, integrating an ASU may sometimes be more economical than relying solely on by-product O_2. To bridge occasional O_2 demand gaps, 21.5% of O_2 is generated from ASU, though excess O_2 is discarded when renewable energy is abundant, resulting in an overall O_2 disposal rate of 6.7%. In contrast to O_2, a larger share of CO_2 is allocated to liquid storage rather than gaseous storage, as methanol synthesis load adjustments occur over prolonged cycles.

We extend the optimization model to each existing cement plant in China and summarize key parameters—such as annual charge-discharge cycles and storage durations of storage systems, levelized costs of electricity and molecules, storage utilization proportions, electricity curtailment, and facility utilization factors—in the following figures:

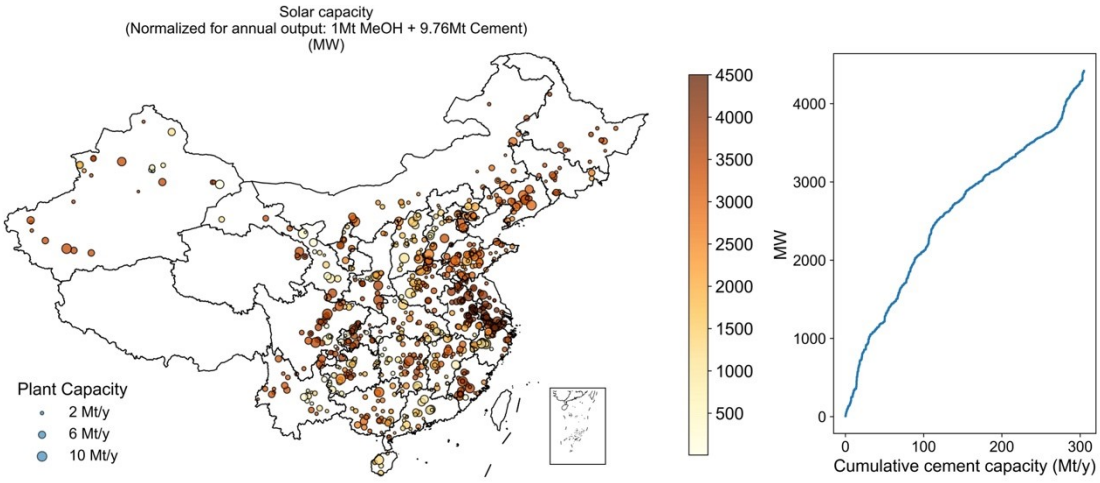

Fig. S1 Plant-level solar capacity under net-zero methanol production scenarios.

Each dot marks an existing cement plant with different capacity (size) and normalized solar capacity (color). The normalized solar capacity is defined as the solar capacity required to produce 1 Mt of methanol and 9.76 Mt of cement annually, representing the solar capacity intensity per unit of co-produced output. The right plot shows the curve sorted in ascending order of solar capacity versus cumulative cement capacity.

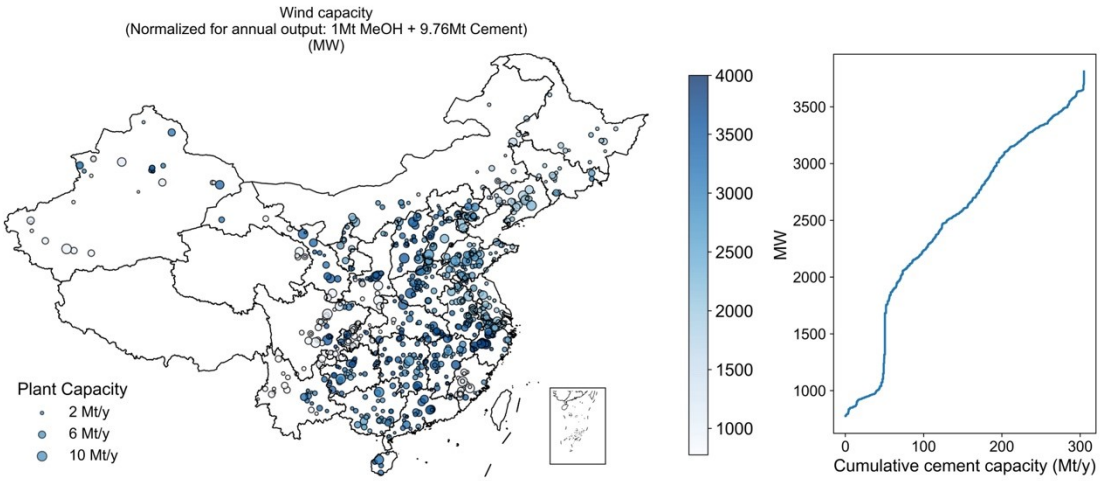

Fig. S2 Plant-level wind capacity under net-zero methanol production scenarios.

Each dot marks an existing cement plant with different capacity (size) and normalized wind capacity (color). The normalized wind capacity is defined as the wind capacity required to produce 1 Mt of methanol and 9.76 Mt of cement annually, representing the wind capacity intensity per unit of co-produced output. The right plot shows the curve sorted in ascending order of wind capacity versus cumulative cement capacity.

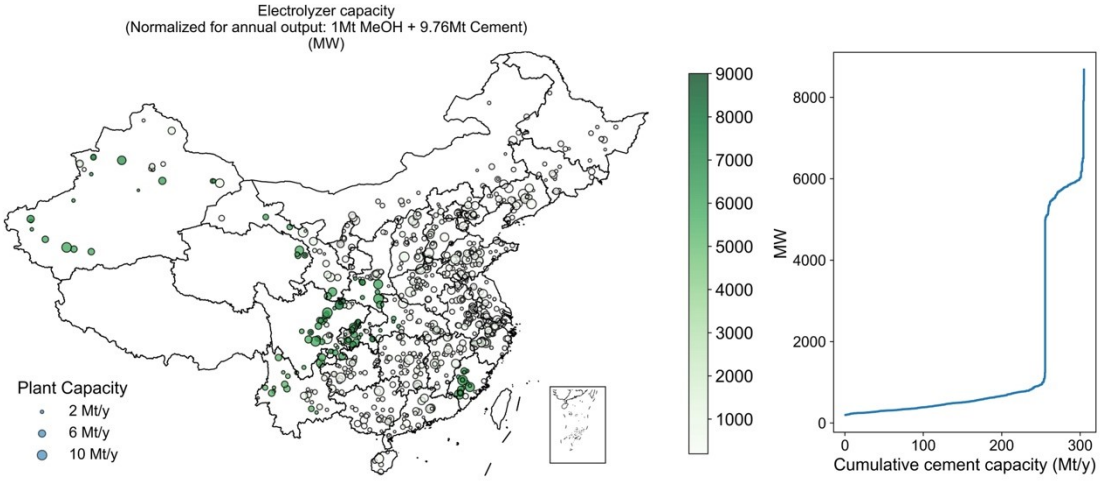

Fig. S3 Plant-level electrolyzer capacity under net-zero methanol production scenarios.

Each dot marks an existing cement plant with different capacity (size) and normalized electrolyzer capacity (color). The normalized electrolyzer capacity is defined as the electrolyzer capacity required to produce 1 Mt of methanol and 9.76 Mt of cement annually, representing the electrolyzer capacity intensity per unit of co-produced output. The right plot shows the curve sorted in ascending order of electrolyzer capacity versus cumulative cement capacity.

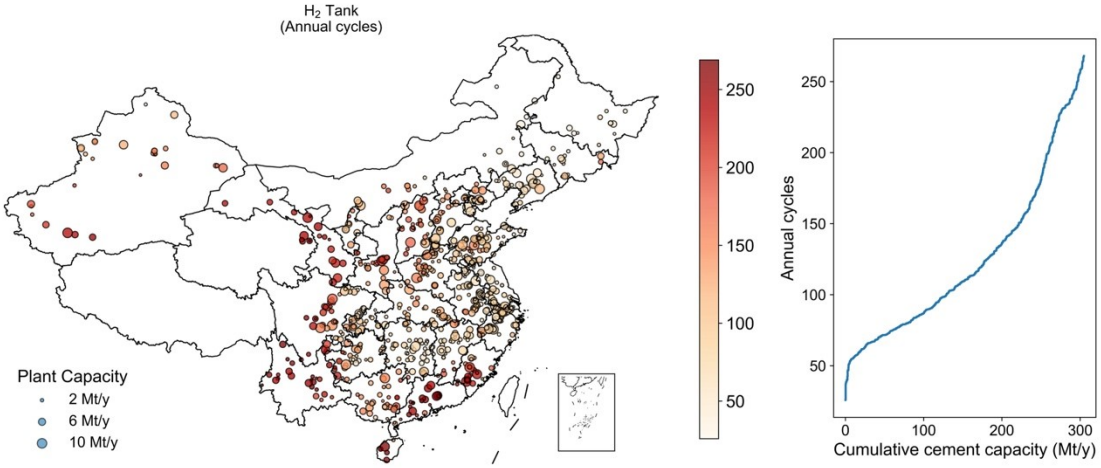

Fig. S4 Plant-level H_2 tank annual cycles under net-zero methanol production scenarios.

Each dot marks an existing cement plant with different capacity (size) and H_2 tank annual cycles (color). A cycle is defined as one full charge-discharge round of a storage system and annual cycles are the total number of such cycles counted over a year. The stoichiometric data is 9.76 tonne of cement per tonne of methanol under net zero methanol production scenarios. The right plot shows the curve sorted in ascending order of numbers of annual cycles versus cumulative cement capacity.

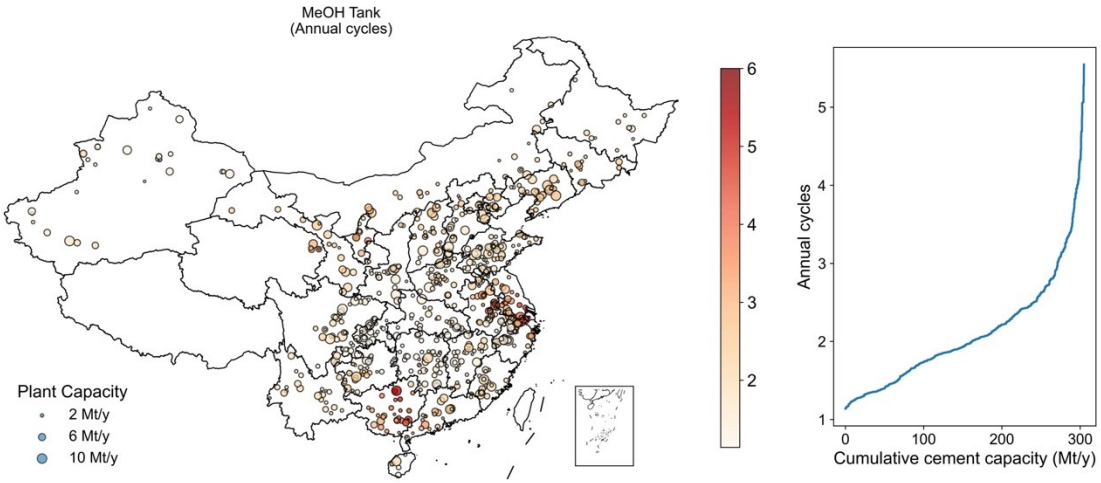

Fig. S5 Plant-level MeOH tank annual cycles under net-zero methanol production scenarios.

Each dot marks an existing cement plant with different capacity (size) and MeOH tank annual cycles (color). A cycle is defined as one full charge-discharge round of a storage system and annual cycles are the total number of such cycles counted over a year. The stoichiometric data is 9.76 tonne of cement per tonne of methanol under net zero methanol production scenarios. The right plot shows the curve sorted in ascending order of numbers of annual cycles versus cumulative cement capacity.

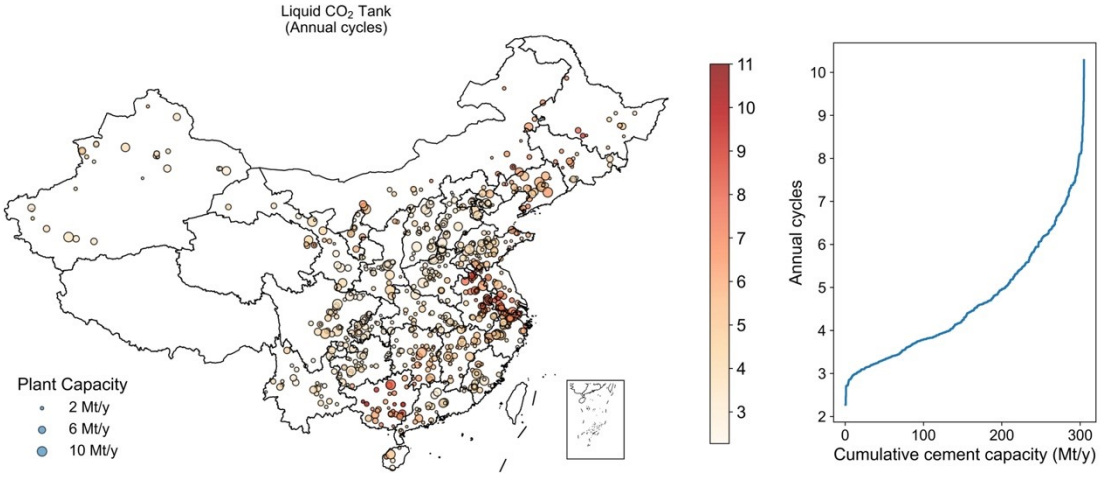

Fig. S6 Plant-level LCO_2 tank annual cycles under net-zero methanol production scenarios.

Each dot marks an existing cement plant with different capacity (size) and LCO_2 tank annual cycles (color). A cycle is defined as one full charge-discharge round of a storage system and annual cycles are the total number of such cycles counted over a year. The stoichiometric data is 9.76 tonne of cement per tonne of methanol under net zero methanol production scenarios. The right plot shows the curve sorted in ascending order of numbers of annual cycles versus cumulative cement capacity.

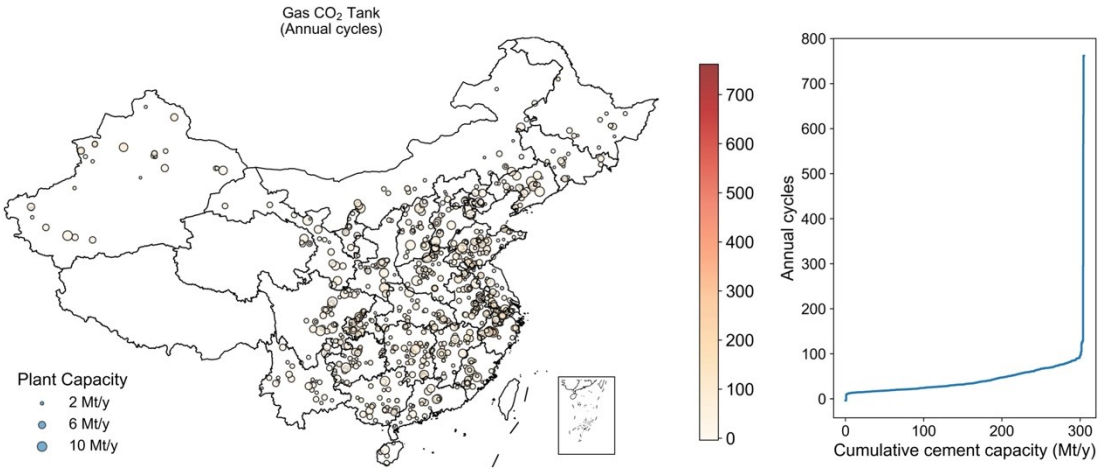

Fig. S7 Plant-level GCO_2 tank annual cycles under net-zero methanol production scenarios.

Each dot marks an existing cement plant with different capacity (size) and GCO_2 tank annual cycles (color). A cycle is defined as one full charge-discharge round of a storage system and annual cycles are the total number of such cycles counted over a year. The stoichiometric data is 9.76 tonne of cement per tonne of methanol under net zero methanol production scenarios. The right plot shows the curve sorted in ascending order of numbers of annual cycles versus cumulative cement capacity.

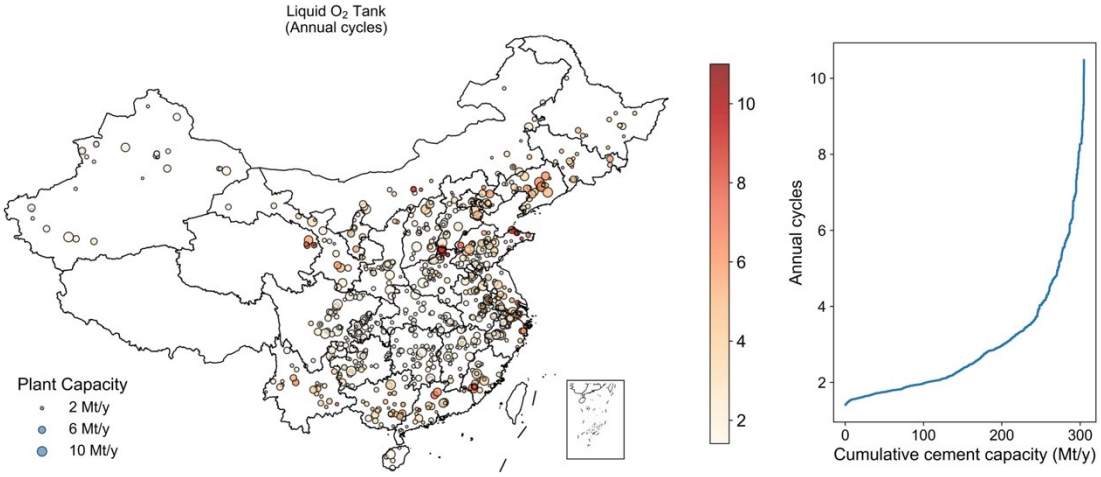

Fig. S8 Plant-level LO_2 tank annual cycles under net-zero methanol production scenarios.

Each dot marks an existing cement plant with different capacity (size) and LO_2 tank annual cycles (color). A cycle is defined as one full charge-discharge round of a storage system and annual cycles are the total number of such cycles counted over a year. The stoichiometric data is 9.76 tonne of cement per tonne of methanol under net zero methanol production scenarios. The right plot shows the curve sorted in ascending order of numbers of annual cycles versus cumulative cement capacity.

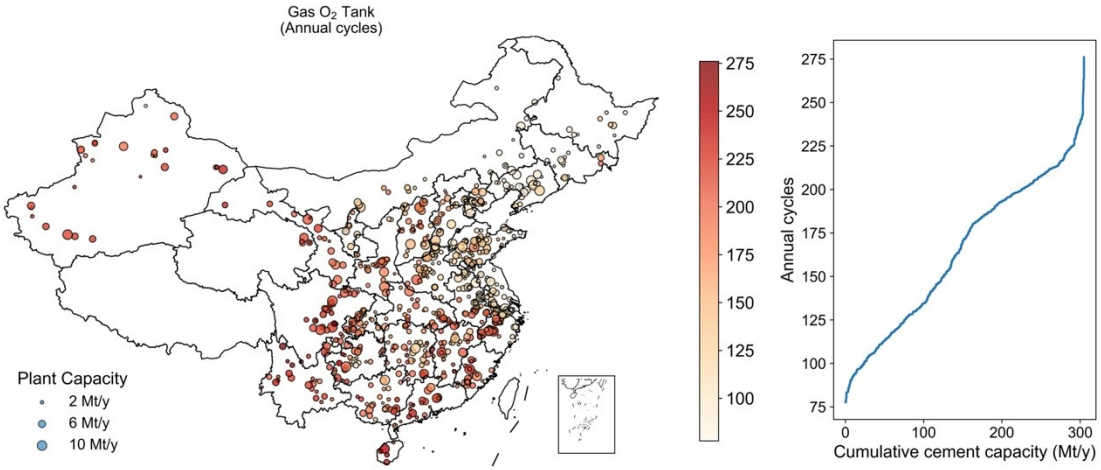

Fig. S9 Plant-level GO_2 tank annual cycles under net-zero methanol production scenarios.

Each dot marks an existing cement plant with different capacity (size) and GO_2 tank annual cycles (color). A cycle is defined as one full charge-discharge round of a storage system and annual cycles are the total number of such cycles counted over a year. The stoichiometric data is 9.76 tonne of cement per tonne of methanol under net zero methanol production scenarios. The right plot shows the curve sorted in ascending order of numbers of annual cycles versus cumulative cement capacity.

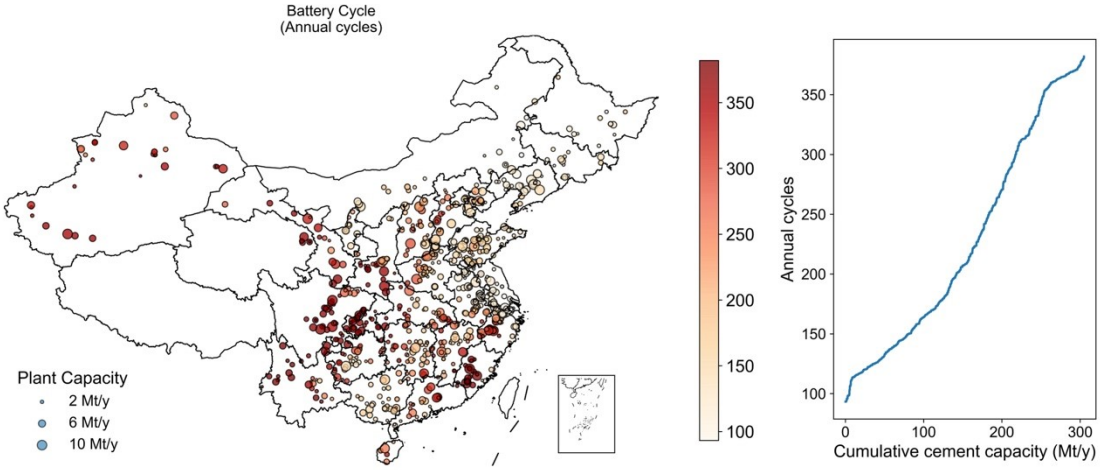

Fig. S10 Plant-level battery annual cycles under net-zero methanol production scenarios.

Each dot marks an existing cement plant with different capacity (size) and battery annual cycles (color). A cycle is defined as one full charge-discharge round of a storage system and annual cycles are the total number of such cycles counted over a year. The stoichiometric data is 9.76 tonne of cement per tonne of methanol under net zero methanol production scenarios. The right plot shows the curve sorted in ascending order of numbers of annual cycles versus cumulative cement capacity.

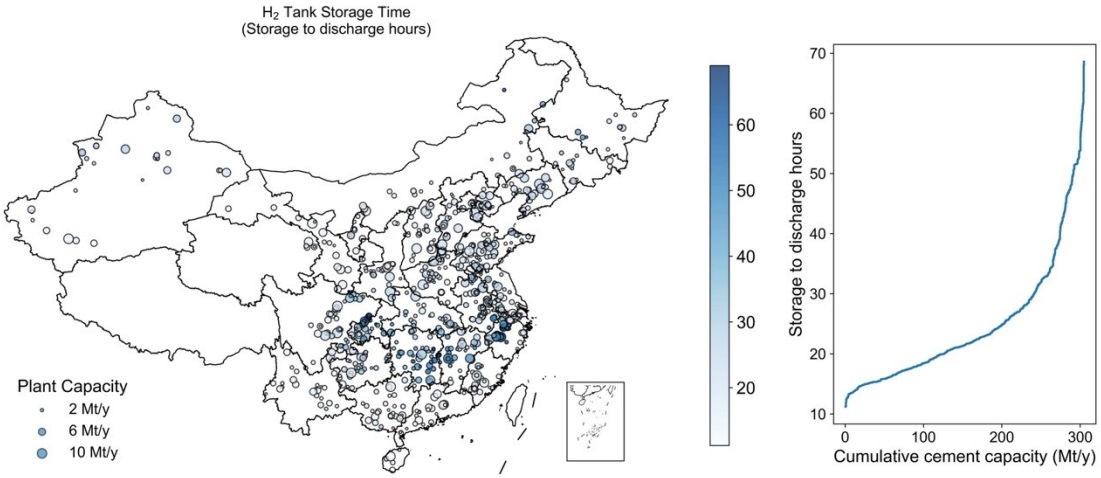

Fig. S11 Plant-level H_2 tank storage duration under net-zero methanol production scenarios.

Each dot marks an existing cement plant with different capacity (size) and H_2 storage duration (color). Storage duration is defined as the full storage volume divided by the discharge load, representing the length of time the storage can sustain downstream operations without additional input. The stoichiometric data is 9.76 tonne of cement per tonne of methanol under net zero methanol production scenarios. The right plot shows the curve sorted in ascending order of storage duration versus cumulative cement capacity.

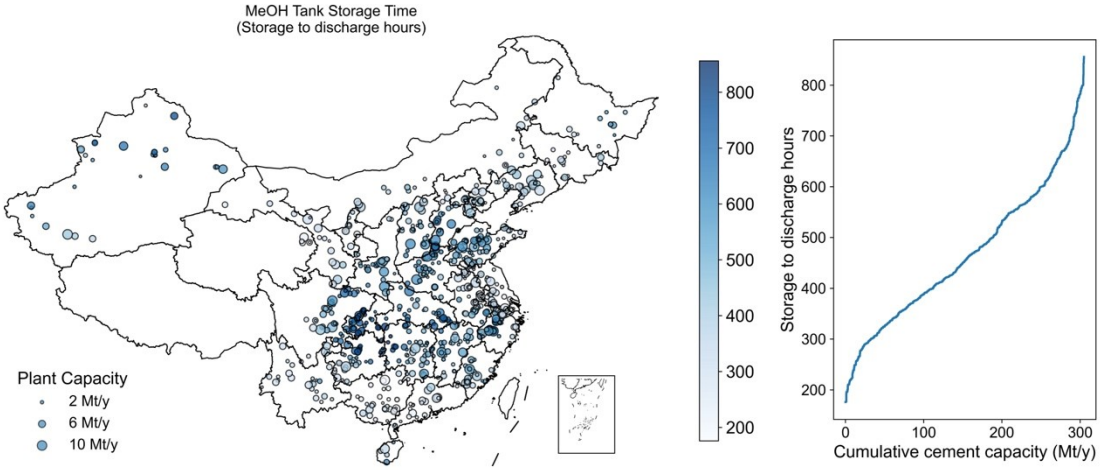

Fig. S12 Plant-level MeOH tank storage duration under net-zero methanol production scenarios.

Each dot marks an existing cement plant with different capacity (size) and MeOH storage duration (color). Storage duration is defined as the full storage volume divided by the discharge load, representing the length of time the storage can sustain exogeneous demand without additional input. The stoichiometric data is 9.76 tonne of cement per tonne of methanol under net zero methanol production scenarios. The right plot shows the curve sorted in ascending order of storage duration versus cumulative cement capacity.

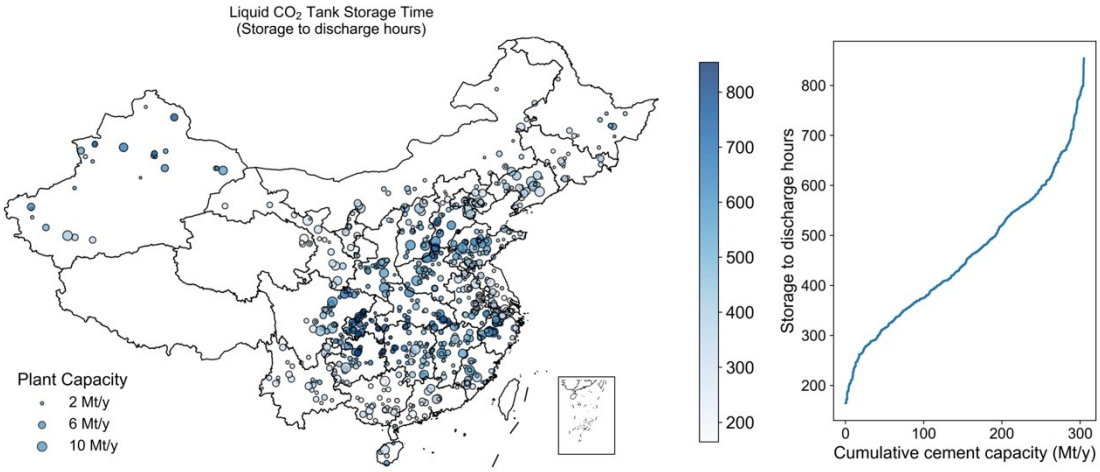

Fig. S13 Plant-level LCO_2 tank storage duration under net-zero methanol production scenarios.

Each dot marks an existing cement plant with different capacity (size) and LCO_2 storage duration (color). Storage duration is defined as the full storage volume divided by the discharge load, representing the length of time the storage can sustain downstream operations without additional input. The stoichiometric data is 9.76 tonne of cement per tonne of methanol under net zero methanol production scenarios. The right plot shows the curve sorted in ascending order of storage duration versus cumulative cement capacity.

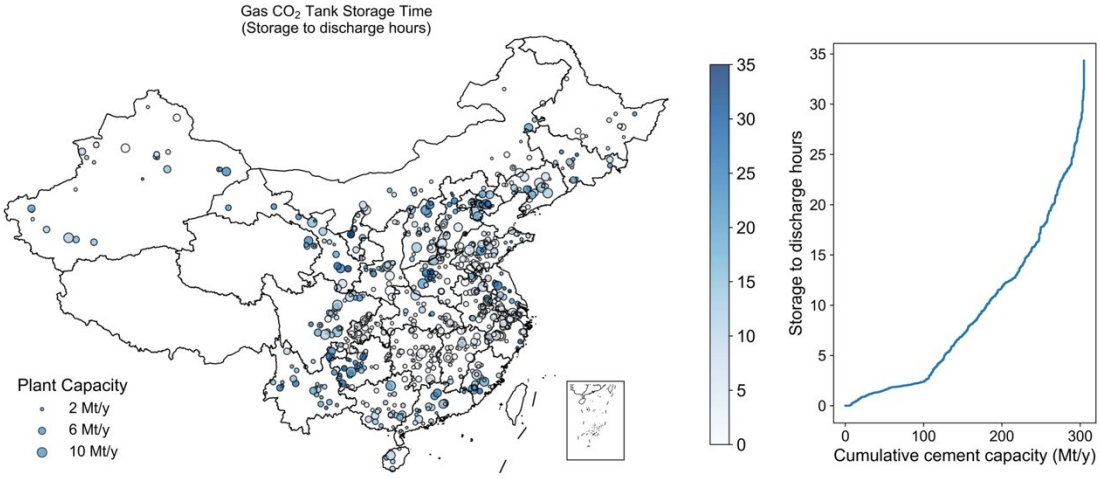

Fig. S14 Plant-level GCO_2 tank storage duration under net-zero methanol production scenarios.

Each dot marks an existing cement plant with different capacity (size) and GCO_2 storage duration (color). Storage duration is defined as the full storage volume divided by the discharge load, representing the length of time the storage can sustain downstream operations without additional input. The stoichiometric data is 9.76 tonne of cement per tonne of methanol under net zero methanol production scenarios. The right plot shows the curve sorted in ascending order of storage duration versus cumulative cement capacity.

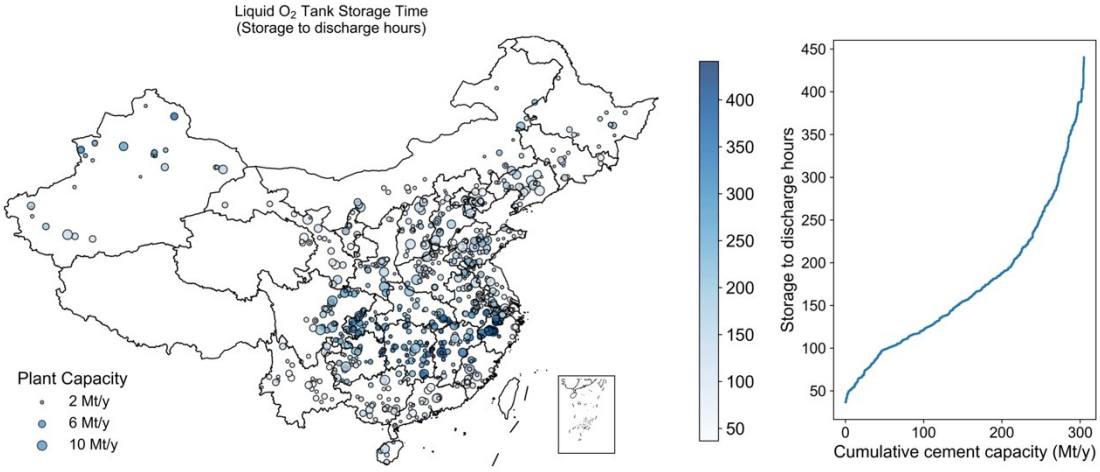

Fig. S15 Plant-level LO_2 tank storage duration under net-zero methanol production scenarios.

Each dot marks an existing cement plant with different capacity (size) and LO_2 storage duration (color). Storage duration is defined as the full storage volume divided by the discharge load, representing the length of time the storage can sustain downstream operations without additional input. The stoichiometric data is 9.76 tonne of cement per tonne of methanol under net zero methanol production scenarios. The right plot shows the curve sorted in ascending order of storage duration versus cumulative cement capacity.

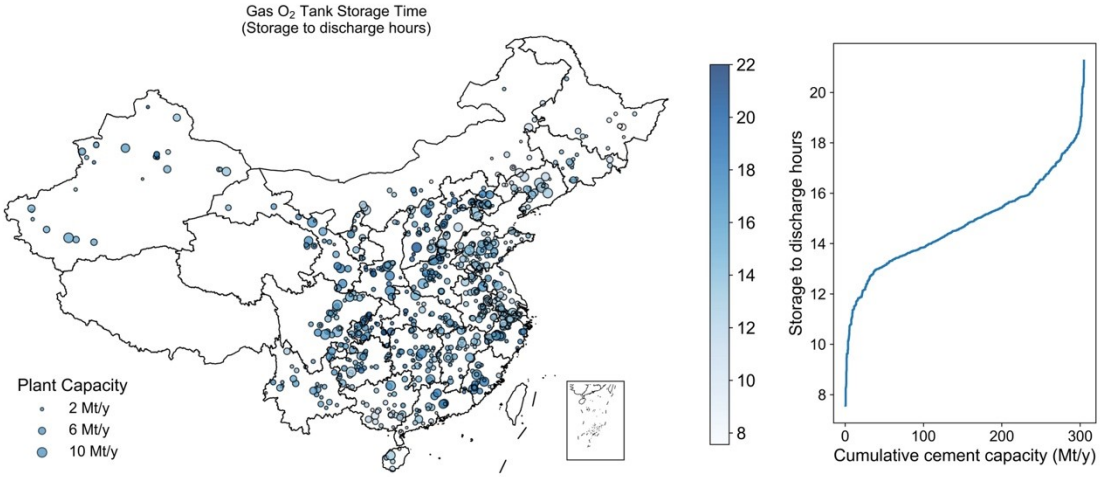

Fig. S16 Plant-level GO_2 tank storage duration under net-zero methanol production scenarios.

Each dot marks an existing cement plant with different capacity (size) and GO_2 storage duration (color). Storage duration is defined as the full storage volume divided by the discharge load, representing the length of time the storage can sustain downstream operations without additional input. The stoichiometric data is 9.76 tonne of cement per tonne of methanol under net zero methanol production scenarios. The right plot shows the curve sorted in ascending order of storage duration versus cumulative cement capacity.

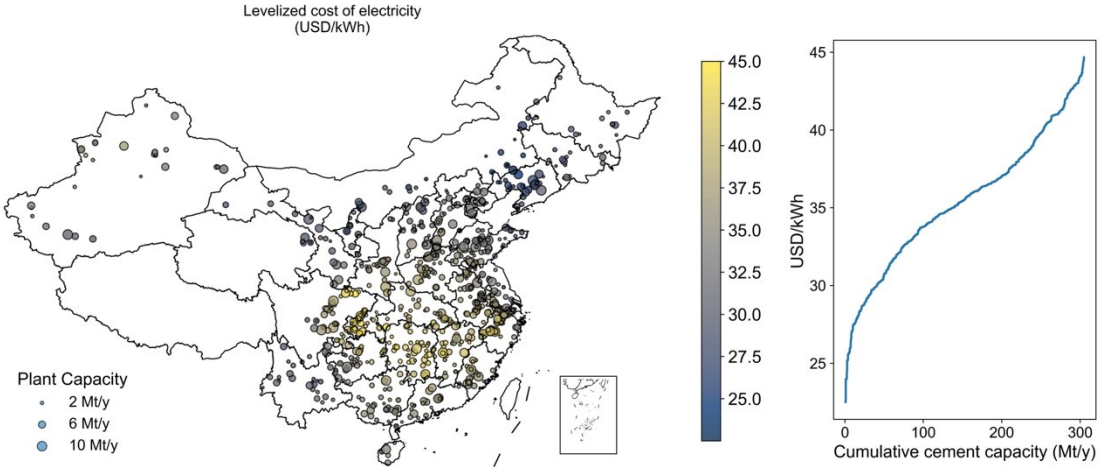

Fig. S17 Plant-level levelized cost of electricity (LCOE) under net-zero methanol production scenarios.

Each dot marks an existing cement plant with different capacity (size) and LCOE (color). The stoichiometric data is 9.76 tonne of cement per tonne of methanol under net zero methanol production scenarios. The right plot shows the curve sorted in ascending order of LCOE versus cumulative cement capacity.

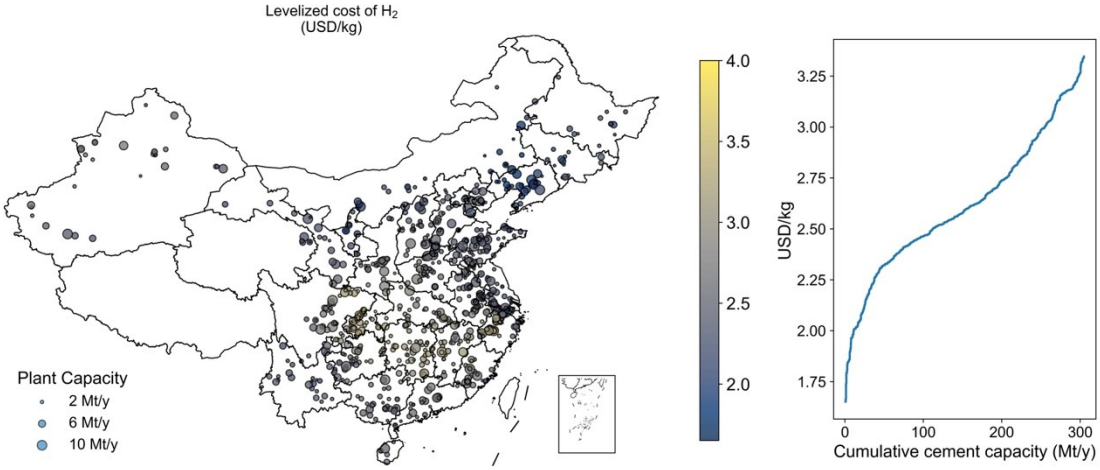

Fig. S18 Plant-level levelized cost of H_2 (LCOH) under net-zero methanol production scenarios.

Each dot marks an existing cement plant with different capacity (size) and LCOH (color). The stoichiometric data is 9.76 tonne of cement per tonne of methanol under net zero methanol production scenarios. The right plot shows the curve sorted in ascending order of LCOH versus cumulative cement capacity.

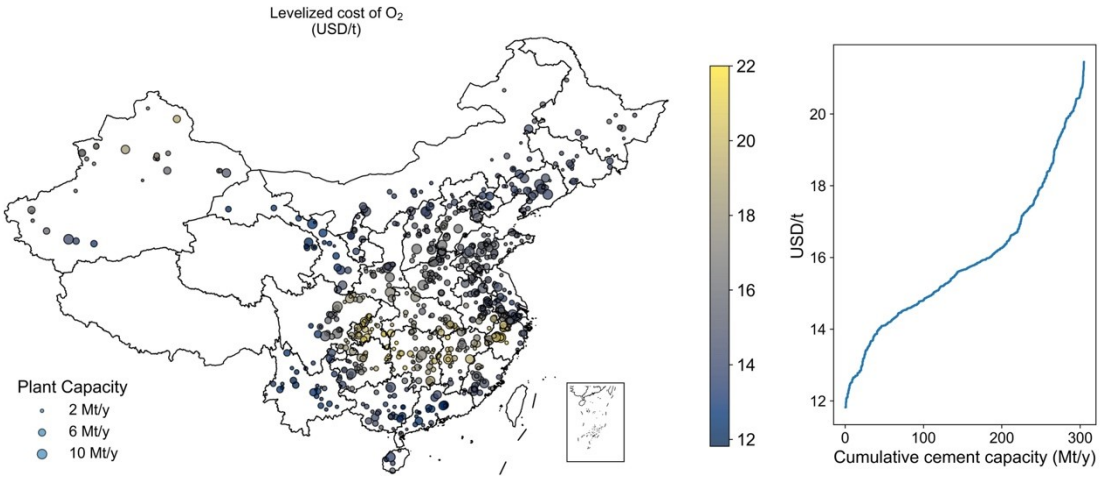

Fig. S19 Plant-level levelized cost of O_2 (LCOO) under net-zero methanol production scenarios.

Each dot marks an existing cement plant with different capacity (size) and LCOO (color). The stoichiometric data is 9.76 tonne of cement per tonne of methanol under net zero methanol production scenarios. The right plot shows the curve sorted in ascending order of LCOO versus cumulative cement capacity.

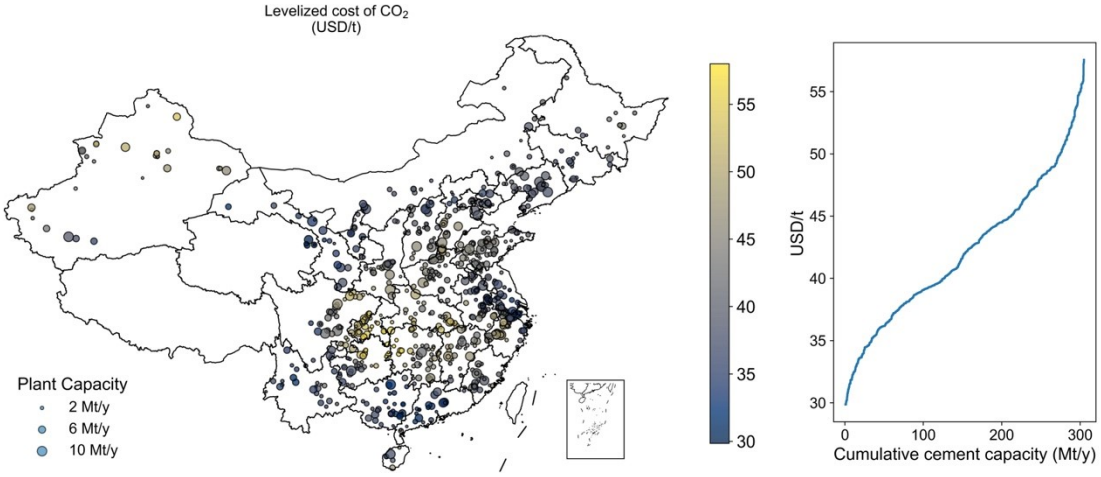

Fig. S20 Plant-level levelized cost of CO_2 (LCOC) under net-zero methanol production scenarios.

Each dot marks an existing cement plant with different capacity (size) and LCOC (color). The stoichiometric data is 9.76 tonne of cement per tonne of methanol under net zero methanol production scenarios. The right plot shows the curve sorted in ascending order of LCOC versus cumulative cement capacity.

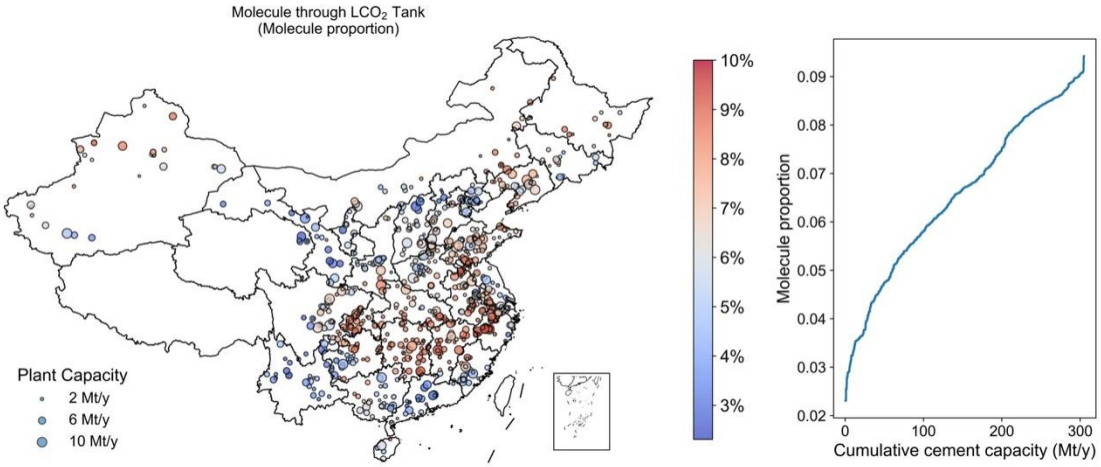

Fig. S21 Plant-level CO_2 proportion through LCO_2 tank under net-zero methanol production scenarios.

Each dot marks an existing cement plant with different capacity (size) and CO_2 proportion through LCO_2 tank (color). The molecule proportion is defined as the total volume of a molecule utilizing a specific storage method divided by the total volume of molecule generation. The stoichiometric data is 9.76 tonne of cement per tonne of methanol under net zero methanol production scenarios. The right plot shows the curve sorted in ascending order of molecule proportion versus cumulative cement capacity.

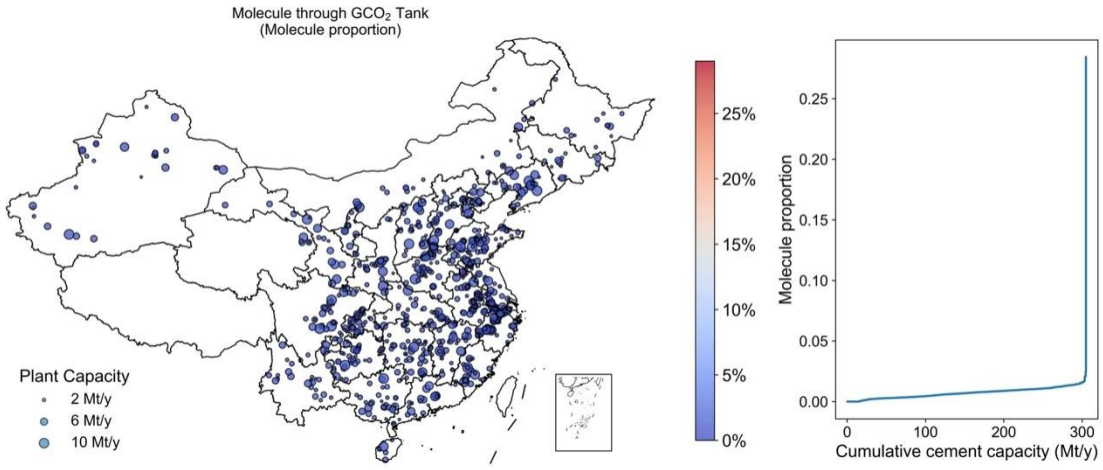

Fig. S22 Plant-level CO_2 proportion through GCO_2 tank under net-zero methanol production scenarios.

Each dot marks an existing cement plant with different capacity (size) and CO_2 proportion through GCO_2 tank (color). The molecule proportion is defined as the total volume of a molecule utilizing a specific storage method divided by the total volume of molecule generation. The stoichiometric data is 9.76 tonne of cement per tonne of methanol under net zero methanol production scenarios. The right plot shows the curve sorted in ascending order of molecule proportion versus cumulative cement capacity.

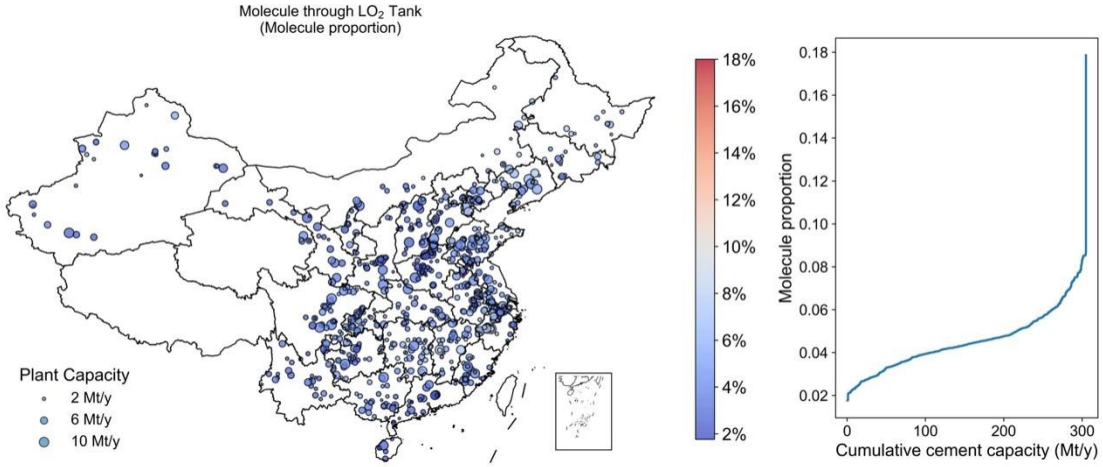

Fig. S23 Plant-level O_2 proportion through GO_2 tank under net-zero methanol production scenarios.

Each dot marks an existing cement plant with different capacity (size) and O_2 proportion through GO_2 tank (color). The molecule proportion is defined as the total volume of a molecule utilizing a specific storage method divided by the total volume of molecule generation. The stoichiometric data is 9.76 tonne of cement per tonne of methanol under net zero methanol production scenarios. The right plot shows the curve sorted in ascending order of molecule proportion versus cumulative cement capacity.

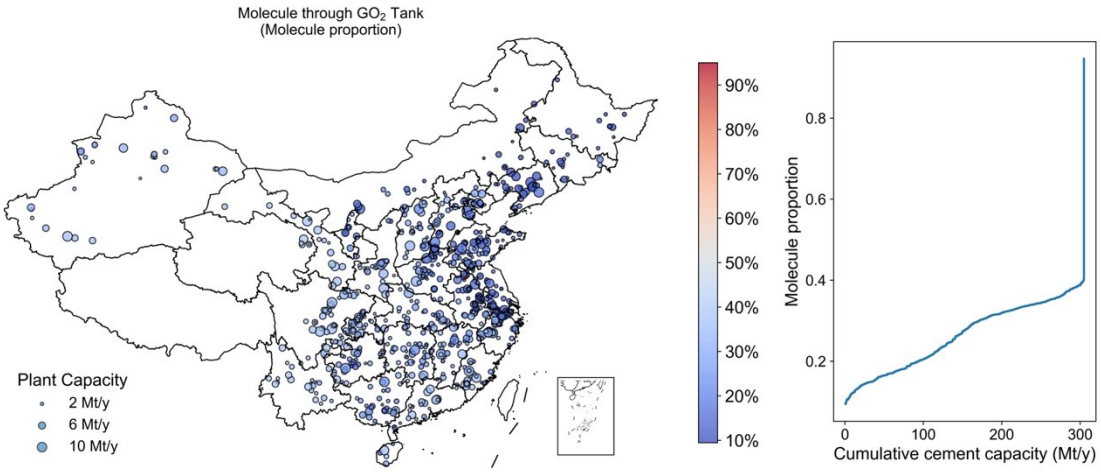

Fig. S24 Plant-level O_2 proportion through LO_2 tank under net-zero methanol production scenarios.

Each dot marks an existing cement plant with different capacity (size) and O_2 proportion through LO_2 tank (color). The molecule proportion is defined as the total volume of a molecule utilizing a specific storage method divided by the total volume of molecule generation. The stoichiometric data is 9.76 tonne of cement per tonne of methanol under net zero methanol production scenarios. The right plot shows the curve sorted in ascending order of molecule proportion versus cumulative cement capacity.

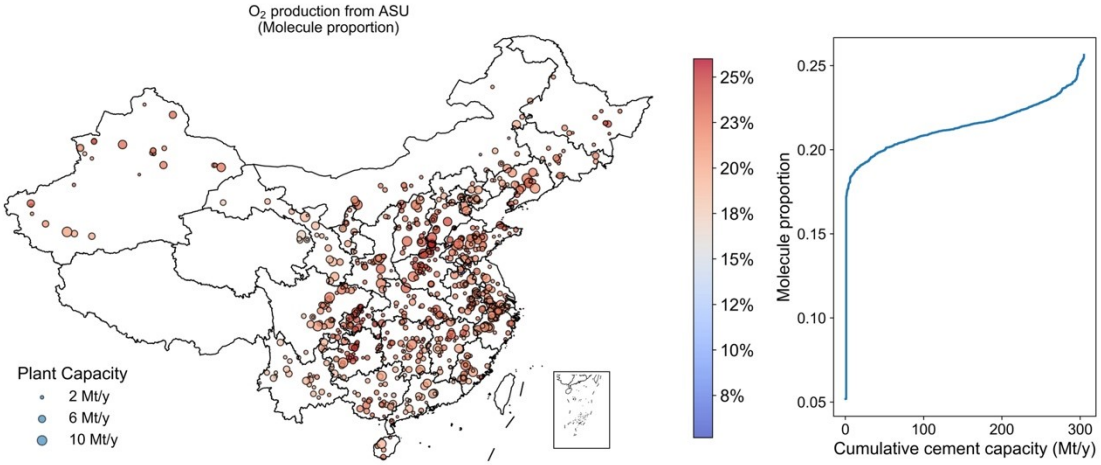

Fig. S25 Plant-level O_2 proportion generated from ASU under net-zero methanol production scenarios.

Each dot marks an existing cement plant with different capacity (size) and O_2 proportion generated from ASU (color). The molecule proportion is defined as the total volume of a molecule from a specific source divided by the total volume of molecule generation. The stoichiometric data is 9.76 tonne of cement per tonne of methanol under net zero methanol production scenarios. The right plot shows the curve sorted in ascending order of molecule proportion versus cumulative cement capacity.

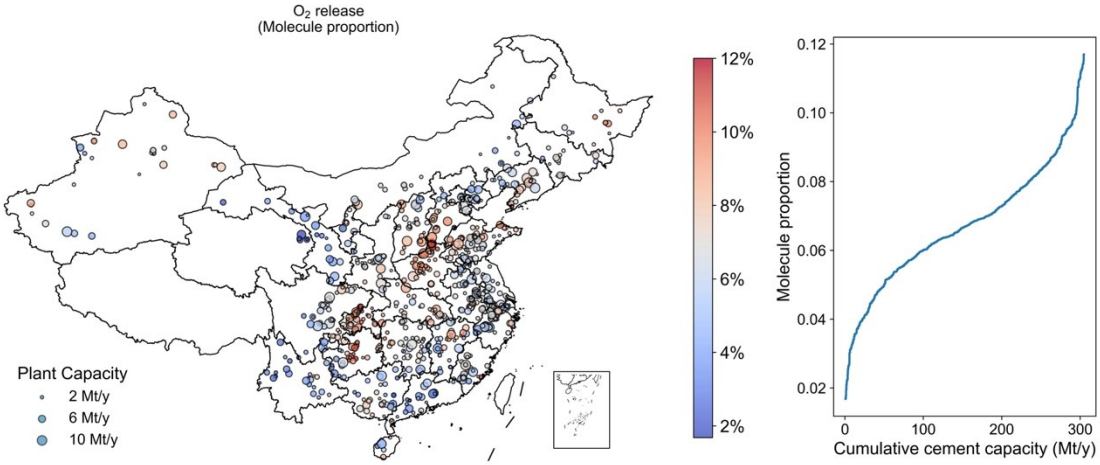

Fig. S26 Plant-level O_2 proportion released to atmosphere under net-zero methanol production scenarios.

Each dot marks an existing cement plant with different capacity (size) and O_2 proportion released to atmosphere (color). The molecule proportion is defined as the total volume of a molecule released to atmosphere divided by the total volume of molecule generation. The stoichiometric data is 9.76 tonne of cement per tonne of methanol under net zero methanol production scenarios. The right plot shows the curve sorted in ascending order of molecule proportion versus cumulative cement capacity.

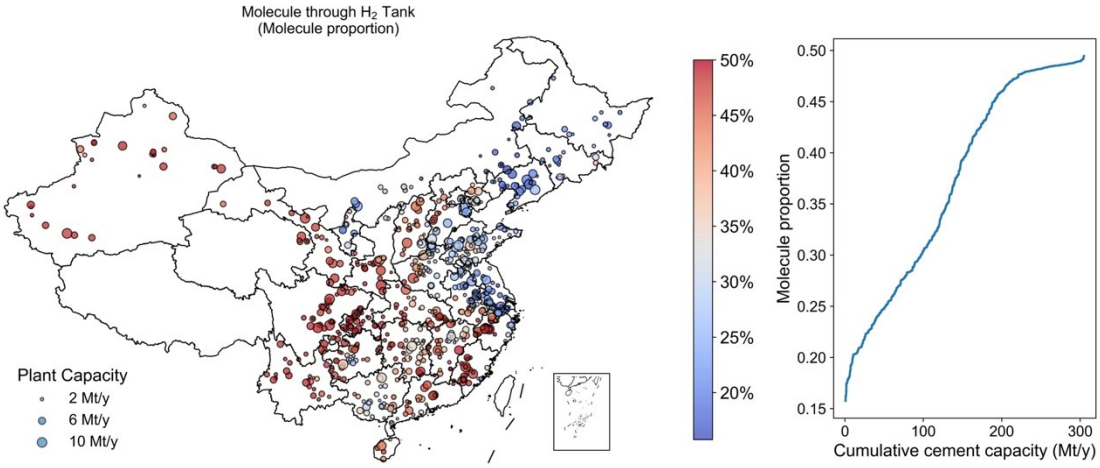

Fig. S27 Plant-level H_2 proportion through H_2 tank under net-zero methanol production scenarios.

Each dot marks an existing cement plant with different capacity (size) and H_2 proportion through H_2 tank (color). The molecule proportion is defined as the total volume of a molecule utilizing a specific storage method divided by the total volume of molecule generation. The stoichiometric data is 9.76 tonne of cement per tonne of methanol under net zero methanol production scenarios. The right plot shows the curve sorted in ascending order of molecule proportion versus cumulative cement capacity.

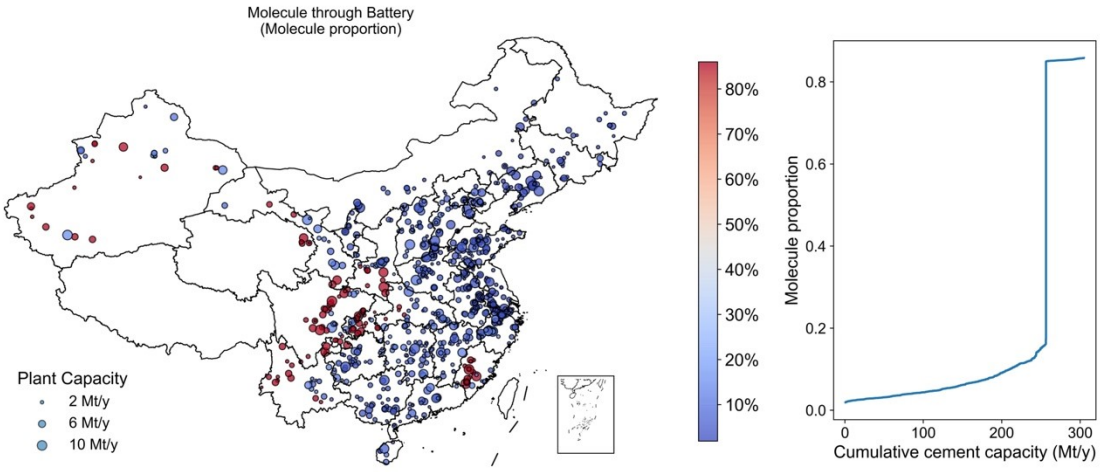

Fig. S28 Plant-level electricity proportion through battery under net-zero methanol production scenarios.

Each dot marks an existing cement plant with different capacity (size) and electricity proportion through battery (color). The stoichiometric data is 9.76 tonne of cement per tonne of methanol under net zero methanol production scenarios. The right plot shows the curve sorted in ascending order of electricity proportion versus cumulative cement capacity.

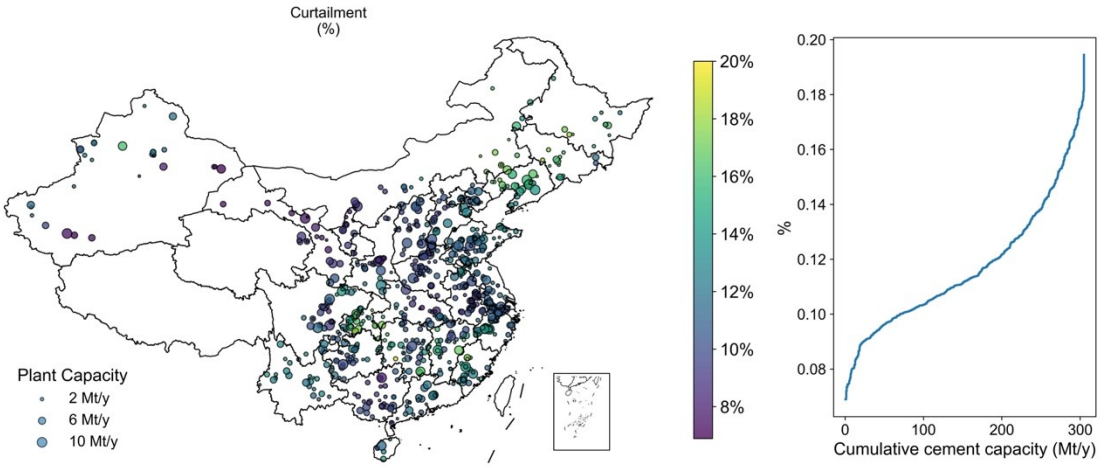

Fig. S29 Plant-level electricity curtailment rate under net-zero methanol production scenarios.

Each dot marks an existing cement plant with different capacity (size) and electricity curtailment rate (color). The stoichiometric data is 9.76 tonne of cement per tonne of methanol under net zero methanol production scenarios. The right plot shows the curve sorted in ascending order of electricity curtailment rate versus cumulative cement capacity.

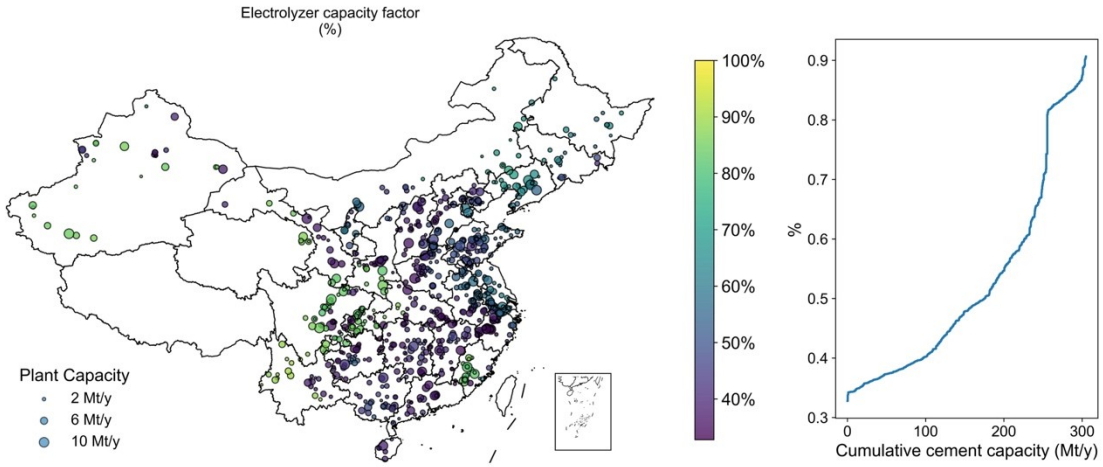

Fig. S30 Plant-level electrolyzer capacity factor under net-zero methanol production scenarios.

Each dot marks an existing cement plant with different capacity (size) and electrolyzer capacity factor (color). The stoichiometric data is 9.76 tonne of cement per tonne of methanol under net zero methanol production scenarios. The right plot shows the curve sorted in ascending order of electrolyzer capacity factor versus cumulative cement capacity.

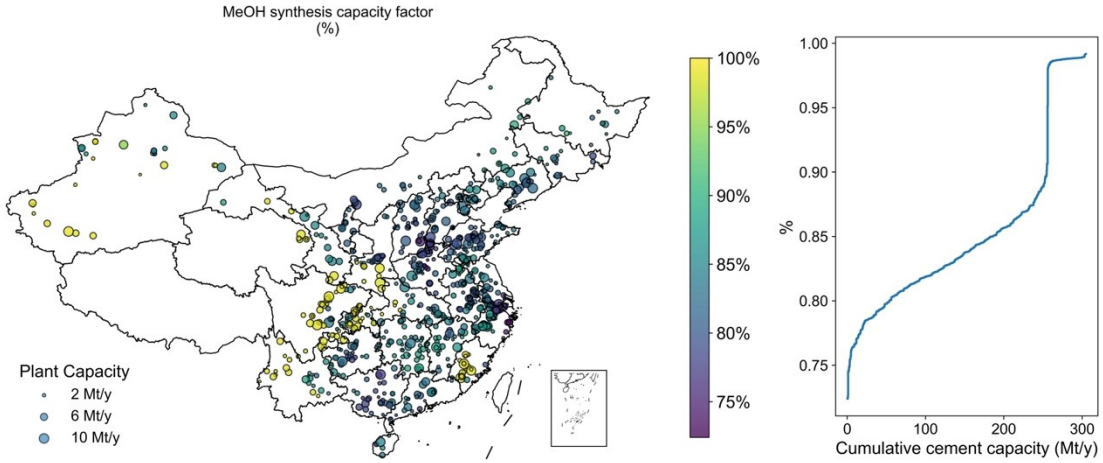

Fig. S31 Plant-level MeOH plant capacity factor under net-zero methanol production scenarios.

Each dot marks an existing cement plant with different capacity (size) and MeOH plant capacity factor (color). The stoichiometric data is 9.76 tonne of cement per tonne of methanol under net zero methanol production scenarios. The right plot shows the curve sorted in ascending order of MeOH plant capacity factor versus cumulative cement capacity.

2. Optimization model details

The objective function minimizes the total annualized cost of the cement and methanol co-production system, including annuitized capital investments, operation and maintenance (O&M) costs, raw material inputs, energy expenses, and labor expenditures (Equations (1)–(3)). Fixed costs are categorized into five components—electricity, industrial plants, H_2, O_2, and CO_2 systems—with detailed formulations provided in Equations (4)–(8). For each component, the fixed cost is computed as the product of the installed capacity and its associated annuity value, which encompasses both capital investment and fixed O&M costs. The electricity system includes solar PV, wind turbines, and batteries (covering both power and energy capacity). The industrial plant category comprises the raw meal grinder, cement grinder, clinker kiln, kiln retrofit cost, methanol synthesis unit, and methanol storage tank. The H_2 system consists of alkaline electrolyzers, H_2 compressors, and gaseous H_2 storage tanks. The O_2 system includes the air separation unit (ASU), O_2 compressors, liquefaction units, and both gaseous and liquid O_2 storage tanks. The CO_2 system includes CO_2 compressors, liquefaction units, and storage tanks for gaseous and liquid CO_2. Variable costs arise from biomass consumption, cement raw materials, labor, and CO_2 sequestration. These are calculated as the product of time-varying operational parameters (e.g., hourly biomass use) and unit costs, as described in Equation (9).

$$totc = fixc_{tot} + varc_{tot} \tag{1}$$

$$fixc_{tot} = fixc_{ele} + fixc_{plant} + fixc_{h2} + fixc_{o2} + fixc_{co2} \tag{2}$$

$$varc_{tot} = varc_{bio} + varc_{mat} + varc_{labor} + varc_{co2-seq} \tag{3}$$

$$fixc_{ele} = \sum_i cap_i \cdot ANNC_i \qquad i \in (solar, wind, battery) \tag{4}$$

$$fixc_{plant} = \sum_i cap_i \cdot ANNC_i \qquad i \in (cement, methanol, MeOH\ tank) \tag{5}$$

$$fixc_{h2} = \sum_i cap_i \cdot ANNC_i \qquad i \in (electrolyzer, H2\ tank, H2\ comp.) \tag{6}$$

$$fixc_{o2} = \sum_i cap_i \cdot ANNC_i \qquad i \in (ASU, LO2\ tank, GO2\ tank, O2\ liq., O2\ comp.) \tag{7}$$

$$fixc_{o2} = \sum_i cap_i \cdot ANNC_i \qquad i \in (LCO2\ tank, GCO2\ tank, CO2\ liq., CO2\ comp.) \tag{8}$$

$$varc_j = \sum_t \sum_j var_{t,j} \cdot UNITC_j \qquad j \in (bio., mat., labor, CO2\_seq.) \tag{9}$$

Balance constraints: Balance constraints are imposed on electricity, H_2, O_2, CO_2, methanol, and cement-related materials to ensure system-wide mass and energy equilibrium (Equations (10)–(15)). These constraints require that, for each commodity, generation plus net discharge from storage must equal demand or supply in each time period. Electricity demand is disaggregated into four end-use categories: H_2 supply (electrolyzers and H_2 compressors), O_2 supply (air separation unit, O_2 compressors, and liquefaction units), CO_2 supply (CO_2 compressors and liquefaction units), and plant operations (grinders and methanol synthesis). For O_2 and CO_2 balance equations, both gaseous and liquid storage pathways are modeled. O_2 generated from electrolysis or ASU can be directly used in the clinker kiln for oxy-fuel combustion, stored into different states or discarded if in excess.

Captured CO_2 is allocated to either methanol synthesis as a feedstock or directed to underground sequestration ultimately, depending on the stoichiometric balance, and can be stored into different forms as well.

$$ele\_gen_{t,solar} + ele\_gen_{t,wind} + bat\_out_t - bat\_in_t = ele\_con_{t,h2} + ele\_con_{t,o2} + ele\_con_{t,co2} + ele\_c \quad (10)$$

$$h2\_gen_t + h2\_out_t - h2\_in_t = meth\_h2_t \quad (11)$$

$$o2\_gen_{t,ely} + o2\_gen_{t,asu} + go2\_out_t - go2\_in_t + lo2\_out_t - lo2\_in_t = kiln\_o2_t + ex\_o2_t \quad (12)$$

$$co2\_gen_{t,kiln} \cdot CCR + gco2\_out_t - gco2\_in_t + lco2\_out_t - lco2\_in_t = meth\_co2_t + seq\_co2_t \quad (13)$$

$$meth\_gen_t + meth\_out_t - meth\_in_t = METH\_SUPPLY_t \quad (14)$$

$$mat\_gen_{t,i} + mat\_out_{t,i} - mat\_in_{t,i} = mat\_supply_{t,i} \qquad i \in (raw\ meal, clinker, cement) \quad (15)$$

Capacity Constraints: Capacity constraints ensure that the operational load of each facility remains within technically feasible limits. For renewable generation, the output per unit of installed capacity is bounded by weather-dependent maximum generation profiles (Equations (16)–(17)). In the case of batteries, charging and discharging rates are limited by the installed power capacity, while the state of charge (SOC) must remain within the bounds of the energy storage capacity (Equations (18)–(20)). Electrolyzers (Equations (21)–(22)), air separation units (ASU) (Equations (25)–(26)), and liquefaction units (Equations (42)–(43)) operate within predefined output ranges, constrained by both upper and lower operational limits. Compressors are assumed to be fully flexible on an hourly basis and are constrained only by maximum load thresholds (Equation (41)). For gaseous storage systems, both upper SOC limits and minimum SOC requirements (serving as operational cushion) are enforced (Equations (23)–(24), Equations (29)–(30), and Equations (33)–(34)). Liquid storage systems, by contrast, are only subject to upper SOC constraints due to their higher capital costs and slower dynamics (Equations (27)–(28) and Equations (31)–(32)). If flexible operation is enabled for methanol synthesis, its output must remain within specified upper and lower load boundaries (Equations (35)–(36)). In inflexible scenarios, methanol synthesis operates at a fixed full-load level. Meanwhile, the methanol is stored in the liquid state, with an upper limit of SOC (Equation (37)). Cement-related facilities, including grinders and clinker kilns, are also subject to capacity constraints that reflect nominal design capacity (Equations (38)–(39)). As solid-state materials, their storage is comparatively simple and less costly; hence, storage facility costs are omitted, though maximum storage durations are enforced based on engineering experience in current actual projects (Equation (40)).

$$ele\_gen_{t,solar} \le cap_{solar} \cdot MAXGEN_{t,solar} \quad (16)$$

$$ele\_gen_{t,wind} \le cap_{wind} \cdot MAXGEN_{t,wind} \quad (17)$$

$$bat\_out_t \le cap_{batp} \quad (18)$$

$$bat\_in_t \le cap_{batp} \quad (19)$$

$$bat\_soc_t \le cap_{bate} \quad (20)$$

$$ely\_p_t \le cap_{ely} \cdot MAX\_LOAD_{ely} \quad (21)$$

$$ely\_p_t \ge cap_{ely} \cdot MIN\_LOAD_{ely} \quad (22)$$

$$h2\_soc_t \le cap_{h2tank} \quad (23)$$

$$h2\_soc_t \ge cap_{h2tank} \cdot MIN\_SOC_{h2} \quad (24)$$

$$o2\_gen_{t,asu} \le cap_{asu} \cdot MAX\_LOAD_{asu} \quad (25)$$

$$o2\_gen_{t,asu} \geq cap_{asu} \cdot MIN\_LOAD_{asu} \quad (26)$$

$$lo2\_soc_t \leq cap_{lo2tank} \quad (27)$$

$$lo2\_soc_t \geq cap_{lo2tank} \cdot MIN\_SOC_{lo2} \quad (28)$$

$$go2\_soc_t \leq cap_{go2tank} \quad (29)$$

$$go2\_soc_t \geq cap_{go2tank} \cdot MIN\_SOC_{go2} \quad (30)$$

$$lco2\_soc_t \leq cap_{lco2tank} \quad (31)$$

$$lco2\_soc_t \geq cap_{lco2tank} \cdot MIN\_SOC_{lco2} \quad (32)$$

$$gco2\_soc_t \leq cap_{gco2tank} \quad (33)$$

$$gco2\_soc_t \geq cap_{gco2tank} \cdot MIN\_SOC_{gco2} \quad (34)$$

$$meth\_gen_t \leq cap_{meth} \cdot MAX\_LOAD_{meth} \quad (35)$$

$$meth\_gen_t \geq cap_{meth} \cdot MIN\_LOAD_{meth} \quad (36)$$

$$meth\_soc_t \leq cap_{methtank} \quad (37)$$

$$mat\_gen_{t,clinker} = cap_{kiln} \quad (38)$$

$$mat\_gen_{t,i} \leq cap_i \qquad i \in (raw\ meal, cement) \quad (39)$$

$$mat\_soc_{t,i} \leq cap_i \cdot MAX\_DURATION_i \qquad i \in (raw\ meal, clinker, cement) \quad (40)$$

$$mole\_comp\_p_{t,i} \leq cap_{comp,i} \qquad i \in (h2, go2, gco2) \quad (41)$$

$$mole\_liq\_p_{t,i} \leq cap_{liq,i} \cdot MAX\_LOAD_{liq,i} \qquad i \in (lo2, lco2) \quad (42)$$

$$mole\_liq\_p_{t,i} \geq cap_{liq,i} \cdot MIN\_LOAD_{liq,i} \qquad i \in (lo2, lco2) \quad (43)$$

Storage constraints: Storage constraints define the evolution of state of charge (SOC) across time steps based on charge and discharge actions. At each time slice, the SOC equals the SOC of the previous time step plus the net charge within the period. For batteries, charging and discharging efficiencies are explicitly considered to reflect energy losses (Equation (44)). For molecular storage (e.g., H_2, O_2, CO_2), methanol and cement-related solid materials, losses are assumed negligible due to the relatively low leakage and loss characteristics of these storage types (Equations (45)–(51)).

$$bat\_soc_t = bat\_soc_{t-1} - bat\_out_t / BAT\_\eta_{out} + bat\_in_t \times BAT\_\eta_{in} \quad (44)$$

$$h2\_soc_t = h2\_soc_{t-1} - h2\_out_t + h2\_in_t \quad (45)$$

$$go2\_soc_t = go2\_soc_{t-1} - go2\_out_t + go2\_in_t \quad (46)$$

$$lo2\_soc_t = lo2\_soc_{t-1} - lo2\_out_t + lo2\_in_t \quad (47)$$

$$gco2\_soc_t = gco2\_soc_{t-1} - gco2\_out_t + gco2\_in_t \quad (48)$$

$$lco2\_soc_t = lco2\_soc_{t-1} - lco2\_out_t + lco2\_in_t \quad (49)$$

$$meth\_soc_t = meth\_soc_{t-1} - meth\_out_t + meth\_in_t \quad (50)$$

$$mat\_soc_{t,i} = mat\_soc_{t-1,i} - mat\_out_{t,i} + mat\_in_{t,i} \qquad i \in (raw\ meal, clinker, cement) \quad (51)$$

Ramp Constraints: Ramp constraints impose limits on the rate of change in facility loads between consecutive hours to ensure operational feasibility. For methanol synthesis, ramp-up and ramp-down rates are constrained to reflect technical limitations and maintain smooth transitions (Equations (52)–(53)). For ASU and liquefaction units, ramping capabilities typically exceed 3% per minute[1,2]. Given this high responsiveness, hourly-resolution models do not require explicit ramp constraints for these components, and such constraints are thus omitted.

$$meth\_gen_{t-1} - meth\_gen_t \leq cap_{meth} \times RAMP\_UP_{meth} \quad (52)$$

$$meth\_gen_t - meth\_gen_{t-1} \leq cap_{meth} \times RAMP\_DOWN_{meth} \quad (53)$$

Stoichiometry Balance: Stoichiometric constraints ensure mass and energy input–output consistency across all conversion and storage processes in the system. For electrolyzers, H_2 and O_2 production are assumed linearly proportional to the electricity input (Equations (54)–(55)). In air separation units (ASUs), each unit of oxygen output corresponds to a certain electricity input (Equation (56)). For gas compression, electricity consumption is associated with the pressurization processes (Equation (57)). H_2 produced by electrolyzers must be compressed from 30 bar to 150 bar before being consumed or stored. For O_2, only the O_2 generated by ASU that is directed to gaseous storage requires compression to 30 bar. In contrast, O_2 from electrolyzers can be fed directly into gaseous storage tanks. Both ASU- and electrolyzer-derived O_2 can also be liquefied and stored in liquid tanks, each with specific liquefaction energy consumption (Equation (58)). For CO_2, the gas destined for methanol synthesis or gaseous storage must be compressed to 50 bar, while that intended for geological sequestration requires compression to 150 bar, incurring different electricity consumption rates. Liquid storage is also an option via CO_2 liquefaction units with certain amount of power consumption. Methanol synthesis consumes fixed ratios of hydrogen, CO_2, and electricity per unit of methanol output (Equations (59)–(61)). Similarly, clinker production requires raw meal, oxygen, and biomass as inputs, and generates CO_2 (Equations (62)–(66)). The cement-to-clinker ratio is used to maintain material flow consistency between the clinker and final cement production stages (Equation (67)).

$$h2\_gen_t \times STOICH_{ele,h2} = ely\_p_t \quad (54)$$

$$o2\_gen_{t,ely} \times STOICH_{ele,o2} = ely\_p_t \quad (55)$$

$$o2\_gen_{t,asu} \times STOICH_{asu\_ele,o2} = asu\_p_t \quad (56)$$

$$mole\_comp_{t,i} \times STOICH_{comp\_ele,i} = mole\_comp\_p_{t,i} \qquad i \in (h2, go2, gco2) \quad (57)$$

$$mole\_liq_{t,i} \times STOICH_{liq\_ele,i} = mole\_liq\_p_{t,i} \qquad i \in (lo2, lco2) \quad (58)$$

$$meth\_gen_t \times STOICH_{h2,meth} = meth\_h2_t \quad (59)$$

$$meth\_gen_t \times STOICH_{ele,meth} = meth\_p_t \quad (60)$$

$$meth\_gen_t \times STOICH_{co2,meth} = meth\_co2_t \quad (61)$$

$$mat\_gen_{t,i} \times STOICH_{ele,i} = mat\_p_{t,i} \qquad i \in (raw\ meal, cement) \quad (62)$$

$$mat\_gen_{t,clinker} \times STOICH_{o2,clinker} = kiln\_o2_t \quad (63)$$

$$mat\_gen_{t,clinker} \times STOICH_{co2,clinker} = co2\_gen_{t,kiln} \quad (64)$$

$$mat\_gen_{t,clinker} \times STOICH_{bio,clinker} = kiln\_bio_t \quad (65)$$

$$mat\_gen_{t,clinker} \times STOICH_{raw\ meal,clinker} = mat\_supply_{t,raw\ meal} \quad (66)$$

$$mat\_gen_{t,cement} \times STOICH_{clinker,cement} = mat\_supply_{t,clinker} \quad (67)$$

Emission Constraints: Emission constraints are scenario-specific and designed to ensure consistency between carbon flows and assumed system boundaries. In the net-methanol scenario, total CO_2 originating from biomass combustion must equal the sum of non-captured CO_2 emitted into the atmosphere and the CO_2 incorporated into methanol as a carbon feedstock. In the no-CO_2 sequestration scenario, all CO_2 captured from clinker production is directed exclusively to methanol

synthesis, with no CO_2 allocated for geological sequestration. These constraints are implemented to reflect realistic carbon accounting and to enable assessment of different carbon utilization strategies.

$$\sum_t kiln\_bio_t \cdot CF_{bio} = \sum_t meth\_co2_t + co2\_gen_{t,kiln} \cdot (1 - CCR) \quad (68)$$

$$seq\_co2_t = 0 \quad (69)$$

Table S1 Costs of labor and other materials.

Items	Value	Unit	Source
Methanol labor	12.5	\$/t MeOH	[3]
CO_2 from DAC	203.6	\$/t CO_2	[3]
Cement labor	4.5	\$/t cement	Cement company 2022 annual report
Cement other materials	5.9	\$/t cement	Cement company 2022 annual report
Biomass	17.4	\$/MWh	[4]

Table S2 Stoichiometric data. Low heat value is used. For clinker kilns, their power consumption is neglected since it is almost equal to the power generation from waste heat recovery. For the stoichiometric data of clinker kilns, coal-based data are provided in the literature. We calculate the corresponding data of biomass by converting heat value and emission factors, assuming heat requirements per tonne clinker are the same.

	Value	Unit	Source
Power to H_2	1.650	MWh/MWh H_2	[5]
Power to O_2 (electrolyzer)	6.875	MWh/t O_2	[5]
Power to O_2 (ASU)	0.282	MWh/t O_2	[6] and ASEPN
H_2 compression (30 bar to 150 bar)	0.025	MWh/MWh H_2	[3]
O_2 compression (ASU outlet to 30 bar)	0.108	MWh/t O_2	ASEPN
CO_2 compression (to 50 bar)	0.099	MWh/t CO_2	[3]
CO_2 compression (to 150 bar)	0.134	MWh/t CO_2	[7]
O_2 liquefaction (from ASU outlet)	0.434	MWh/t O_2	[8]
O_2 liquefaction (from electrolyzer outlet)	0.312	MWh/t O_2	[8] and ASEPN
CO_2 liquefaction	0.160	MWh/t CO_2	[3]
H_2 to methanol	6.633	MWh H_2/t MeOH	[3]
Power to methanol	0.169	MWh/t MeOH	[3]
CO_2 to methanol	1.460	t CO_2/t MeOH	[3]
Raw grinder power	0.057	MWh/t raw	[9]
Cement grinder power	0.044	MWh/t cement	[9]
Raw to clinker	1	t raw/t clinker	Equivalent

Clinker to cement	0.678	t clinker/t cement	raw meal [10]
O_2 to clinker	0.286	t O_2/t clinker	[11] and own calculations
Clinker CO_2 production	0.862	t CO_2/t clinker	[12] and Own calculations
Biomass to clinker	0.887	MWh/t clinker	[12] and Own calculations
Process CO_2 emission factor	0.556	t CO_2/t clinker	[10]
Biomass CO_2 emission factor	0.346	t CO_2/MWh	[13] and Own calculations

Table S3 CAPEX and fixed OPEX data. The renewable technology-related data used in this study are specific to China. The retrofit cost of clinker kiln is derived from the actual oxy-fuel combustion project of a certain cement plant in China. We investigate the gas storage tank manufacturing companies in China and conduct consistency checks with the literature data.

	CAPEX (2035)	Unit	OPEX	Lifetime	Source
solar	417	$/kW	1.4%	25	[14]
wind	662	$/kW	1.9%	25	[14]
battery power	274	$/kW	5.0%	15	[14]
battery energy	137	$/kWh	/	15	[14]
electrolyzer	232	$/kW	2.0%	12	[15]
H_2 tank	394	$/kg H_2	2.0%	25	[16]
H_2 compressor	2843	$/kW	4.0%	20	[3]
ASU	200	$/(t O_2/y)	4.0%	30	[17]
GO_2 tank	24318	$/t O_2	1.3%	30	[3] and Own calculations
GCO_2 tank	17577	$/t CO_2	1.3%	30	[3] and Own calculations
LCO_2 tank	4049	$/t CO_2	1.2%	30	[3]
LO_2 tank	1616	$/t O_2	2.0%	30	[18]
CO_2 liquefaction	186	$/(t CO_2/y)	4.0%	20	[19]
O_2 liquefaction (from ASU)	101	$/(t O_2/y)	6.0%	10	[8] and Aspen Plus Economic Analyzer
O_2 liquefaction (from electrolyzer)	79	$/(t O_2/y)	6.0%	10	[8] and Aspen Plus Economic Analyzer
CO_2 compressor	3884	$/kW	4.0%	20	[3]

Raw grinder	37	$/(t clinker/y)	5.0%	25	[9]
Clinker kiln	64	$/(t clinker/y)	5.0%	25	[20] and Own calculations
Cement grinder	19	$/(t cement/y)	5.0%	25	[21]
Retrofit clinker	90	$/(t clinker/y)	5.0%	25	[22]
MeOH	435	$/(t MeOH/y)	3%	30	[23]
MeOH_tank	81	$/t MeOH	4%	30	[3]

Table S4 Technical data and boundaries.

	Value	Source
Lithium-ion battery round-trip efficiency	86%	[24]
Alkaline electrolyzer min load	5%	[25]
Alkaline electrolyzer max load	110%	[25]
Gaseous tank min SOC	10%	[3]
Methanol synthesis min load	50%	[3]
Methanol synthesis ramp-up rate	2%	[3]
Methanol synthesis ramp-down rate	20%	[3]
ASU and liquefaction min load	70%	[19]

3. CO_2 abatement cost

(1) Incumbent and separate decarbonization technologies calculation

Table S5 Cost breakdown of incumbent cement plants. CAPEX, OPEX and stoichiometric data are referenced to Table S1, Table S3, and Table S2. Grid power prices are based on average industrial power prices in China, which is $91.7 per MWh[26]. Coal prices refer to the domestic thermal-coal benchmark of $98.4 per tonne (5500 kcal/t)[27].

Item	Cost ($/t cement)
Annualized CAPEX & Fixed OPEX	10.4
Var OPEX (other materials, labor, etc.)	10.4
Coal	9.3
Power	7.6
SUM	37.6

Table S6 Cost breakdown of cement plants with oxy-fuel combustion CCUS technology. CAPEX, OPEX and stoichiometric data are referenced to Table S1, Table S3, and Table S2. While the thermal input remains essentially unchanged, power consumption increases due to additional CO_2 processing steps such as compression[9].

Item	Cost ($/t cement)
Annualized CAPEX & Fixed OPEX	17.6
Var OPEX	10.4
Coal	9.3
Power	14.0
Annualized CAPEX & Fixed OPEX of ASU	4.8
Power of ASU	5.3
CO_2 transport & sequestration	7.6
SUM (excl. CO_2 transport & sequestration)	61.3
SUM (incl. CO_2 transport & sequestration)	68.9

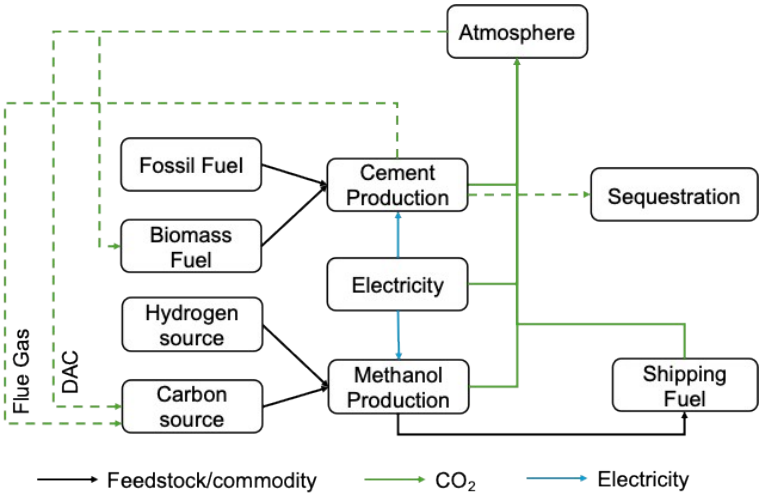

Fig. S32 CO_2 emission accounting boundary.

Carbon accounting covers net-CO_2 released to the atmosphere from cement and methanol production and from methanol combustion when used as a shipping fuel. Carbon sourced from DAC or biomass is treated as atmosphere-neutral, and geological sequestration is assumed to offset emissions that would otherwise be vented.

Table S7 CO_2 emission breakdown of incumbent cement plants and plants with oxy-fuel combustion CCUS technology. The emission factor of grid power is set as 1.000 kg CO_2/kWh, which is the grid emission factor in Inner Mongolia in 2020[28].

Item	Incumbent coal-based cement (t CO_2/t cement)	Coal-based cement with CCUS (t CO_2/t cement)
Coal & Process	0.582	0.058
Power	0.083	0.210
Total	0.664	0.268

Table S8 Cost breakdown of incumbent methanol plants. CAPEX, OPEX and stoichiometric data are referenced to Table S1, Table S3, and Table S2. Grid power prices are based on average industrial power prices in China, which is \$91.7 per MWh[26]. The coal price is based on the chemical coal price, which is estimated to be 1.2 times the price of thermal coal.

Item	Cost (\$/t methanol)
Annualized CAPEX & Fixed OPEX	72.2
Var OPEX (other materials, labor, etc.)	12.5
Coal	251.9
Power	11.5
SUM	348.0

Table S9 Cost estimations of DAC.

Source	Projected Cost (\$/tCO_2 removed)	DAC Tech Type
Fasihi & Breyer (2024)[3]	~\$180–215 (in 2030)	Solid sorbent DAC
Sievert et al. (2024)[29]	\$341 (\$226–544, 1 GtCO_2/yr scale)	Liquid solvent DAC
	\$374 (\$281–579, 1 GtCO_2/yr scale)	Solid sorbent DAC
	\$371 (\$230–835, 1 GtCO_2/yr scale)	CaO looping
Young et al. (2023)[30]	\$100-440 (1 GtCO_2/yr scale)	KOH–Ca looping
	\$450-1350 (1 GtCO_2/yr scale)	KOH–BPMED
	\$170-730 (1 GtCO_2/yr scale)	Solid sorbent
	\$100-540 (1 GtCO_2/yr scale)	MgO ambient weathering
Al-Juaied & Whitmore (2023)[31]	~\$200–400 (in 2050)	N/A
IEAGHG (2021)[32]	~\$194–230 (1 MtCO_2/yr scale)	Liquid & solid DAC

Most recent DAC cost projections use a hybrid FOAK-to-NOAK framework: they build a bottom-up first-of-a-kind (FOAK) cost (with contingencies) and then apply learning curves to extrapolate to gigaton-scale deployment. When boundaries include net removal (capture, compression, transport & geological storage), these learning-curve studies typically converge on an

order-of-magnitude cost band of ~$200–600 per tCO_2 at Gt yr^{-1}, with optimistic best-site assumptions occasionally approaching ~$100. Across all routes, outcomes hinge on energy price and carbon intensity, capacity factor, discount rate and learning rate. In this study, we adopt the median estimate from Fasihi & Breyer at ~$200/$tCO_2$ in 2030[3], from their assessment of DAC paired with renewable hydrogen for green-methanol production. This is a relatively optimistic figure; even so, our results show the co-production technology is more cost-effective than using DAC and renewable hydrogen to produce methanol. The advantage only widens under higher DAC cost assumptions.

Table S10 Cost breakdown of renewable-based methanol plants in Inner Mongolia. CAPEX, OPEX and stoichiometric data are referenced to Table S1, Table S3, and Table S2. The renewable profiles are based on the selected case plant in Inner Mongolia. Assume CO_2 is from DAC. Therefore, the renewable-based methanol can be regarded as carbon-neutral across its entire life cycle.

Item	Cost ($/t methanol)
Wind	47.9
Solar	211.8
Battery	50.2
Electrolyzer	95.9
H_2 tank	16.6
H_2 compressor	17.7
MeOH plant	50.2
MeOH tank	0.4
CO_2 cost	297.2
Labor cost	12.5
Total	800.7

Table S11 CO_2 emission breakdown of incumbent methanol plants. The emission factor of grid power is set as 1.000 kg CO_2/kWh, which is the grid emission factor in Inner Mongolia in 2020[28].

Item	Incumbent coal-based methanol (t CO_2/t methanol)
Coal & Process	3.272
Power	0.185
Total	3.456

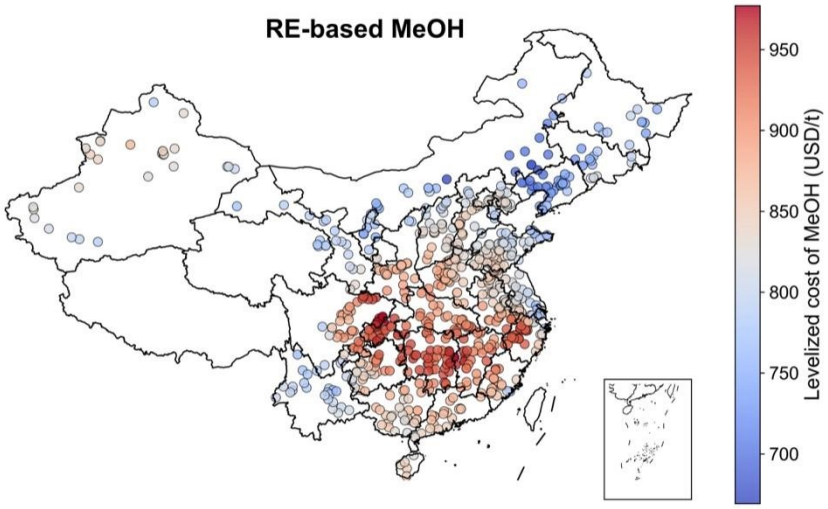

Fig. S33 Renewable-based methanol production cost across existing cement facility sites. Assume CO_2 is from DAC.

(2) CO_2 abatement cost calculation

CO_2 abatement cost is defined as the incremental cost required to avoid one additional tonne of CO_2 emissions when moving from a reference (baseline) scenario to an alternative, lower-emission scenario. Mathematically, it is expressed as:

$$C_{abatement} = \frac{C_1 - C_0}{E_0 - E_1}$$

where

- C_0 and E_0 are the total production cost and CO_2 emissions of the baseline process, and
- C_1 and E_1 are the corresponding cost and emissions under the abatement scenario.

This metric normalizes abatement costs across heterogeneous scenarios, such as different stoichiometric data of cement and methanol production. By converting both cost and emissions reductions into a single "USD per tonne CO_2 avoided" figure, CO_2 abatement cost provides a consistent basis for comparing the economic effectiveness of diverse decarbonization measures and enables transparent prioritization of low-carbon technologies across multiple sectors.

4. Biomass availability

This study assumes that cement kiln fuel is fully supplied by biomass, specifically agricultural and forestry residues. To estimate regional biomass availability, we refer to high-resolution assessments of China's biomass resources[33]. Under the scenario considering only agricultural and forestry residues (excluding energy crops), we obtain the energy potential of such resources for each province. Based on 2023 provincial cement production statistics, we estimate cement kiln fuel demand in each province and derive the maximum biomass substitution potential for the cement sector. Comparing the available biomass with the maximum substitution potential shows that the ratio exceeds 1 in all provinces except Zhejiang (0.99). Most provinces exhibit ratios between 1.5 and 5, while the three northeastern provinces (Liaoning, Jilin, Heilongjiang) and Inner Mongolia exceed 7.5, indicating abundant biomass resources in these regions. Together with our results showing lower deployment costs and higher potential for co-production systems in these areas, the co-location of rich biomass and renewable energy resources further strengthens their regional advantages.

Although this study does not account for competition for biomass from other industries, future cement demand in China is expected to decline, along with retained production capacity, potentially reducing biomass demand from the cement sector. Therefore, in our modeling, biomass availability is not imposed as a hard constraint; all cement plants are assumed to have access to biomass at a uniform cost. Future work could incorporate high-resolution biomass supply chain modeling to refine the upstream representation of co-production systems.

Table S12 Biomass availability and fuel substitution potential comparison in each province.

Province	Maximum biomass substitution potential (PJ)	Biomass potential (PJ)	Supply–demand ratio	Surplus / Gap (PJ)
Guangdong	331.1	511.2	1.54	180.1
Jiangsu	330.2	687.4	2.08	357.2
Anhui	306.4	936.1	3.06	629.7
Shandong	298.1	1293.2	4.34	995.1
Zhejiang	293.9	292.3	0.99	-1.6
Sichuan	280.9	825.5	2.94	544.5
Guangxi	231.2	1059.5	4.58	828.4
Hebei	230.8	955.4	4.14	724.6
Hubei	228.7	723.2	3.16	494.5
Yunnan	222.2	837.1	3.77	614.9
Henan	220.9	1388.9	6.29	1168.0
Jiangxi	192.9	633.5	3.28	440.6
Hunan	191.6	840.8	4.39	649.2
Fujian	185.9	518.8	2.79	333.0
Guizhou	136.0	349.5	2.57	213.5

Shaanxi	133.4	360.1	2.7	226.7
Chongqing	126.7	234.6	1.85	108.0
Xinjiang	111.2	566.0	5.09	454.7
Shanxi	107.8	350.2	3.25	242.4
Gansu	95.4	244.3	2.56	148.9
Liaoning	88.2	664.6	7.54	576.4
Inner Mongolia	86.2	758.3	8.79	672.0
Jilin	47.0	976.1	20.78	929.2
Heilongjiang	45.0	1424.8	31.69	1379.8
Ningxia	38.6	70.2	1.82	31.6
Hainan	35.7	141.6	3.96	105.9
Tibet	27.7	97.8	3.53	70.1
Qinghai	27.6	42.4	1.54	14.9
Tianjin	11.2	49.2	4.4	38.0
Shanghai	10.2	17.7	1.74	7.5
Beijing	4.6	28.6	6.19	24.0

5. ASPEN plus application

The gas compression train is modeled as a multistage compressor with interstage cooling (Mcompr, Aspen Plus module name, same below) (**Fig. S34**). We specified the discharge pressure from the last stage, and selected an equal pressure ratio between stages. Other parameters, including polytropic and mechanical efficiency, and the cooler outlet temperature and pressure drop, were adopted from [34].

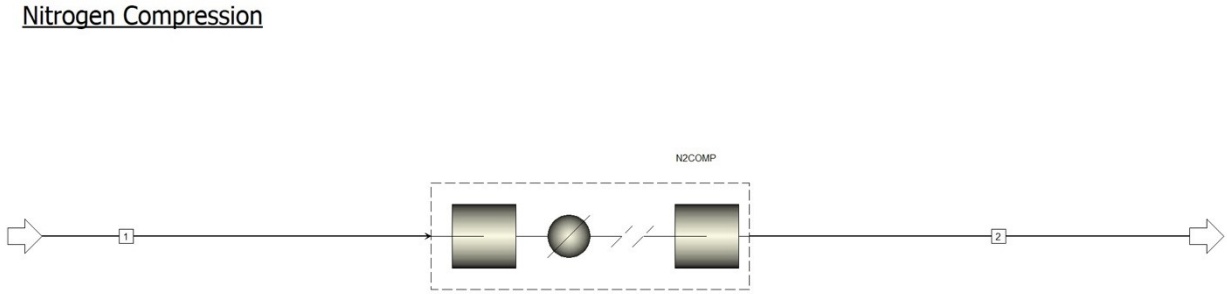

Fig. S34 Aspen Plus process flowsheet for nitrogen compression.
This flowsheet also applicable to the compression of other gases.

The liquefaction process is modeled using the flowsheet proposed by [8] (**Fig. S35**). Fresh and recycled O_2 streams are first combined, and then cooled in a cold box (MHeatX) and a precooler (HeatX). The resulting cold, gaseous O_2 stream is expanded in a flash drum (Flash2), where it is partially condensed to produce liquid O_2. The vapor leaving the flash drum flows back through the precooler and the cold box to recover cold duty, and then enters a compression train with interstage cooling (Compr and Heater) to increase its pressure so that it can be mixed with the fresh O_2 stream. The cold box is primarily chilled by a hydrocarbon refrigerant circulating in a standard cycle (i.e., compression (Compr), cooling (Heater), and expansion (Valve)).

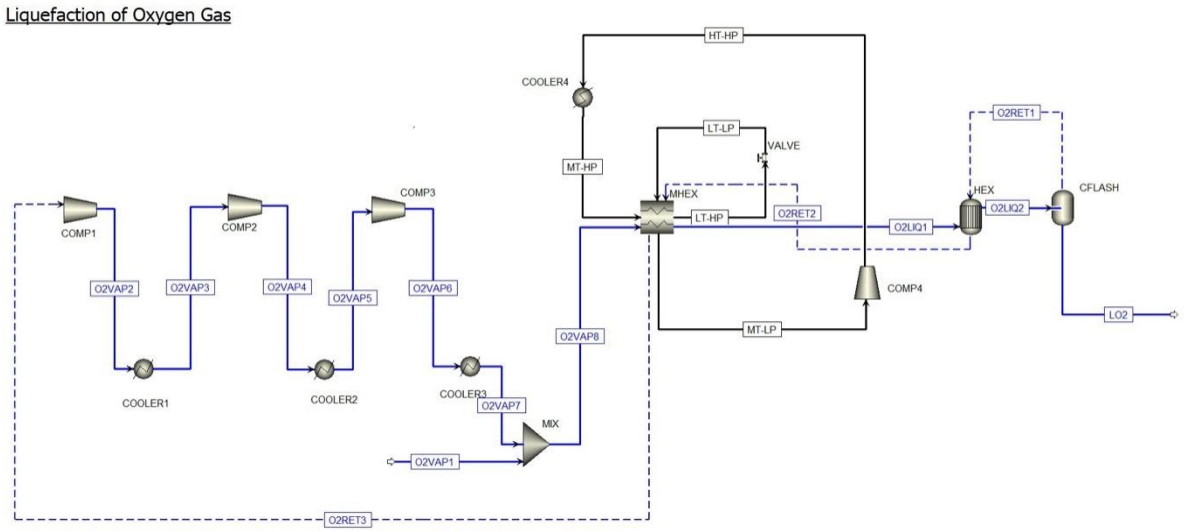

Fig. S35 Aspen Plus process flowsheet for oxygen liquefaction.

This flowsheet also applicable to the compression of other gases.

The methanol synthesis process is modeled by extending the reactor design from [35] with all necessary upstream and downstream unit operations (**Fig. S36**). Fresh and recycled syngas streams are combined, heated in a preheater (HeatX), and then sent to the vapor-phase methanol reactor (RPlug), where temperature control is achieved by steam generation. The reactor effluent flows back through the precooler to recover heat, then through a cooler (Heater) for partial condensation, and finally into a drum (Flash2) to separate raw methanol from light gases. A small fraction of the light gases is purged, and the balance is recompressed so that it can be mixed with the fresh syngas stream. The raw methanol first flows through a valve (Valve) for pressure reduction and then enters another drum (Flash2) for further phase separation. The liquid leaving the drum is pumped (Pump) and heated (Heater) to meet the inlet conditions of the distillation section, while the vapor leaving the drum is purged. The distillation section has two columns (RadFrac), where methanol is recovered in high purity from the top of the second column. The vapor leaving the top of the first column is combined with other purge streams for use in the onsite gas turbine combined cycle.

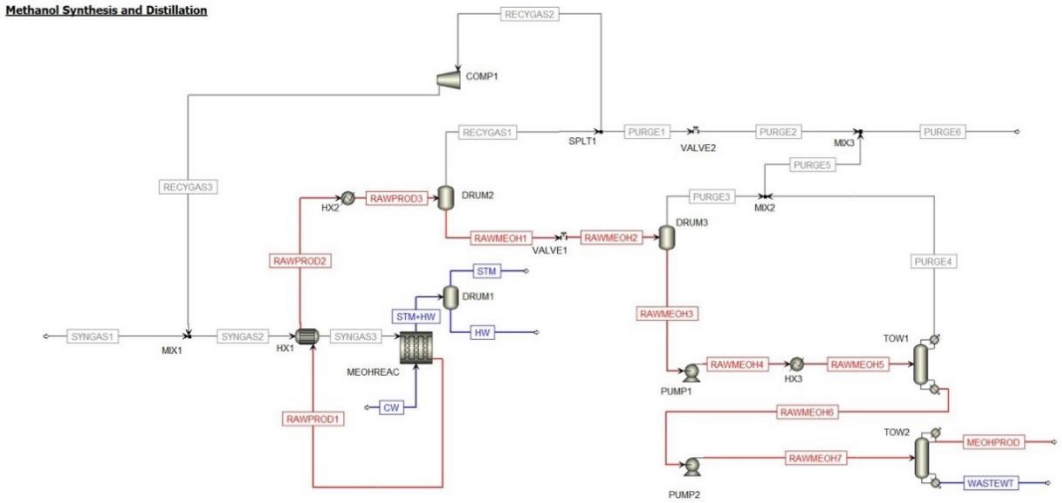

Fig. S36 Aspen Plus process flowsheet for methanol synthesis and distillation.

6. SimCCS-China introduction

SimCCS is a tool used for simulating and optimizing the performance of CCS systems. The process typically involves capturing CO_2 from industrial emissions, compressing and transporting it to suitable storage sites, and injecting it into geological formations for long-term storage.

This study uses SimCCS to obtain the CCS network and related costs around China, by optimizing the process of capturing CO_2 from cement plants, transporting captured CO_2 via pipelines, and injecting it into selected CO_2 storage sites

(1) Source estimation

For each cement plant, we first compute the annual CO_2 available for sequestration, assuming the capacity utilization factor is 80%.

$$Sequestered\ CO_2\ \ (Mt/yr) = Cement\ output\ (Mt/yr) \times CO_2\ \ sequestration\ \ factor\ (t\ CO_2\ /t\ cement)$$

- **Net-zero methanol co-production scenario:**

  From the plant optimization model, we find that when CO_2 from biomass equals to CO_2 released to the atmosphere and consumed in methanol synthesis, the sequestration factor is 0.38 t CO_2 per tonne of cement.

- **Cement-decarbonization-only scenario:**

  We increase the sequestration factor to 0.52 t CO_2 per tonne of cement, corresponding to 100 % of the capturable CO_2 being sequestered.

Next, we obtain the plant-by-plant results and convert the co-production costs (excluding CO_2 transport and sequestration costs) into equivalent CO_2 capture cost required by SimCCS inputs.

$$Eq.capture\ cost(\$/tCO_2) = co-production\ cost(\$/(t\ MeOH + xt\ cement))/stoichiometry(x)/C$$
$$(tCO_2\ /t\ cement)$$

Where x is the stoichiometric data of cement and methanol. Under the net-zero methanol scenario, x is equal to 9.76.

Table S13 Plant level information as in CO_2 source inputs in SimCCS-China.

Plant number	Capacity (Mt/yr)	Longitude	Latitude	Co-production CO_2 seq. amount (Mt/yr)	Eq. capture cost ($/t CO_2)	Cement-only CO_2 seq. amount (Mt/yr)
p1	2.7	118.4	31.2	0.8	299.0	1.1
p2	5	111.8	26.7	1.5	320.7	2.1
p3	2.8	118.9	30.7	0.8	322.7	1.2

p4	6.6	106.4	26.7	2.0	290.5	2.8
p5	3.3	116.9	30.6	1.0	302.7	1.4
p6	7	117.8	30.8	2.1	310.0	2.9
p7	4.4	118.2	32.2	1.3	282.0	1.8
p8	2.2	113.4	29.5	0.7	321.1	0.9
p9	2.8	114.7	27.9	0.8	332.9	1.2
p10	4	109.8	22.7	1.2	285.2	1.7
p11	2	119.1	29.3	0.6	330.8	0.8
p12	2.2	117.4	35.6	0.7	292.7	0.9
p13	5	112.0	27.4	1.5	316.6	2.1
p14	4.4	107.3	30.9	1.3	344.1	1.8
p15	3.2	119.0	30.8	1.0	318.4	1.3
p16	6.4	113.4	24.3	1.9	299.6	2.7
p17	6.6	112.0	22.4	2.0	290.8	2.8
p18	3.24	106.7	35.5	1.0	285.7	1.4
p19	4.4	111.2	27.8	1.3	334.7	1.8
p20	4.4	111.3	29.6	1.3	325.9	1.8
p21	4	110.7	25.6	1.2	310.9	1.7
p22	6.2	107.9	22.7	1.9	287.6	2.6
p23	2.2	107.0	34.7	0.7	302.8	0.9
p24	4.4	118.0	31.1	1.3	301.9	1.8
p25	4.86	117.4	28.6	1.5	320.3	2.0
p26	2.2	107.1	34.5	0.7	305.1	0.9
p27	1.5	105.4	25.1	0.5	295.2	0.6
p28	2.2	107.8	34.5	0.7	308.6	0.9
p29	2.2	99.3	25.1	0.7	277.1	0.9
p30	2.2	106.8	32.4	0.7	339.0	0.9
p31	4.5	117.9	31.5	1.4	289.8	1.9
p32	1.8	119.1	32.2	0.5	281.0	0.8
p33	1.6	108.0	30.2	0.5	335.3	0.7
p34	4.05	114.9	25.5	1.2	304.6	1.7
p35	4.4	105.9	32.6	1.3	332.2	1.8
p36	3.2	105.7	26.2	1.0	290.1	1.3
p37	2.2	111.7	28.2	0.7	332.0	0.9
p38	2.52	110.7	26.7	0.8	338.4	1.1
p39	2.2	111.5	25.2	0.7	307.6	0.9
p40	2.2	107.5	30.5	0.7	344.2	0.9
p41	2.2	111.9	27.7	0.7	320.4	0.9
p42	4.4	108.6	34.6	1.3	307.8	1.8
p43	2	107.7	23.1	0.6	289.8	0.8
p44	2.2	108.2	34.7	0.7	305.6	0.9
p45	2	109.0	35.0	0.6	295.9	0.8

p46	2.2	111.4	27.2	0.7	328.9	0.9
p47	2.1	105.0	26.5	0.6	288.9	0.9
p48	4.4	117.1	34.0	1.3	292.9	1.8
p49	4.4	109.1	27.5	1.3	334.0	1.8
p50	4	103.7	23.8	1.2	276.7	1.7
p51	1.44	97.8	24.5	0.4	277.9	0.6
p52	3.24	107.0	27.8	1.0	326.6	1.4
p53	1.5	116.0	28.5	0.5	301.3	0.6
p54	2.4	117.4	32.9	0.7	283.9	1.0
p55	1.5	121.4	31.0	0.5	261.1	0.6
p56	3.2	120.6	32.0	1.0	269.9	1.3
p57	4.4	119.0	33.4	1.3	281.1	1.8
p58	4.4	116.7	32.7	1.3	287.5	1.8
p59	3.3	116.3	31.7	1.0	312.6	1.4
p60	2.2	118.5	29.9	0.7	331.1	0.9
p61	3.2	121.1	31.8	1.0	261.3	1.3
p62	1.85	121.2	31.5	0.6	259.0	0.8
p63	3.8	118.5	31.8	1.1	285.5	1.6
p64	3.2	121.9	29.9	1.0	267.9	1.3
p65	4.4	121.5	29.5	1.3	291.7	1.8
p66	1.8	117.2	32.0	0.5	287.4	0.8
p67	3.2	110.3	21.3	1.0	284.4	1.3
p68	3.2	113.1	22.2	1.0	287.0	1.3
p69	4	116.0	28.8	1.2	305.0	1.7
p70	1.65	119.0	33.6	0.5	282.2	0.7
p71	4.4	121.7	29.5	1.3	283.3	1.8
p72	2.9	116.1	29.6	0.9	310.6	1.2
p73	2.2	116.4	28.3	0.7	309.3	0.9
p74	1.5	110.8	21.7	0.5	288.5	0.6
p75	4.4	119.8	32.3	1.3	276.7	1.8
p76	2	121.1	28.2	0.6	287.2	0.8
p77	7	116.3	33.5	2.1	290.7	2.9
p78	2.05	114.9	25.7	0.6	306.5	0.9
p79	2	115.4	29.9	0.6	325.0	0.8
p80	6	103.9	31.0	1.8	307.9	2.5
p81	7.2	114.5	30.7	2.2	313.1	3.0
p82	1.4	114.3	30.3	0.4	318.9	0.6
p83	2.3	114.1	30.6	0.7	310.4	1.0
p84	3	119.4	32.3	0.9	280.0	1.3
p85	1.5	114.2	36.4	0.5	291.6	0.6
p86	5	116.9	40.1	1.5	288.4	2.1
p87	5	116.0	39.6	1.5	288.8	2.1

p88	3	117.0	40.1	0.9	288.3	1.3
p89	3.5	114.6	38.8	1.1	297.1	1.5
p90	10	117.1	39.3	3.0	277.0	4.2
p91	5	115.3	40.1	1.5	279.6	2.1
p92	3	106.0	29.2	0.9	328.3	1.3
p93	1.5	107.5	34.5	0.5	307.9	0.6
p94	2.4	123.0	41.2	0.7	255.4	1.0
p95	2	108.6	34.6	0.6	308.1	0.8
p96	5	113.1	35.2	1.5	301.8	2.1
p97	1.5	118.8	39.8	0.5	281.9	0.6
p98	1.5	118.3	40.8	0.5	279.3	0.6
p99	2	113.6	36.5	0.6	291.0	0.8
p100	2	114.2	38.2	0.6	301.0	0.8
p101	2	112.2	41.0	0.6	265.4	0.8
p102	2.5	106.2	29.7	0.8	330.0	1.0
p103	2	106.4	30.0	0.6	333.8	0.8
p104	3.19	127.1	45.4	1.0	267.0	1.3
p105	1.8	126.2	42.9	0.5	265.3	0.8
p106	2	126.3	43.5	0.6	265.3	0.8
p107	3	111.3	35.4	0.9	305.4	1.3
p108	5	114.5	37.4	1.5	298.0	2.1
p109	2	115.6	39.4	0.6	293.6	0.8
p110	4	111.6	38.2	1.2	282.4	1.7
p111	5	114.3	38.4	1.5	302.1	2.1
p112	3	111.5	29.7	0.9	319.7	1.3
p113	3	112.7	37.9	0.9	288.3	1.3
p114	1.8	114.8	38.9	0.5	297.7	0.8
p115	1.5	118.2	39.9	0.5	287.6	0.6
p116	1.65	118.5	39.8	0.5	284.2	0.7
p117	2	110.7	37.5	0.6	288.6	0.8
p118	1.5	115.0	40.8	0.5	267.9	0.6
p119	3	113.7	37.9	0.9	281.5	1.3
p120	1.5	113.4	37.0	0.5	288.8	0.6
p121	3	111.6	40.7	0.9	277.8	1.3
p122	1.6	123.4	41.6	0.5	257.6	0.7
p123	8	115.6	38.0	2.4	286.5	3.3
p124	3	118.2	40.0	0.9	287.9	1.3
p125	1.5	115.1	40.6	0.5	274.6	0.6
p126	2.5	112.4	31.7	0.8	309.4	1.0
p127	4	113.8	29.9	1.2	321.6	1.7
p128	2	111.6	30.9	0.6	315.9	0.8
p129	10	111.7	32.5	3.0	317.7	4.2

p130	3	111.3	29.6	0.9	325.3	1.3
p131	1.5	111.5	30.1	0.5	321.2	0.6
p132	3	110.7	31.2	0.9	318.9	1.3
p133	5	112.3	31.3	1.5	306.3	2.1
p134	2	113.9	30.7	0.6	307.3	0.8
p135	2.555	114.1	36.1	0.8	289.2	1.1
p136	2	119.3	29.3	0.6	333.0	0.8
p137	1.5	117.9	35.0	0.5	294.0	0.6
p138	3	116.2	37.5	0.9	281.0	1.3
p139	5	118.3	32.2	1.5	281.8	2.1
p140	3	111.6	29.1	0.9	320.1	1.3
p141	2	113.3	28.2	0.6	334.0	0.8
p142	2.5	117.5	34.9	0.8	293.4	1.0
p143	1.5	117.6	35.4	0.5	293.7	0.6
p144	6	113.2	34.0	1.8	299.2	2.5
p145	4	118.5	29.0	1.2	319.4	1.7
p146	2.5	110.8	24.9	0.8	298.8	1.0
p147	3.2	112.8	26.3	1.0	327.4	1.3
p148	2.5	117.0	35.2	0.8	293.4	1.0
p149	3	113.0	25.6	0.9	327.3	1.3
p150	3.5	118.3	28.7	1.1	321.5	1.5
p151	1.5	119.6	31.4	0.5	290.3	0.6
p152	6	114.5	37.3	1.8	297.3	2.5
p153	2	113.1	41.7	0.6	235.3	0.8
p154	5	113.1	34.4	1.5	303.1	2.1
p155	2.9	111.5	33.1	0.9	318.8	1.2
p156	1.5	119.6	31.3	0.5	290.4	0.6
p157	1.5	112.1	26.8	0.5	318.4	0.6
p158	4	119.8	31.1	1.2	295.2	1.7
p159	9	119.9	30.9	2.7	297.0	3.8
p160	9	116.4	36.0	2.7	287.9	3.8
p161	1.7	119.7	29.8	0.5	334.3	0.7
p162	4.38	118.4	36.8	1.3	281.8	1.8
p163	1.5	119.6	31.0	0.5	300.1	0.6
p164	3.6	119.7	31.1	1.1	296.7	1.5
p165	1.5	118.8	35.7	0.5	283.2	0.6
p166	5	119.3	31.4	1.5	293.0	2.1
p167	2	114.9	26.8	0.6	319.2	0.8
p168	2	112.0	23.1	0.6	294.6	0.8
p169	3	113.8	27.7	0.9	343.1	1.3
p170	1.5	112.0	23.0	0.5	294.5	0.6
p171	5	117.8	31.5	1.5	290.7	2.1

p172	2	113.2	28.0	0.6	330.8	0.8
p173	2	112.8	28.0	0.6	322.2	0.8
p174	5	119.7	30.7	1.5	314.1	2.1
p175	8	114.1	36.2	2.4	290.1	3.3
p176	7	117.2	32.8	2.1	284.7	2.9
p177	2.7	119.7	31.1	0.8	295.4	1.1
p178	1.65	120.1	30.6	0.5	308.6	0.7
p179	7	119.8	29.9	2.1	333.5	2.9
p180	1.5	119.7	29.9	0.5	334.1	0.6
p181	2	119.6	31.1	0.6	299.5	0.8
p182	5	109.4	22.7	1.5	281.7	2.1
p183	2	117.3	34.4	0.6	295.6	0.8
p184	2.19	115.9	25.8	0.7	308.9	0.9
p185	3	113.3	26.6	0.9	330.9	1.3
p186	2	109.9	28.7	0.6	340.5	0.8
p187	4.5	113.0	26.8	1.4	324.3	1.9
p188	3	112.7	28.2	0.9	319.6	1.3
p189	10	112.2	27.7	3.0	317.4	4.2
p190	6	119.7	31.1	1.8	295.6	2.5
p191	5	120.0	30.9	1.5	295.7	2.1
p192	5	119.8	31.0	1.5	295.3	2.1
p193	3	119.8	31.2	0.9	290.2	1.3
p194	3	119.8	31.2	0.9	290.3	1.3
p195	10	114.7	27.4	3.0	335.8	4.2
p196	4	115.7	28.2	1.2	307.1	1.7
p197	3	114.7	27.4	0.9	336.3	1.3
p198	3	118.3	28.7	0.9	321.6	1.3
p199	8	116.7	27.4	2.4	331.9	3.3
p200	3	113.7	27.7	0.9	342.3	1.3
p201	3	114.6	28.2	0.9	336.7	1.3
p202	1.5	117.3	35.6	0.5	292.4	0.6
p203	2	114.5	37.5	0.6	297.7	0.8
p204	1.4	112.4	34.2	0.4	307.3	0.6
p205	3	119.0	32.0	0.9	282.2	1.3
p206	2.19	109.0	19.2	0.7	286.7	0.9
p207	1.5	111.5	27.1	0.5	325.7	0.6
p208	2	111.8	23.1	0.6	295.3	0.8
p209	2	111.7	22.7	0.6	292.9	0.8
p210	4	117.3	35.0	1.2	293.6	1.7
p211	4	120.7	42.9	1.2	239.3	1.7
p212	3	106.8	39.4	0.9	265.8	1.3
p213	2.3	106.8	39.4	0.7	264.2	1.0

p214	4	121.1	37.5	1.2	267.8	1.7
p215	3	118.3	35.7	0.9	290.3	1.3
p216	3	120.3	30.1	0.9	316.6	1.3
p217	1.6	118.5	28.9	0.5	320.2	0.7
p218	7	119.6	29.2	2.1	333.3	2.9
p219	1.5	120.3	30.1	0.5	315.5	0.6
p220	4	115.9	34.9	1.2	293.0	1.7
p221	2.6	120.2	30.6	0.8	303.5	1.1
p222	3	120.7	30.5	0.9	284.9	1.3
p223	1.5	116.9	33.5	0.5	289.0	0.6
p224	2.5	116.8	33.7	0.8	291.3	1.0
p225	3	113.0	29.2	0.9	316.4	1.3
p226	2	119.3	29.3	0.6	332.7	0.8
p227	5	119.2	29.4	1.5	332.5	2.1
p228	2	117.1	28.3	0.6	329.7	0.8
p229	4	115.3	27.5	1.2	318.9	1.7
p230	8	115.9	28.6	2.4	301.9	3.3
p231	3	114.6	29.2	0.9	335.6	1.3
p232	2.5	120.8	30.8	0.8	274.2	1.0
p233	3	120.9	30.8	0.9	274.5	1.3
p234	1.5	120.6	30.7	0.5	280.8	0.6
p235	2	119.2	29.2	0.6	332.5	0.8
p236	3	112.5	34.8	0.9	308.5	1.3
p237	8	121.1	30.8	2.4	268.8	3.3
p238	3	119.6	35.4	0.9	279.9	1.3
p239	2	121.2	30.9	0.6	264.4	0.8
p240	3	117.9	33.4	0.9	285.8	1.3
p241	3	117.0	33.8	0.9	291.8	1.3
p242	6	117.2	34.9	1.8	294.8	2.5
p243	8	120.4	30.5	2.4	294.5	3.3
p244	10	117.9	33.2	3.0	284.5	4.2
p245	10	120.6	31.0	3.0	274.2	4.2
p246	2	119.6	34.2	0.6	282.8	0.8
p247	1.5	113.4	33.6	0.5	298.5	0.6
p248	1.5	117.7	34.3	0.5	294.0	0.6
p249	1.5	120.9	30.5	0.5	279.5	0.6
p250	1.5	120.3	29.8	0.5	323.5	0.6
p251	10	117.0	24.8	3.0	299.8	4.2
p252	2.5	109.6	22.9	0.8	285.8	1.0
p253	2	106.8	23.7	0.6	293.7	0.8
p254	2	110.5	23.5	0.6	297.1	0.8
p255	4	107.9	22.2	1.2	292.2	1.7

p256	2	109.7	23.5	0.6	293.3	0.8
p257	1.5	109.6	21.7	0.5	282.2	0.6
p258	9	113.1	36.3	2.7	285.2	3.8
p259	3	111.0	37.5	0.9	291.1	1.3
p260	1.5	109.2	23.2	0.5	283.7	0.6
p261	5	114.4	23.6	1.5	294.8	2.1
p262	3	110.2	22.6	0.9	286.2	1.3
p263	5	100.5	25.3	1.5	271.7	2.1
p264	2	100.2	26.7	0.6	269.2	0.8
p265	6	106.6	27.5	1.8	319.9	2.5
p266	1.5	110.3	21.4	0.5	285.2	0.6
p267	1.5	113.6	22.9	0.5	289.7	0.6
p268	3	118.8	25.0	0.9	258.0	1.3
p269	3	109.5	18.9	0.9	295.7	1.3
p270	2.5	108.5	21.8	0.8	284.3	1.0
p271	10	112.3	33.4	3.0	313.2	4.2
p272	3	114.6	31.9	0.9	300.2	1.3
p273	8	123.3	41.3	2.4	257.4	3.3
p274	1.5	121.4	39.6	0.5	259.8	0.6
p275	7	112.9	33.9	2.1	303.2	2.9
p276	3.5	117.0	34.1	1.1	294.2	1.5
p277	6	122.7	40.8	1.8	254.4	2.5
p278	7	123.4	41.3	2.1	258.0	2.9
p279	6	112.6	34.3	1.8	306.7	2.5
p280	1.5	113.2	34.4	0.5	301.0	0.6
p281	2	123.3	41.4	0.6	257.5	0.8
p282	3	122.2	41.2	0.9	250.3	1.3
p283	1.5	113.2	33.7	0.5	298.9	0.6
p284	2	123.4	41.6	0.6	257.6	0.8
p285	2	117.4	38.6	0.6	274.0	0.8
p286	3	112.6	33.3	0.9	309.1	1.3
p287	3	113.9	34.0	0.9	292.3	1.3
p288	3	113.7	34.1	0.9	292.1	1.3
p289	4.5	122.2	40.3	1.4	257.5	1.9
p290	1.5	113.8	34.7	0.5	293.0	0.6
p291	2	112.9	33.8	0.6	303.1	0.8
p292	4	114.6	33.6	1.2	293.3	1.7
p293	2	120.1	29.9	0.6	327.9	0.8
p294	5	117.8	30.8	1.5	310.8	2.1
p295	3	82.1	44.8	0.9	299.8	1.3
p296	4	117.0	30.6	1.2	303.3	1.7
p297	8	84.8	44.4	2.4	310.7	3.3

p298	2	119.9	33.0	0.6	276.2	0.8
p299	3	116.1	29.7	0.9	309.0	1.3
p300	3	121.4	28.7	0.9	292.4	1.3
p301	3	116.3	32.6	0.9	290.0	1.3
p302	7.5	114.3	23.7	2.3	294.6	3.1
p303	2	116.2	24.9	0.6	301.4	0.8
p304	2	116.1	24.6	0.6	299.3	0.8
p305	3	119.7	29.8	0.9	334.2	1.3
p306	3	119.2	29.4	0.9	332.0	1.3
p307	1.5	115.5	28.2	0.5	311.6	0.6
p308	2	106.8	30.2	0.6	343.2	0.8
p309	2.5	117.4	25.4	0.8	301.3	1.0
p310	3.5	117.7	25.8	1.1	304.4	1.5
p311	10	119.2	29.2	3.0	331.6	4.2
p312	3	106.9	26.5	0.9	297.5	1.3
p313	2.5	104.8	28.4	0.8	325.4	1.0
p314	5	107.3	22.4	1.5	292.6	2.1
p315	2	108.9	27.4	0.6	333.3	0.8
p316	2.5	113.1	27.1	0.8	326.6	1.0
p317	4	108.2	23.1	1.2	285.2	1.7
p318	2	99.3	25.4	0.6	276.5	0.8
p319	4.5	111.9	25.6	1.4	315.2	1.9
p320	2.19	111.5	26.6	0.7	333.2	0.9
p321	5	119.5	29.2	1.5	333.5	2.1
p322	1.5	116.3	28.0	0.5	312.7	0.6
p323	1.5	115.1	27.1	0.5	316.2	0.6
p324	2	120.1	28.7	0.6	331.8	0.8
p325	6	119.5	29.2	1.8	333.5	2.5
p326	1.5	118.5	25.0	0.5	277.1	0.6
p327	4	117.6	24.7	1.2	296.9	1.7
p328	2	114.0	31.9	0.6	300.4	0.8
p329	3.8	115.4	29.9	1.1	324.8	1.6
p330	2.2	107.4	29.6	0.7	335.5	0.9
p331	3.53	115.3	30.1	1.1	324.8	1.5
p332	1.6	114.0	29.7	0.5	326.0	0.7
p333	1.4	106.4	29.9	0.4	333.3	0.6
p334	2.6	111.2	30.5	0.8	320.9	1.1
p335	1.62	111.4	27.6	0.5	333.3	0.7
p336	2.2	112.9	25.7	0.7	329.2	0.9
p337	1.44	107.1	30.8	0.4	344.1	0.6
p338	1.7	111.9	31.8	0.5	310.6	0.7
p339	3.5	111.5	30.3	1.1	321.5	1.5

p340	1.5	103.8	27.4	0.5	281.8	0.6
p341	2.1	113.1	27.6	0.6	322.0	0.9
p342	1.8	110.7	30.9	0.5	321.8	0.8
p343	2	111.4	25.6	0.6	314.7	0.8
p344	2.48	114.9	30.2	0.7	324.8	1.0
p345	1.8	112.4	22.0	0.5	289.4	0.8
p346	2	102.5	25.2	0.6	271.5	0.8
p347	2	110.8	32.8	0.6	321.2	0.8
p348	1.4	102.9	25.1	0.4	269.4	0.6
p349	1.4	113.2	29.5	0.4	316.7	0.6
p350	1.9	114.4	30.6	0.6	312.2	0.8
p351	2	119.9	49.3	0.6	265.0	0.8
p352	5	126.0	43.2	1.5	262.8	2.1
p353	4	126.7	45.8	1.2	264.8	1.7
p354	5	125.9	43.3	1.5	259.0	2.1
p355	2	126.2	41.8	0.6	280.0	0.8
p356	2	126.6	43.9	0.6	268.8	0.8
p357	3.2	129.7	43.0	1.0	277.5	1.3
p358	10	123.1	41.6	3.0	256.5	4.2
p359	4	103.7	31.0	1.2	303.6	1.7
p360	2	105.1	32.0	0.6	324.3	0.8
p361	5	105.9	37.9	1.5	265.7	2.1
p362	3.4	105.7	37.4	1.0	256.9	1.4
p363	2	106.0	38.5	0.6	275.5	0.8
p364	1.5	104.1	36.6	0.5	274.4	0.6
p365	5	105.4	34.6	1.5	288.3	2.1
p366	2.5	106.3	39.0	0.8	274.2	1.0
p367	2	120.0	41.4	0.6	247.3	0.8
p368	5	116.9	36.6	1.5	286.0	2.1
p369	8	119.0	36.7	2.4	279.3	3.3
p370	4	116.9	36.6	1.2	286.3	1.7
p371	2.5	116.4	35.4	0.8	292.5	1.0
p372	1.5	120.8	37.7	0.5	268.7	0.6
p373	4.5	121.6	39.5	1.4	262.2	1.9
p374	10	123.3	41.2	3.0	257.9	4.2
p375	4	117.6	34.5	1.2	295.0	1.7
p376	2.5	117.8	36.6	0.8	283.3	1.0
p377	4	120.1	43.9	1.2	247.7	1.7
p378	2	126.6	42.0	0.6	277.9	0.8
p379	2.5	113.9	35.5	0.8	293.0	1.0
p380	2	118.4	36.4	0.6	282.7	0.8
p381	1.5	111.0	37.6	0.5	291.0	0.6

p382	2.5	121.0	37.4	0.8	268.8	1.0
p383	1.5	112.7	38.2	0.5	286.9	0.6
p384	1.5	116.7	35.1	0.5	294.1	0.6
p385	3	113.1	36.8	0.9	288.6	1.3
p386	1.5	118.7	43.6	0.5	247.1	0.6
p387	3	118.0	37.5	0.9	277.0	1.3
p388	2	115.6	35.0	0.6	291.7	0.8
p389	4	118.4	37.0	1.2	281.8	1.7
p390	5	116.0	35.4	1.5	292.1	2.1
p391	2	118.4	37.5	0.6	274.9	0.8
p392	1.5	121.4	45.0	0.5	247.3	0.6
p393	6	122.0	41.1	1.8	249.7	2.5
p394	1.8	120.0	36.7	0.5	281.5	0.8
p395	2	121.5	37.0	0.6	268.5	0.8
p396	2	120.4	36.3	0.6	282.0	0.8
p397	3	115.5	36.0	0.9	287.3	1.3
p398	1.5	123.6	41.5	0.5	258.6	0.6
p399	10	117.4	38.9	3.0	273.3	4.2
p400	3	122.2	43.7	0.9	246.2	1.3
p401	2	119.0	37.1	0.6	277.1	0.8
p402	3	122.1	37.3	0.9	261.6	1.3
p403	8	122.1	46.1	2.4	249.1	3.3
p404	2.5	118.6	35.7	0.8	286.2	1.0
p405	2.5	110.0	38.4	0.8	272.0	1.0
p406	2.5	121.0	41.0	0.8	247.6	1.0
p407	3	118.9	36.7	0.9	278.9	1.3
p408	2	116.2	37.4	0.6	281.4	0.8
p409	4.5	115.8	36.5	1.4	284.0	1.9
p410	1.5	120.5	36.8	0.5	279.1	0.6
p411	4	103.5	29.5	1.2	312.3	1.7
p412	1.5	103.5	29.5	0.5	312.5	0.6
p413	3.5	87.6	43.7	1.1	297.4	1.5
p414	3	110.1	27.6	0.9	340.0	1.3
p415	3	119.3	32.2	0.9	280.6	1.3
p416	4	105.6	26.0	1.2	294.4	1.7
p417	2	106.3	26.4	0.6	281.2	0.8
p418	6	106.9	30.5	1.8	343.0	2.5
p419	1.5	106.7	30.2	0.5	339.0	0.6
p420	2	109.6	26.5	0.6	323.0	0.8
p421	2	123.5	41.3	0.6	258.7	0.8
p422	2	105.4	28.8	0.6	325.6	0.8
p423	5	119.0	36.0	1.5	281.4	2.1

p424	10	109.3	32.8	3.0	316.0	4.2
p425	9	109.3	34.1	2.7	309.1	3.8
p426	2.5	107.8	32.9	0.8	317.5	1.0
p427	5	80.2	37.0	1.5	278.0	2.1
p428	4	106.6	26.4	1.2	289.3	1.7
p429	10	109.0	34.8	3.0	304.0	4.2
p430	8	109.2	34.9	2.4	299.3	3.3
p431	2.5	109.0	34.9	0.8	298.6	1.0
p432	3	109.2	33.4	0.9	312.8	1.3
p433	5	81.9	36.8	1.5	272.8	2.1
p434	3	109.6	35.1	0.9	300.0	1.3
p435	9	118.5	28.9	2.7	320.0	3.8
p436	4	118.3	28.7	1.2	321.5	1.7
p437	4	119.6	31.0	1.2	301.3	1.7
p438	2.5	117.9	31.7	0.8	288.2	1.0
p439	1.5	113.3	28.1	0.5	335.3	0.6
p440	3	104.4	31.6	0.9	313.6	1.3
p441	3.5	103.8	31.0	1.1	308.9	1.5
p442	2	117.2	35.9	0.6	291.0	0.8
p443	2.5	119.2	29.4	0.8	332.6	1.0
p444	3	114.9	28.2	0.9	329.2	1.3
p445	1.5	125.3	42.8	0.5	253.6	0.6
p446	5	117.3	29.1	1.5	307.2	2.1
p447	5	113.1	23.3	1.5	290.3	2.1
p448	3	106.6	30.1	0.9	337.6	1.3
p449	7	106.3	30.0	2.1	332.7	2.9
p450	3	106.9	28.9	0.9	343.1	1.3
p451	1.5	108.4	30.7	0.5	337.8	0.6
p452	2.5	108.8	29.4	0.8	337.9	1.0
p453	5	107.0	29.8	1.5	339.5	2.1
p454	6	106.4	29.3	1.8	333.2	2.5
p455	3	109.1	28.4	0.9	339.8	1.3
p456	3	106.4	29.4	0.9	333.1	1.3
p457	6	107.2	29.2	1.8	337.9	2.5
p458	4	117.3	32.8	1.2	283.8	1.7
p459	2	121.7	39.3	0.6	263.3	0.8
p460	3	122.1	39.6	0.9	263.5	1.3
p461	3	107.3	30.8	0.9	343.8	1.3
p462	2	112.9	34.3	0.6	304.6	0.8
p463	3	120.7	31.0	0.9	272.2	1.3
p464	4	117.3	26.0	1.2	309.5	1.7
p465	2	117.8	26.8	0.6	319.9	0.8

p466	5	117.5	26.8	1.5	322.5	2.1
p467	4	117.1	25.1	1.2	301.6	1.7
p468	5	117.2	25.2	1.5	301.9	2.1
p469	3	107.1	23.5	0.9	292.9	1.3
p470	2	109.3	24.4	0.6	282.1	0.8
p471	2	106.4	26.6	0.6	289.0	0.8
p472	1.5	114.3	38.1	0.5	302.6	0.6
p473	6	114.2	38.2	1.8	301.2	2.5
p474	3	129.6	46.7	0.9	279.0	1.3
p475	10	113.9	35.4	3.0	293.7	4.2
p476	2	112.2	34.5	0.6	307.1	0.8
p477	5	114.2	35.9	1.5	288.1	2.1
p478	1.5	113.9	35.4	0.5	293.0	0.6
p479	5	114.0	32.8	1.5	297.2	2.1
p480	4.5	113.3	35.3	1.4	298.9	1.9
p481	5	116.8	34.0	1.5	292.8	2.1
p482	2.6	114.9	30.0	0.8	328.1	1.1
p483	1.5	113.0	30.9	0.5	304.8	0.6
p484	4	110.2	27.9	1.2	338.0	1.7
p485	1.8	112.3	28.3	0.5	321.0	0.8
p486	10	107.0	39.4	3.0	262.0	4.2
p487	2	117.5	26.7	0.6	320.6	0.8
p488	1.5	119.3	31.4	0.5	292.2	0.6
p489	1.5	120.4	32.8	0.5	271.7	0.6
p490	5	117.1	28.7	1.5	311.7	2.1
p491	1.8	115.9	25.8	0.5	308.9	0.8
p492	10	113.3	35.3	3.0	298.6	4.2
p493	6	112.6	39.4	1.8	274.4	2.5
p494	10	119.6	29.1	3.0	333.4	4.2
p495	7	115.9	29.6	2.1	317.3	2.9
p496	2.1	119.6	29.2	0.6	333.4	0.9
p497	5	130.8	46.2	1.5	264.5	2.1
p498	5	99.1	24.9	1.5	276.7	2.1
p499	1.8	102.4	24.9	0.5	270.6	0.8
p500	4	102.6	24.8	1.2	271.3	1.7
p501	2.2	106.9	27.5	0.7	321.8	0.9
p502	3	104.7	28.4	0.9	322.2	1.3
p503	1.5	124.1	41.9	0.5	260.2	0.6
p504	7.5	123.7	42.1	2.3	257.3	3.1
p505	3	119.6	31.5	0.9	285.1	1.3
p506	8	104.9	33.4	2.4	291.2	3.3
p507	2	103.4	23.3	0.6	282.6	0.8

p508	2	129.5	44.4	0.6	272.2	0.8
p509	1.5	105.6	37.4	0.5	256.9	0.6
p510	5	119.4	31.7	1.5	285.0	2.1
p511	2	114.2	38.2	0.6	300.8	0.8
p512	1.8	123.5	41.4	0.5	258.9	0.8
p513	8	101.7	36.9	2.4	268.4	3.3
p514	10	104.4	29.5	3.0	309.3	4.2
p515	3	107.0	27.6	0.9	324.0	1.3
p516	5	112.9	23.4	1.5	292.1	2.1
p517	4	107.8	34.2	1.2	306.6	1.7
p518	3	118.1	36.8	0.9	283.0	1.3
p519	2	117.5	34.5	0.6	295.3	0.8
p520	1.5	117.6	34.5	0.5	294.9	0.6
p521	3	109.5	35.1	0.9	298.0	1.3
p522	1.5	110.3	33.9	0.5	308.8	0.6
p523	2	104.8	29.7	0.6	311.0	0.8
p524	2	106.9	30.5	0.6	342.9	0.8
p525	4	103.9	29.2	1.2	315.7	1.7
p526	3	106.8	30.1	0.9	341.6	1.3
p527	1.5	107.6	26.6	0.5	317.7	0.6
p528	2	104.5	31.3	0.6	313.2	0.8
p529	2.5	112.8	23.2	0.8	291.8	1.0
p530	3	93.4	42.7	0.9	287.0	1.3
p531	2	106.8	35.5	0.6	285.9	0.8
p532	3.5	87.7	43.9	1.1	303.0	1.5
p533	2	119.2	31.5	0.6	288.8	0.8
p534	4	101.6	36.4	1.2	267.5	1.7
p535	5	119.6	31.5	1.5	285.5	2.1
p536	3	111.5	30.1	0.9	321.8	1.3
p537	3	108.9	19.2	0.9	285.7	1.3
p538	6	118.9	36.0	1.8	281.3	2.5
p539	1.5	112.4	37.9	0.5	288.6	0.6
p540	3.5	112.7	37.8	1.1	288.0	1.5
p541	3	114.0	35.4	0.9	292.4	1.3
p542	6	106.9	39.6	1.8	260.9	2.5
p543	4	118.0	31.1	1.2	300.6	1.7
p544	3	113.2	31.0	0.9	303.5	1.3
p545	4	104.1	26.2	1.2	277.8	1.7
p546	3	100.6	26.3	0.9	268.3	1.3
p547	2.5	120.2	29.8	0.8	327.8	1.0
p548	2	115.8	26.4	0.6	311.8	0.8
p549	1.5	118.5	28.7	0.5	322.3	0.6

p550	2.5	116.9	26.3	0.8	313.9	1.0
p551	5	119.5	29.2	1.5	333.6	2.1
p552	2	119.7	30.0	0.6	335.0	0.8
p553	8	118.0	36.6	2.4	283.8	3.3
p554	5	100.3	25.7	1.5	269.8	2.1
p555	3.5	117.9	31.5	1.1	290.7	1.5
p556	2.5	106.0	37.9	0.8	266.8	1.0
p557	2.5	106.9	30.5	0.8	343.0	1.0
p558	9	109.3	19.4	2.7	288.7	3.8
p559	3	111.6	22.1	0.9	289.9	1.3
p560	3	109.3	22.7	0.9	281.1	1.3
p561	6	110.4	22.8	1.8	288.3	2.5
p562	1.5	110.4	22.8	0.5	288.2	0.6
p563	3	110.5	23.5	0.9	297.2	1.3
p564	2	104.4	23.5	0.6	277.8	0.8
p565	8	114.2	23.6	2.4	294.5	3.3
p566	4	102.9	23.6	1.2	280.0	1.7
p567	2	114.4	23.6	0.6	294.8	0.8
p568	3	108.9	23.7	0.9	284.5	1.3
p569	2	102.9	24.2	0.6	277.1	0.8
p570	3	102.5	24.4	0.9	275.0	1.3
p571	3	109.7	24.4	0.9	285.9	1.3
p572	7.2	113.7	24.5	2.2	302.5	3.0
p573	6	102.2	24.7	1.8	274.4	2.5
p574	5	117.1	24.9	1.5	300.7	2.1
p575	3	117.1	25.0	0.9	301.0	1.3
p576	3	105.8	25.0	0.9	302.3	1.3
p577	3	103.2	25.0	0.9	268.0	1.3
p578	4	109.2	25.1	1.2	295.6	1.7
p579	6	104.9	25.3	1.8	284.2	2.5
p580	2	114.4	25.3	0.6	308.3	0.8
p581	3.5	98.5	25.4	1.1	280.0	1.5
p582	9	118.0	25.4	2.7	300.8	3.8
p583	5	113.0	25.5	1.5	324.8	2.1
p584	2	118.0	25.5	0.6	301.9	0.8
p585	9	113.0	25.6	2.7	328.4	3.8
p586	3	104.6	25.8	0.9	281.5	1.3
p587	2	104.6	26.0	0.6	282.3	0.8
p588	10	117.3	26.0	3.0	309.1	4.2
p589	2.5	117.3	26.0	0.8	309.4	1.0
p590	10	105.7	26.2	3.0	288.9	4.2
p591	4	105.0	26.5	1.2	289.2	1.7

p592	3	108.0	26.6	0.9	322.5	1.3
p593	2.5	101.5	26.6	0.8	270.5	1.0
p594	2	114.9	26.8	0.6	318.8	0.8
p595	1.8	106.7	26.9	0.5	305.1	0.8
p596	3	106.1	27.0	0.9	295.8	1.3
p597	2.5	102.2	27.1	0.8	275.2	1.0
p598	2	113.9	27.1	0.6	340.2	0.8
p599	1.8	105.6	27.2	0.5	293.3	0.8
p600	1.5	103.6	27.2	0.5	278.2	0.6
p601	1.5	105.3	27.2	0.5	293.4	0.6
p602	4	113.4	27.2	1.2	336.4	1.7
p603	2	105.4	27.2	0.6	294.1	0.8
p604	2	106.8	27.3	0.6	315.9	0.8
p605	8	103.8	27.4	2.4	281.5	3.3
p606	5	106.8	27.4	1.5	319.8	2.1
p607	1.5	109.1	27.7	0.5	336.1	0.6
p608	3.5	110.4	27.9	1.1	338.2	1.5
p609	5	99.7	27.9	1.5	265.7	2.1
p610	2.5	107.0	27.9	0.8	331.1	1.0
p611	6	103.9	27.9	1.8	292.3	2.5
p612	6	105.8	28.0	1.8	318.0	2.5
p613	2	109.6	28.2	0.6	338.6	0.8
p614	4	105.2	28.3	1.2	323.9	1.7
p615	1.8	118.6	28.7	0.5	322.3	0.8
p616	2	105.2	28.9	0.6	326.1	0.8
p617	5	106.9	29.0	1.5	344.0	2.1
p618	4	119.6	29.1	1.2	333.3	1.7
p619	8	119.1	29.2	2.4	331.2	3.3
p620	10	103.3	29.3	3.0	305.7	4.2
p621	3	118.9	29.3	0.9	329.1	1.3
p622	5	105.7	29.3	1.5	324.2	2.1
p623	6	102.6	29.4	1.8	283.5	2.5
p624	4	108.7	29.5	1.2	337.6	1.7
p625	6	109.4	29.5	1.8	340.6	2.5
p626	5	114.0	29.6	1.5	328.9	2.1
p627	1.5	120.2	29.8	0.5	327.3	0.6
p628	4	104.6	29.8	1.2	310.5	1.7
p629	2	104.6	29.8	0.6	310.5	0.8
p630	2	107.6	29.8	0.6	335.7	0.8
p631	1.5	106.1	29.8	0.5	329.1	0.6
p632	2	120.1	29.9	0.6	327.8	0.8
p633	4	102.8	30.0	1.2	294.6	1.7

p634	1.5	102.8	30.0	0.5	295.5	0.6
p635	2.5	108.1	30.1	0.8	332.0	1.0
p636	3	102.0	30.1	0.9	270.8	1.3
p637	6	114.8	30.2	1.8	325.3	2.5
p638	2.5	115.1	30.2	0.8	325.8	1.0
p639	6	119.8	30.2	1.8	330.2	2.5
p640	2	109.5	30.2	0.6	328.1	0.8
p641	4	106.7	30.2	1.2	340.1	1.7
p642	5	114.9	30.3	1.5	323.8	2.1
p643	5	117.5	30.5	1.5	314.7	2.1
p644	5	103.5	30.5	1.5	306.1	2.1
p645	5	118.9	30.7	1.5	323.3	2.1
p646	2	117.7	30.9	0.6	309.5	0.8
p647	3	107.4	30.9	0.9	344.2	1.3
p648	2	104.2	31.0	0.6	307.0	0.8
p649	1.5	118.0	31.1	0.5	301.4	0.6
p650	3	119.3	31.4	0.9	292.9	1.3
p651	4	104.2	31.4	1.2	309.2	1.7
p652	3.5	117.9	31.5	1.1	289.9	1.5
p653	1.5	117.8	31.6	0.5	288.9	0.6
p654	10	104.4	31.7	3.0	313.4	4.2
p655	8	118.3	32.0	2.4	282.6	3.3
p656	6	118.4	32.0	1.8	281.9	2.5
p657	2.5	119.3	32.1	0.8	280.7	1.0
p658	5	106.5	32.2	1.5	334.3	2.1
p659	3	106.1	32.3	0.9	334.8	1.3
p660	8	105.6	32.3	2.4	332.4	3.3
p661	6	109.4	32.3	1.8	314.9	2.5
p662	2	105.6	32.5	0.6	336.1	0.8
p663	6	104.5	33.0	1.8	286.7	2.5
p664	2	113.0	33.9	0.6	301.7	0.8
p665	1.5	107.7	34.2	0.5	306.2	0.6
p666	2	107.6	34.3	0.6	307.0	0.8
p667	3	113.2	34.3	0.9	301.5	1.3
p668	2	117.4	34.5	0.6	295.6	0.8
p669	8	104.7	34.6	2.4	280.7	3.3
p670	3	117.5	34.7	0.9	294.7	1.3
p671	3	117.7	34.8	0.9	294.2	1.3
p672	6	104.4	34.8	1.8	278.0	2.5
p673	4.5	118.2	34.9	1.4	292.5	1.9
p674	3	109.1	34.9	0.9	299.3	1.3
p675	3.2	113.8	35.5	1.0	293.1	1.3

p676	3	113.8	35.6	0.9	293.1	1.3
p677	3.2	118.9	35.7	1.0	282.5	1.3
p678	5	104.3	35.8	1.5	271.6	2.1
p679	2	111.5	35.8	0.6	304.8	0.8
p680	3	116.8	35.8	0.9	288.9	1.3
p681	10	117.7	36.1	3.0	289.6	4.2
p682	8.8	114.1	36.2	2.7	289.7	3.7
p683	10	116.6	36.2	3.0	287.8	4.2
p684	5	106.1	36.2	1.5	267.0	2.1
p685	10	111.8	36.4	3.0	303.0	4.2
p686	6	118.5	36.4	1.8	281.8	2.5
p687	4	102.3	36.5	1.2	269.4	1.7
p688	1.5	102.3	36.5	0.5	269.4	0.6
p689	3	101.5	36.6	0.9	267.2	1.3
p690	6	117.8	36.6	1.8	283.4	2.5
p691	10	114.1	36.7	3.0	292.9	4.2
p692	2	118.1	36.7	0.6	283.4	0.8
p693	3	103.7	36.8	0.9	272.7	1.3
p694	2.5	103.2	36.9	0.8	274.1	1.0
p695	10	79.5	37.1	3.0	279.4	4.2
p696	5	106.7	37.1	1.5	256.8	2.1
p697	6	105.7	37.4	1.8	256.9	2.5
p698	4	112.0	37.5	1.2	291.2	1.7
p699	1.5	112.0	37.5	0.5	291.3	0.6
p700	2	112.0	37.6	0.6	289.8	0.8
p701	7	103.1	37.7	2.1	272.1	2.9
p702	2	120.6	37.7	0.6	269.5	0.8
p703	1.5	120.6	37.7	0.5	269.3	0.6
p704	5	77.5	37.8	1.5	286.9	2.1
p705	2	112.0	37.8	0.6	284.5	0.8
p706	2.5	112.6	38.2	0.8	286.7	1.0
p707	1.5	106.7	38.2	0.5	266.4	0.6
p708	10	102.1	38.4	3.0	271.8	4.2
p709	1.5	102.3	38.5	0.5	271.1	0.6
p710	2	76.2	38.7	0.6	288.6	0.8
p711	4	100.8	38.9	1.2	273.1	1.7
p712	3	111.2	38.9	0.9	278.1	1.3
p713	6	112.8	39.1	1.8	283.3	2.5
p714	2	121.7	39.3	0.6	263.2	0.8
p715	3	115.3	39.3	0.9	292.6	1.3
p716	2	76.1	39.3	0.6	293.6	0.8
p717	10	112.6	39.4	3.0	274.9	4.2

p718	8	111.2	39.4	2.4	278.2	3.3
p719	6	76.1	39.5	1.8	294.6	2.5
p720	1.5	118.5	39.6	0.5	280.3	0.6
p721	4	94.3	39.6	1.2	266.0	1.7
p722	2	112.8	39.6	0.6	274.5	0.8
p723	1.5	115.9	39.7	0.5	289.4	0.6
p724	4	98.5	39.7	1.2	273.4	1.7
p725	3	118.5	39.8	0.9	284.0	1.3
p726	6	106.8	39.8	1.8	259.8	2.5
p727	7	113.0	39.8	2.1	275.0	2.9
p728	3	114.8	39.8	0.9	278.8	1.3
p729	10	118.2	39.9	3.0	287.2	4.2
p730	5	118.4	39.9	1.5	286.7	2.1
p731	1.5	118.2	39.9	0.5	287.3	0.6
p732	6	117.6	39.9	1.8	287.8	2.5
p733	2.5	113.1	39.9	0.8	274.5	1.0
p734	4.5	116.8	40.0	1.4	287.6	1.9
p735	1.5	117.8	40.6	0.5	284.8	0.6
p736	7	118.5	40.7	2.1	279.2	2.9
p737	6	117.9	40.7	1.8	283.4	2.5
p738	10	123.9	40.8	3.0	266.9	4.2
p739	2	120.7	40.8	0.6	251.5	0.8
p740	3	109.2	41.0	0.9	269.0	1.3
p741	3	111.5	41.0	0.9	266.7	1.3
p742	4	111.5	41.0	1.2	266.2	1.7
p743	2	80.2	41.1	0.6	296.3	0.8
p744	2.5	118.0	41.2	0.8	275.3	1.0
p745	5	120.8	41.2	1.5	248.0	2.1
p746	3.1	123.7	41.3	0.9	260.5	1.3
p747	2	123.5	41.4	0.6	258.6	0.8
p748	2	119.8	41.5	0.6	247.1	0.8
p749	2.5	120.5	41.6	0.8	246.1	1.0
p750	1.5	126.0	41.8	0.5	278.4	0.6
p751	5	126.3	41.8	1.5	279.0	2.1
p752	1.5	86.4	41.9	0.5	291.3	0.6
p753	8	121.7	42.1	2.4	244.9	3.3
p754	8	121.3	42.4	2.4	235.5	3.3
p755	8	94.1	42.5	2.4	284.3	3.3
p756	2.5	93.6	42.7	0.8	286.2	1.0
p757	6	88.6	42.7	1.8	294.0	2.5
p758	1.5	120.7	42.9	0.5	239.4	0.6
p759	2.5	124.6	43.3	0.8	251.4	1.0

p760	2	81.9	43.3	0.6	298.4	0.8
p761	5	129.7	43.5	1.5	273.0	2.1
p762	2	87.7	43.6	0.6	292.9	0.8
p763	2.5	81.2	43.7	0.8	300.0	1.0
p764	2	87.8	43.7	0.6	293.0	0.8
p765	4	87.7	43.9	1.2	302.3	1.7
p766	3	88.7	44.1	0.9	295.8	1.3
p767	3.5	80.8	44.2	1.1	293.4	1.5
p768	6	80.8	44.2	1.8	294.0	2.5
p769	4	82.1	44.7	1.2	298.6	1.7
p770	1.5	127.5	45.4	0.5	269.6	0.6
p771	3	130.6	46.2	0.9	265.5	1.3
p772	3	130.6	46.2	0.9	265.6	1.3
p773	6	89.5	46.9	1.8	300.7	2.5
p774	2	130.2	47.2	0.6	276.5	0.8
p775	1.8	86.8	47.8	0.5	273.0	0.8
p776	4	123.5	48.1	1.2	270.2	1.7
p777	2.5	125.7	50.1	0.8	274.4	1.0
p778	2	117.8	36.1	0.6	289.5	0.8
p779	3	104.3	30.7	0.9	304.1	1.3
p780	3	108.1	23.0	0.9	286.2	1.3
p781	3	108.0	24.7	0.9	297.5	1.3
p782	5	114.1	36.1	1.5	289.4	2.1
p783	3	122.7	46.8	0.9	254.3	1.3
p784	4	109.5	18.3	1.2	297.5	1.7
p785	5	120.4	30.5	1.5	294.7	2.1
p786	3	118.2	36.7	0.9	282.9	1.3
p787	3	119.3	42.3	0.9	243.0	1.3
p788	2	110.2	20.0	0.6	287.3	0.8
p789	10	109.3	25.1	3.0	296.8	4.2
p790	3	119.4	25.9	0.9	289.4	1.3
p791	1.5	116.9	28.5	0.5	314.8	0.6
p792	5	119.6	31.3	1.5	290.4	2.1
p793	2.5	118.4	32.0	0.8	281.9	1.0
p794	5	119.5	32.5	1.5	278.3	2.1
p795	2	117.3	32.8	0.6	283.9	0.8
p796	3	114.0	32.8	0.9	297.2	1.3
p797	4	114.0	32.8	1.2	297.0	1.7
p798	2	120.4	32.8	0.6	271.8	0.8
p799	8	119.3	33.3	2.4	280.0	3.3
p800	2	118.4	33.8	0.6	287.1	0.8
p801	5	118.4	33.8	1.5	287.0	2.1

p802	4	107.8	34.2	1.2	306.6	1.7
p803	2	113.5	34.3	0.6	294.7	0.8
p804	2.4	113.5	34.3	0.7	294.8	1.0
p805	3	117.5	34.7	0.9	294.7	1.3
p806	2	114.4	34.8	0.6	291.8	0.8
p807	5	109.0	34.9	1.5	299.2	2.1
p808	2	113.9	35.4	0.6	293.6	0.8
p809	2.5	114.6	35.7	0.8	288.7	1.0
p810	6	114.1	36.1	1.8	289.5	2.5
p811	3	113.0	36.3	0.9	286.2	1.3
p812	2	117.0	36.6	0.6	286.0	0.8
p813	1.8	118.2	36.7	0.5	283.0	0.8
p814	6	120.6	37.7	1.8	269.6	2.5
p815	3	109.7	38.4	0.9	270.6	1.3
p816	4	118.4	39.9	1.2	286.9	1.7
p817	7	122.4	40.6	2.1	254.5	2.9
p818	3	109.7	40.7	0.9	269.0	1.3
p819	2	121.3	41.1	0.6	248.0	0.8
p820	2.5	125.2	44.1	0.8	254.9	1.0
p821	1.6	131.0	45.3	0.5	261.4	0.7
p822	2.5	132.0	47.2	0.8	264.8	1.0
p823	5	110.2	22.5	1.5	286.0	2.1

(2) Sink estimation

In this study, deep saline aquifers were selected as the geological sites for long-term CO_2 storage due to their substantial estimated storage potential. Data from 14 onshore deep saline aquifers were used to estimate CO_2 storage capacity (see **Table S14**). Offshore CO_2 storage was not considered in this analysis, primarily due to the relatively higher costs associated with offshore storage technologies compared to onshore options in China.

Table S14 Selected 14 deep saline aquifers for CO_2 storage in China.

	Depth (m)	Thickness (m)	Permeability (mD)	Porosity (%)	Geothermal gradient (℃/km)	Area (km^2)	Storage capacity (Mt)
Tarim Basin	4000	300	100	0.15	20	100000	
Junggar Basin	1500	300	75	0.15	21	19000	
Qaidam Basin	500	50	5	0.15	30	15000	
Ordos Basin	1000	200	125	0.18	30	35000	
Erlian Basin	1000	300	1000	0.15	40	16000	
Hailaer Basin	2000	100	10	0.15	30	11000	

Songliao Basin	1200	150	200	0.2	42	38000
Bohai Bay Basin	1500	200	800	0.23	55	30000
Southern North China	1000	300	500	0.2	35	52000
Subei Basin	1000	300	5	0.2	30	10000
Jianghan Basin	1000	150	10	0.1	35	2000
Sichuan Basin	3500	400	5	0.1	23	50000
Turpan-Harmi Basin						
Yingen-Ejian Basin						

(3) CO_2 transportation via pipelines

In this study, GIS maps were integrated to provide a comprehensive representation of geographic, topographic, and demographic features relevant to the construction of onshore CO_2 pipelines (**Fig. S37**). The cost of CO_2 pipelines was then assessed on a cell-by-cell basis using these GIS maps, with each cell assigned a cost factor representing the relative expense of constructing pipelines at that location. A value of 1 indicates the standard pipeline construction cost, which depends on pipeline diameter. This baseline cost was calculated using a cost model originally developed by Morgan and later adapted for use in China. Cost factors below 1 reflect areas where construction is expected to be easier and less expensive, such as routes adjacent to existing oil and gas pipelines. Conversely, values above 1 represent areas with higher construction costs, particularly in densely populated regions. The GIS layers were collectively weighted to generate a cost surface with a spatial resolution of 240×240 meters. Details of the GIS maps and the cost factors used in the analysis are available in the supplementary file.

Using the constructed cost surface, the geographical coordinates of CO_2 sources and storage sites were overlaid to optimize least-cost paths for connecting CO_2 capture points at steel plants with potential storage basins. The least-cost path optimization approach has been widely applied in previous studies. This analysis employed the open-source software SimCCS, developed specifically for this purpose. SimCCS enables the aggregation of CO_2 flows from multiple sources into trunk pipelines, thereby maximizing economies of scale, and determines the most cost-effective spatial configuration for connecting known sources and sinks across a defined geographic region.

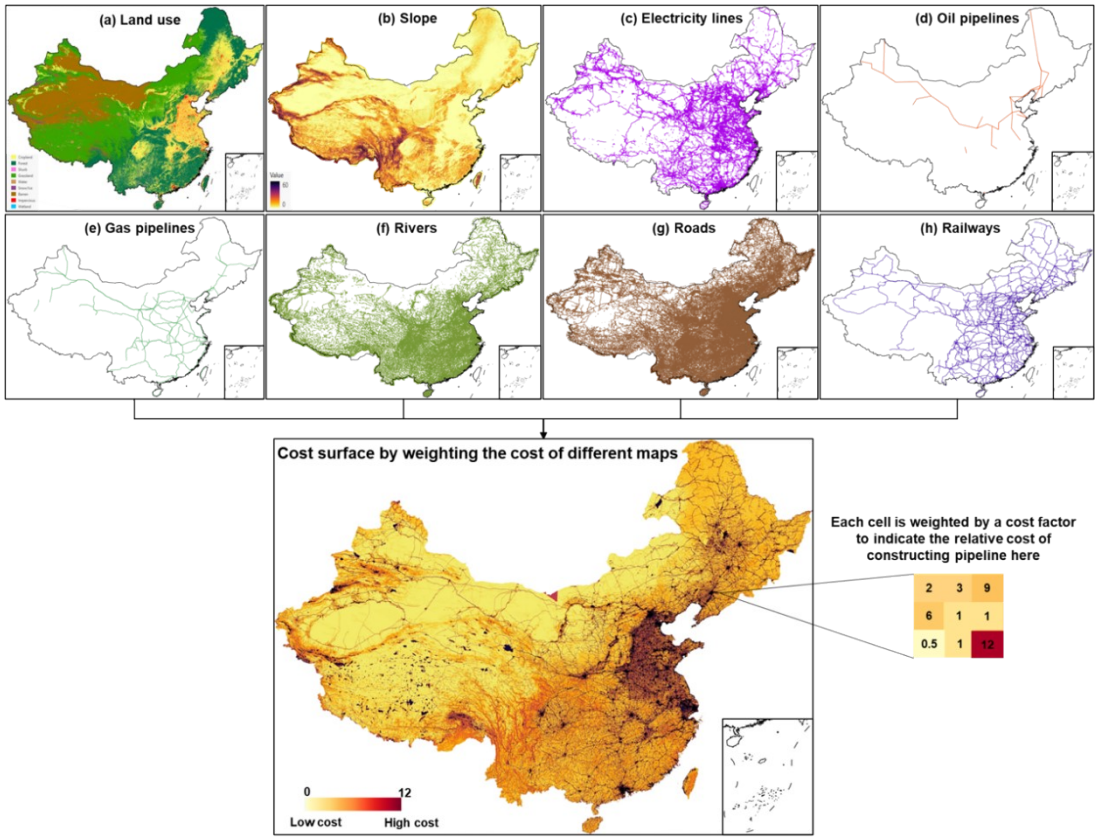

Fig. S37 Cost surface reflecting weightings of CO_2 pipeline construction costs according to map features depicted in panels.

(The resolution of the land-use map is 720×720 m. The resolution of other input maps is 240×240 m. The resolution of the cost surface is 240×240 m. The cost factors in the cost surface are the cost of constructing a CO_2 pipeline relative to the cost for a reference standard pipeline. A value less than 1 means that pipelines in that cell cost less than the standard. A value larger than 1 means higher construction costs.)

7. CO_2 sequestration scenario setting and results

Methanol shipping demand forecast

According to the IEA's prediction[36], China's maritime transport sector consumes about 1.75 EJ of energy in 2035. If methanol accounts for 16 % of that energy[37], the required methanol volume is calculated as

$$MeOH_{2035} = \frac{1.75 \times 10^9\ MJ\ \times\ 0.16}{19.9\ MJ/kg} \approx\ 14.07\ Mt$$

For 2050, assuming total shipping energy of 1.5 EJ and a methanol share of 40 %:

$$MeOH_{2050} = \frac{1.5 \times 10^9\ MJ\ \times\ 0.40}{19.9\ MJ/kg} \approx\ 30.15\ Mt$$

CO_2 sequestration scenarios

We define four scenarios based on the required CO_2 sequestration for cement plants and the corresponding level of methanol production:

1. CO_2 sequestration 26.0 Mt/yr: corresponds to replacing 10% of China's conventional methanol output in 2020 (≈ 7.06 Mt MeOH/yr).
2. CO_2 sequestration 259.7 Mt/yr: corresponds to full substitution of conventional methanol production (≈ 70.6 Mt MeOH/yr).
3. CO_2 sequestration 311.5 Mt/yr: corresponds to full substitution of conventional methanol plus estimated 2035 shipping-fuel demand (≈ 84.7 Mt MeOH/yr).
4. CO_2 sequestration 370.6 Mt/yr: corresponds to full substitution of conventional methanol plus projected 2050 shipping-fuel demand (≈ 100.8 Mt MeOH/yr).

CCS Network Planning

We compute the annual CO_2 sequestration requirement by defining scenarios directly in terms of sequestration volumes (Mt CO_2/yr). For each scenario, the corresponding methanol output is determined by dividing the sequestration volume by a net-sequestration factor of 0.38 t CO_2 per tonne of cement (i.e. the portion of CO_2 that must be sequestered after accounting for that utilized in methanol synthesis), and further scaling by a cement-to-methanol ratio of 9.76 t cement per tonne of methanol (Net-Zero Cement & Methanol). These steps yield the methanol production levels associated with each "CO_2 sequestration" scenario, as reported in Table S14. The resulting sequestration volumes are used as the source terms in SimCCS-China.

At the facility level, the annual CO_2 sequestration of each cement plant is computed as cement output multiplied by the emission factor per tonne of cement, assuming an 80% capacity utilization factor. The theoretical sequestration potential of all existing cement plants is 896.8 Mt CO_2/yr, which indicates that co-production could utilize up to 41.3% of national cement capacity under the

"CO_2 sequestration 370.6 Mt/yr" scenario. For cement-only decarbonization scenarios, the national sequestration total remains the same, but the allocation of CO_2 volumes across plants differs. In this case, the sequestration factor is increased to 0.52 t CO_2 per tonne of cement, implying that 100% of capturable CO_2 is designated for sequestration.

Table S15 Scenarios of CO_2 sequestration requirement and corresponding green methanol production.

Scenario	MeOH production (Mt / yr)
CO_2 sequestration 26.0 Mt/yr	7.06
CO_2 sequestration 259.7 Mt/yr	70.6
CO_2 sequestration 311.5 Mt/yr	84.7
CO_2 sequestration 370.6 Mt/yr	100.8

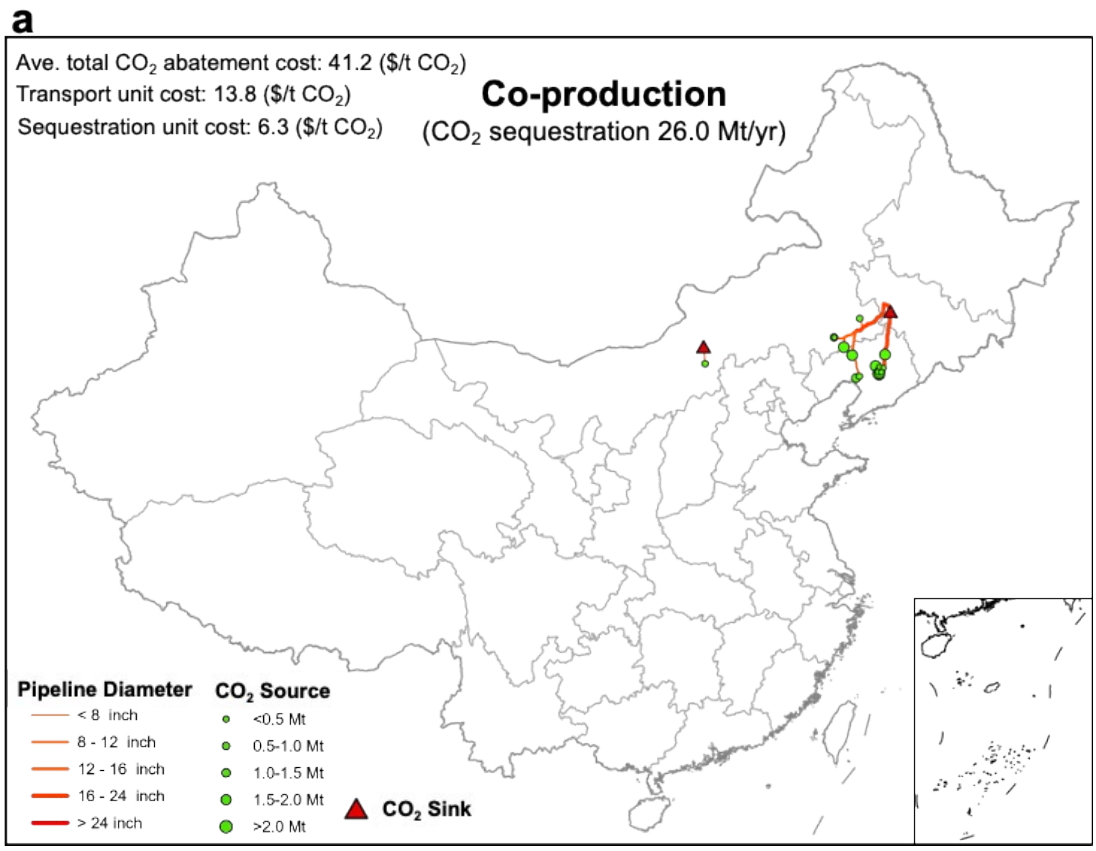

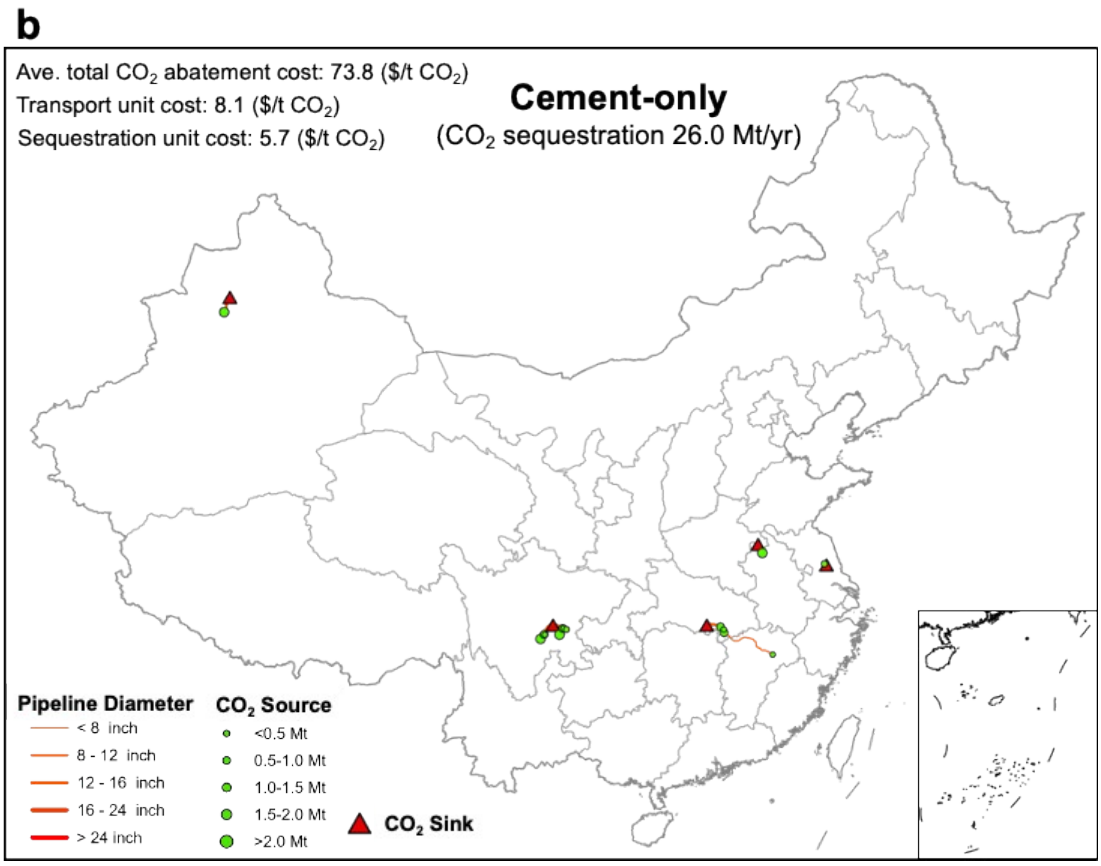

Fig. S38 CO_2 source–sink matching under co-production versus cement-only decarbonization under "CO_2 sequestration 26 Mt/yr" scenarios.

a

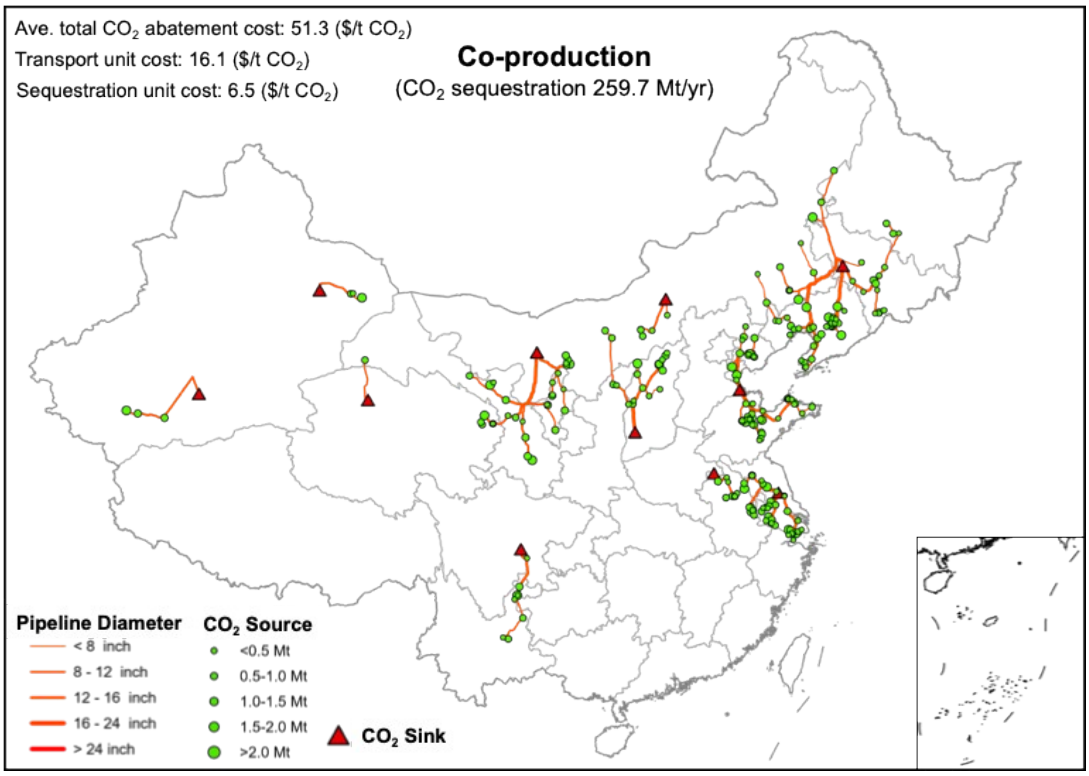
Ave. total CO_2 abatement cost: 51.3 ($/t CO_2)
Transport unit cost: 16.1 ($/t CO_2)
Sequestration unit cost: 6.5 ($/t CO_2)
Co-production
(CO_2 sequestration 259.7 Mt/yr)
Pipeline Diameter
< 8 inch
8 - 12 inch
12 - 16 inch
16 - 24 inch
> 24 inch
CO_2 Source
<0.5 Mt
0.5-1.0 Mt
1.0-1.5 Mt
1.5-2.0 Mt
>2.0 Mt
CO_2 Sink

b

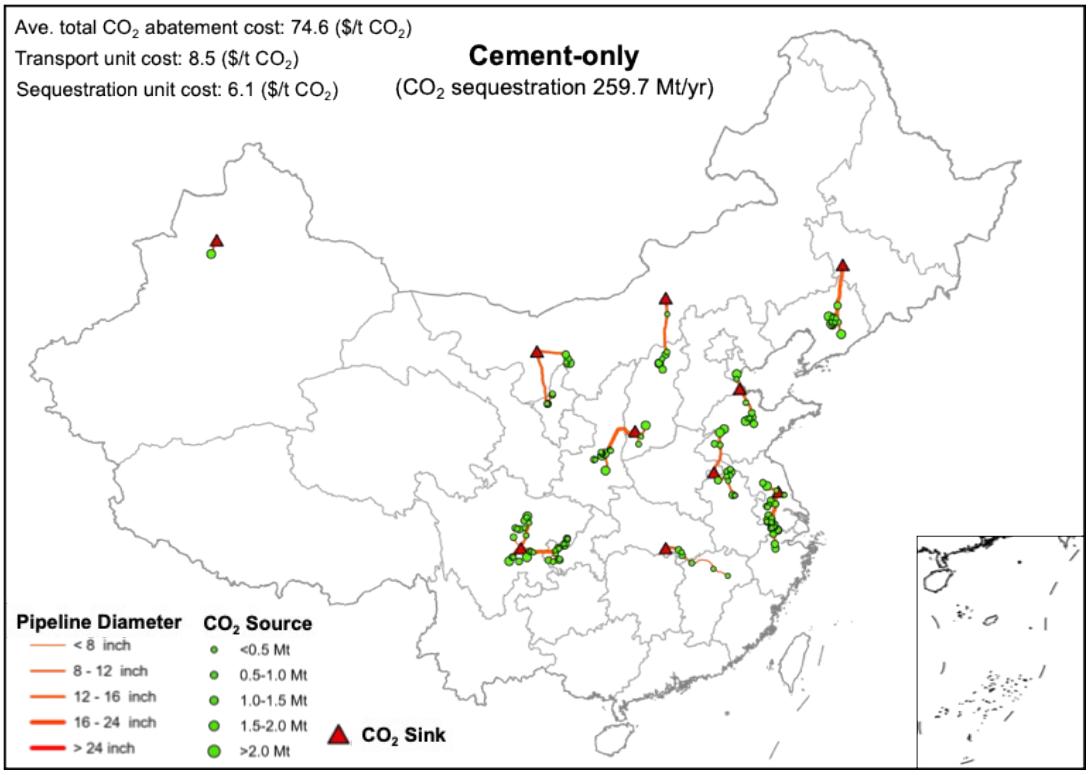
Ave. total CO_2 abatement cost: 74.6 ($/t CO_2)
Transport unit cost: 8.5 ($/t CO_2)
Sequestration unit cost: 6.1 ($/t CO_2)
Cement-only
(CO_2 sequestration 259.7 Mt/yr)
Pipeline Diameter
< 8 inch
8 - 12 inch
12 - 16 inch
16 - 24 inch
> 24 inch
CO_2 Source
<0.5 Mt
0.5-1.0 Mt
1.0-1.5 Mt
1.5-2.0 Mt
>2.0 Mt
CO_2 Sink

c

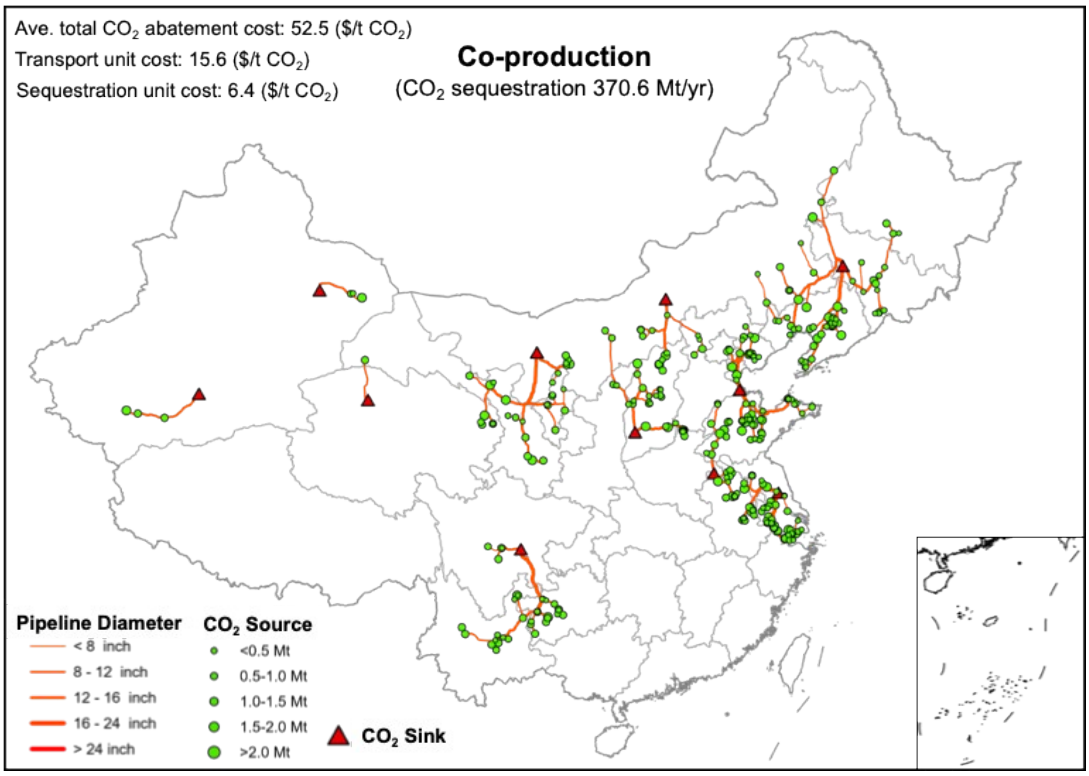
Ave. total CO_2 abatement cost: 52.5 ($/t CO_2)
Transport unit cost: 15.6 ($/t CO_2)
Sequestration unit cost: 6.4 ($/t CO_2)
Co-production
(CO_2 sequestration 370.6 Mt/yr)
Pipeline Diameter
< 8 inch
8 - 12 inch
12 - 16 inch
16 - 24 inch
> 24 inch
CO_2 Source
<0.5 Mt
0.5-1.0 Mt
1.0-1.5 Mt
1.5-2.0 Mt
>2.0 Mt
CO_2 Sink

d

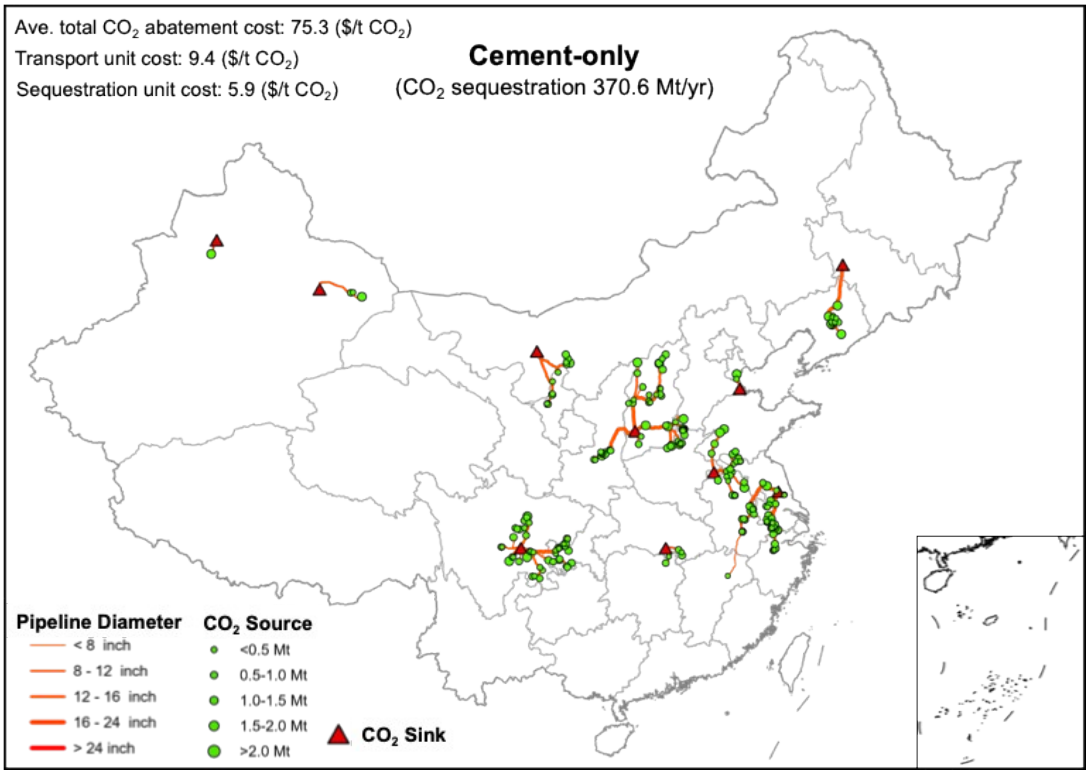
Ave. total CO_2 abatement cost: 75.3 ($/t CO_2)
Transport unit cost: 9.4 ($/t CO_2)
Sequestration unit cost: 5.9 ($/t CO_2)
Cement-only
(CO_2 sequestration 370.6 Mt/yr)
Pipeline Diameter
< 8 inch
8 - 12 inch
12 - 16 inch
16 - 24 inch
> 24 inch
CO_2 Source
<0.5 Mt
0.5-1.0 Mt
1.0-1.5 Mt
1.5-2.0 Mt
>2.0 Mt
CO_2 Sink

Fig. S39 Comparison of CO_2 source–sink matching under co-production versus cement-only decarbonization under additional CO_2 sequestration scenarios.

8. Limitations and future study

(1) Plant heterogeneity and capture economies

In this study, all cement plants are treated as homogeneous with respect to age, design efficiency, and carbon-capture equipment scale. We have not accounted for economies of scale in capture systems across different emission sources.

Future work should build a detailed technology-type database to distinguish individual plant efficiencies and capture-unit characteristics (e.g. retrofit vs. greenfield, capture technology type), enabling more granular modeling of CO_2 removal costs and performance.

(2) Co-location and land-use feasibility

We assume full co-location of cement, methanol synthesis, and renewable power (wind and solar) without verifying land-use constraints. Although most selected plants lie in low-density provinces with ample available land, a robust siting analysis against a high-resolution renewable-energy database is needed.

Future work should incorporate GIS-based land-use and zoning layers to quantify buildable RE capacity, explore partial co-location scenarios, and assess grid-backup options for periods of low renewable output.

(3) Carbon-accounting boundaries

Our carbon accounting covers only process and fossil energy combustion emissions from cement and methanol production and enforces net-zero emissions (including methanol incineration) via certification rules. We have not included lifecycle emissions from renewable-energy facility manufacture or cement product "sponge" carbon sequestration over its service life. Moreover, methanol's downstream product portfolio—some with long service lives—may act as additional carbon sinks.

Future work should develop a comprehensive lifecycle protocol that (a) allocates embodied emissions for all equipment, (b) quantifies post-use cement carbonation, and (c) tailors accounting rules to different methanol end-uses.

(4) Cement transport and regional demand matching

This study ignores transportation costs and logistics constraints for cement products, which are highly sensitive to distance (typically limited to ≤300 km). In China, cement plants tend to be regionally self-sufficient and widely distributed to match local demand. As regional cement demand declines at different rates, optimal plant-retirement strategies and the deployment of low-carbon technologies will vary by location (see our prior work on provincial level decarbonization pathways[38]). However, because even full co-production deployment (including shipping-driven

methanol demand) requires less cement plant capacity than currently exists nationwide, our scope focuses on evaluating co-production technology and prioritizing which plants should adopt it, rather than exploring the industry's overall decarbonization pathway.

Future work should integrate high-resolution spatial demand models and interregional transport cost data to assess regional self-sufficiency constraints and cross-regional trade flows. Meanwhile, it is essential to evaluate how differing decline rates in local cement demand affect plant retirement and low-carbon retrofit strategies.

(5) Practical limits to high alternative-fuel substitution in oxy-fuel cement kilns

High alternative-fuel substitution in cement kilns faces practical constraints related to operability and product quality[39,40]. Heterogeneous fuel properties, including moisture content and variable heating characteristics, can reduce effective heat-release rates and increase the risk of incomplete burnout of solid fuel particles, thereby destabilizing kiln temperature profiles and impairing process stability. In addition, the presence of ash and minor elements may lead to condensation and accumulation in cooler sections of the system, posing further operational challenges and increasing clinker-quality variability. These constraints often necessitate fuel pre-treatment and careful operational control.

Oxy-fuel operation can, in principle, support higher alternative-fuel substitution by enabling temperature regulation through adjustable flue-gas recirculation under CO_2-rich combustion conditions[40,41]. However, its application to clinker burning with high shares of heterogeneous alternative fuels remains site- and fuel-specific. Further pilot-scale validation and targeted research are required to assess robustness, long-term operability, and potential cost and performance penalties at high substitution levels.

9. Methanol fuel transport

Methanol shows strong potential as a shipping fuel. We estimated transport costs (via road or pipeline) from methanol production sites to three representative ports (Tianjin, Shanghai, and Shenzhen) and incorporated these into the co-production cost, excluding CO_2 transport and sequestration (**Fig. S40a-f**). As illustrated in **Fig. S40g**, road transport raises the total co-production cost by more than $100 per tonne methanol and 9.76 tonne cement at Shanghai and Shenzhen ports. While the cost increments are smaller in Tianjin, especially for the lowest-cost 15 % of plants, because most of those facilities are located close to the port. Adopting pipeline transport in place of roads substantially reduces these increases. For the top-15 % plants to Tianjin, pipeline delivery incurs an additional cost of under $20 per tonne methanol and 9.76 tonne cement. Moreover, long distance transportation erodes the competitiveness of sites in Northwest China.

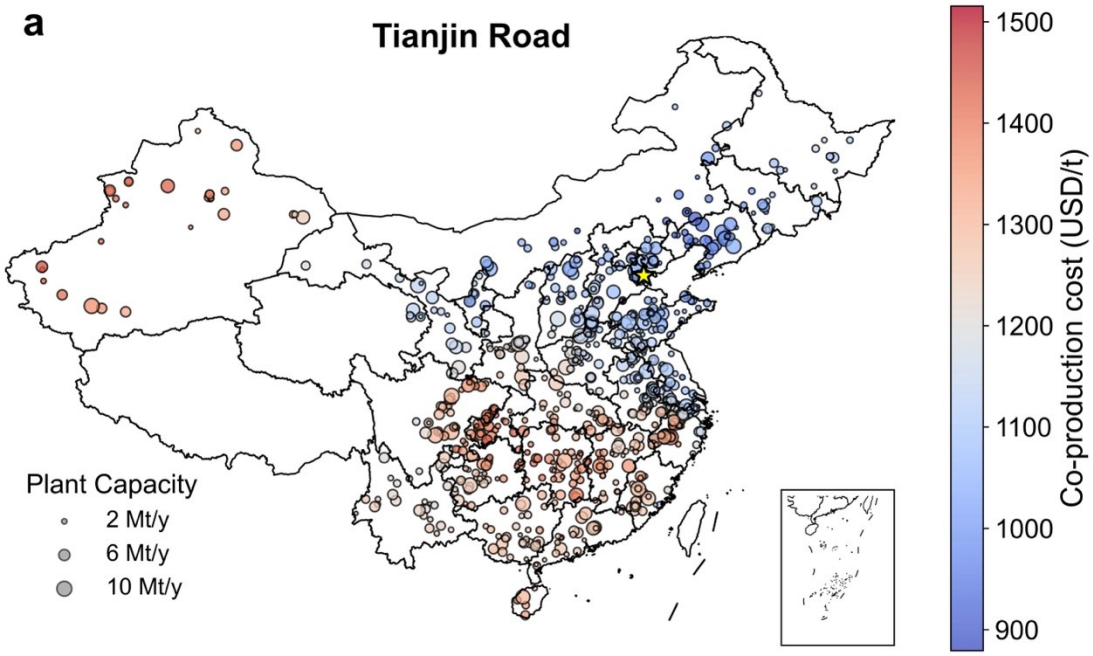

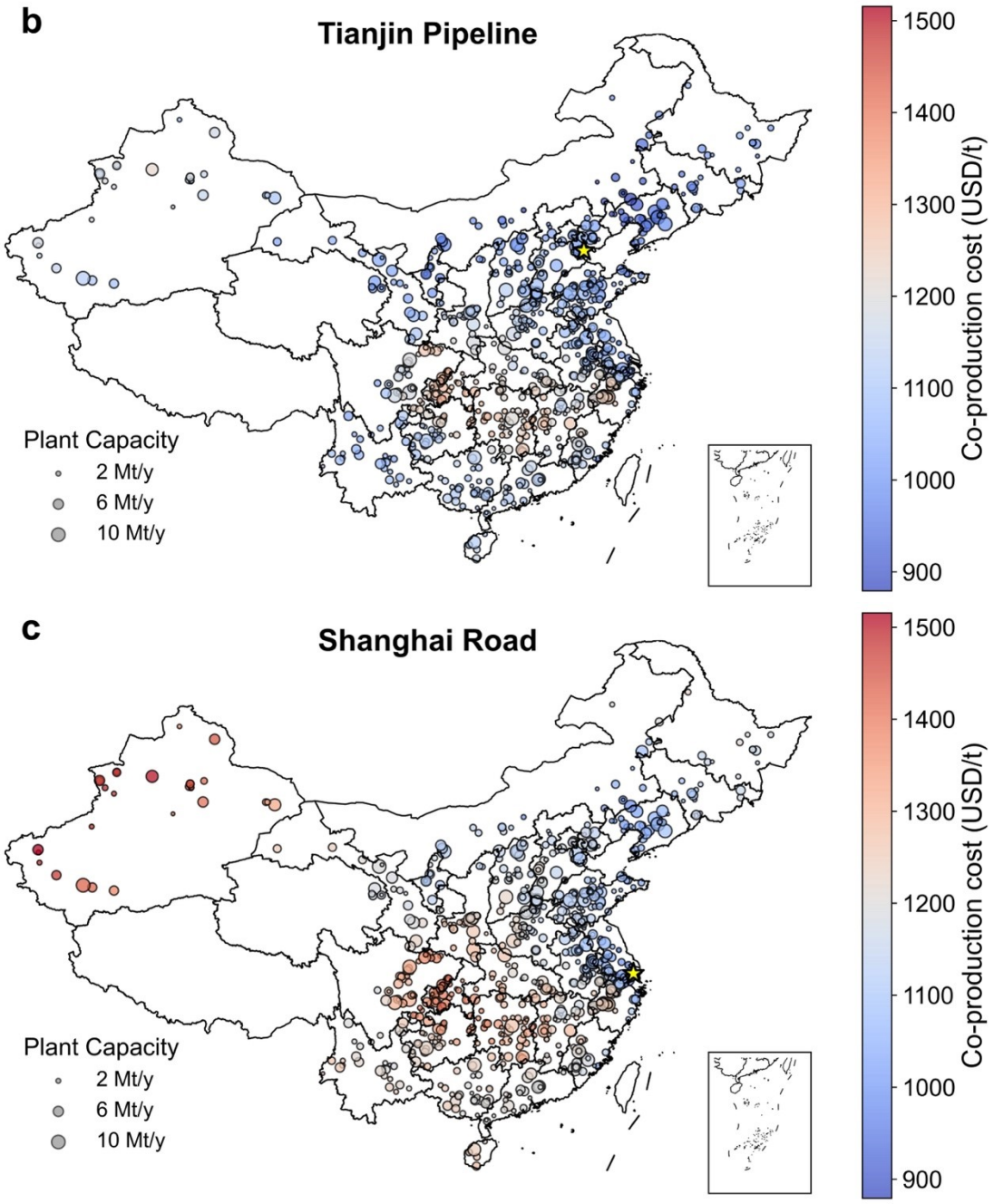
b
Tianjin Pipeline
Plant Capacity
2 Mt/y
6 Mt/y
10 Mt/y
1500
1400
1300
1200
1100
1000
900
Co-production cost (USD/t)
c
Shanghai Road
Plant Capacity
2 Mt/y
6 Mt/y
10 Mt/y
1500
1400
1300
1200
1100
1000
900
Co-production cost (USD/t)

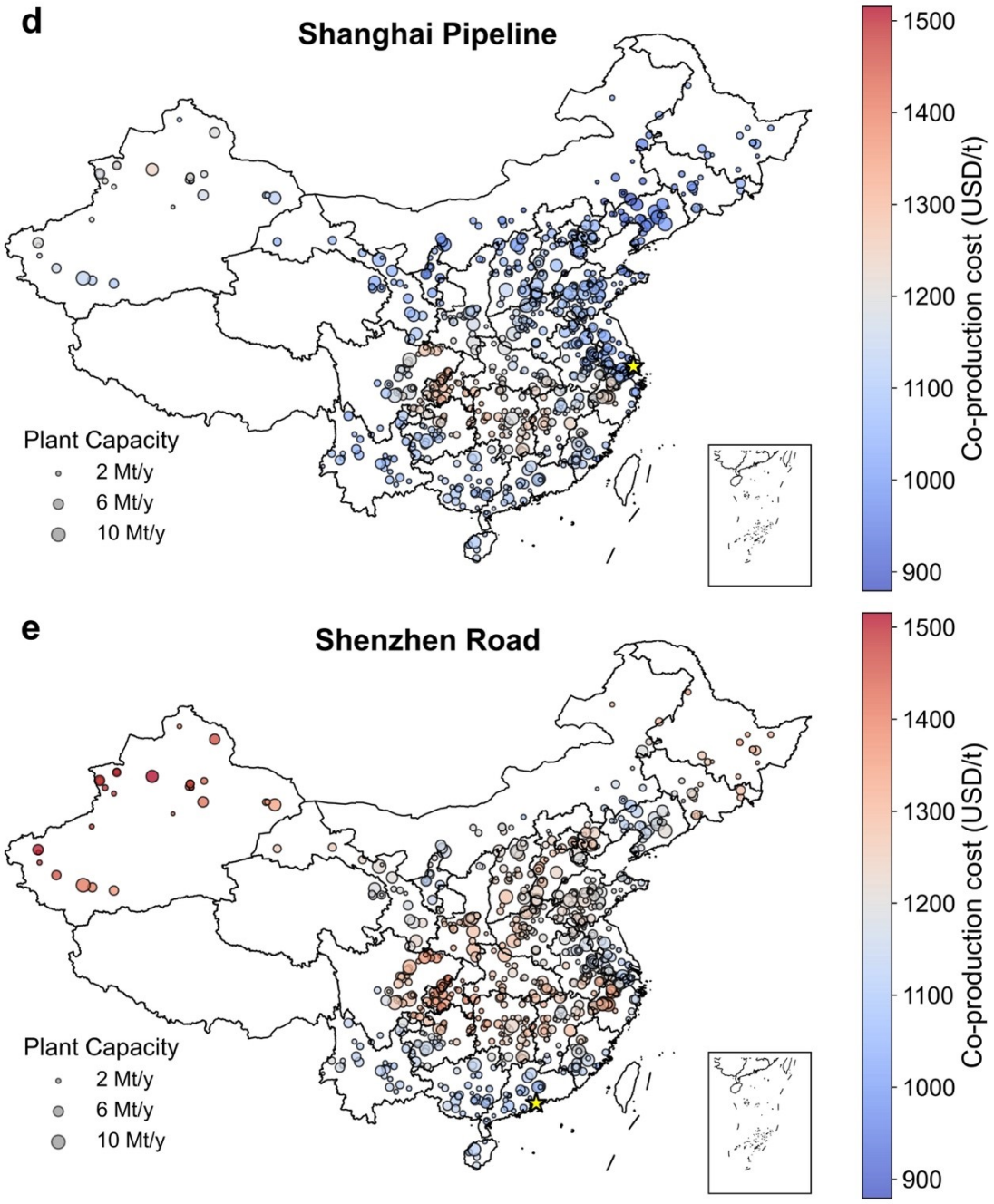
d
Shanghai Pipeline
Plant Capacity
2 Mt/y
6 Mt/y
10 Mt/y
1500
1400
1300
1200
1100
1000
900
Co-production cost (USD/t)
e
Shenzhen Road
Plant Capacity
2 Mt/y
6 Mt/y
10 Mt/y
1500
1400
1300
1200
1100
1000
900
Co-production cost (USD/t)

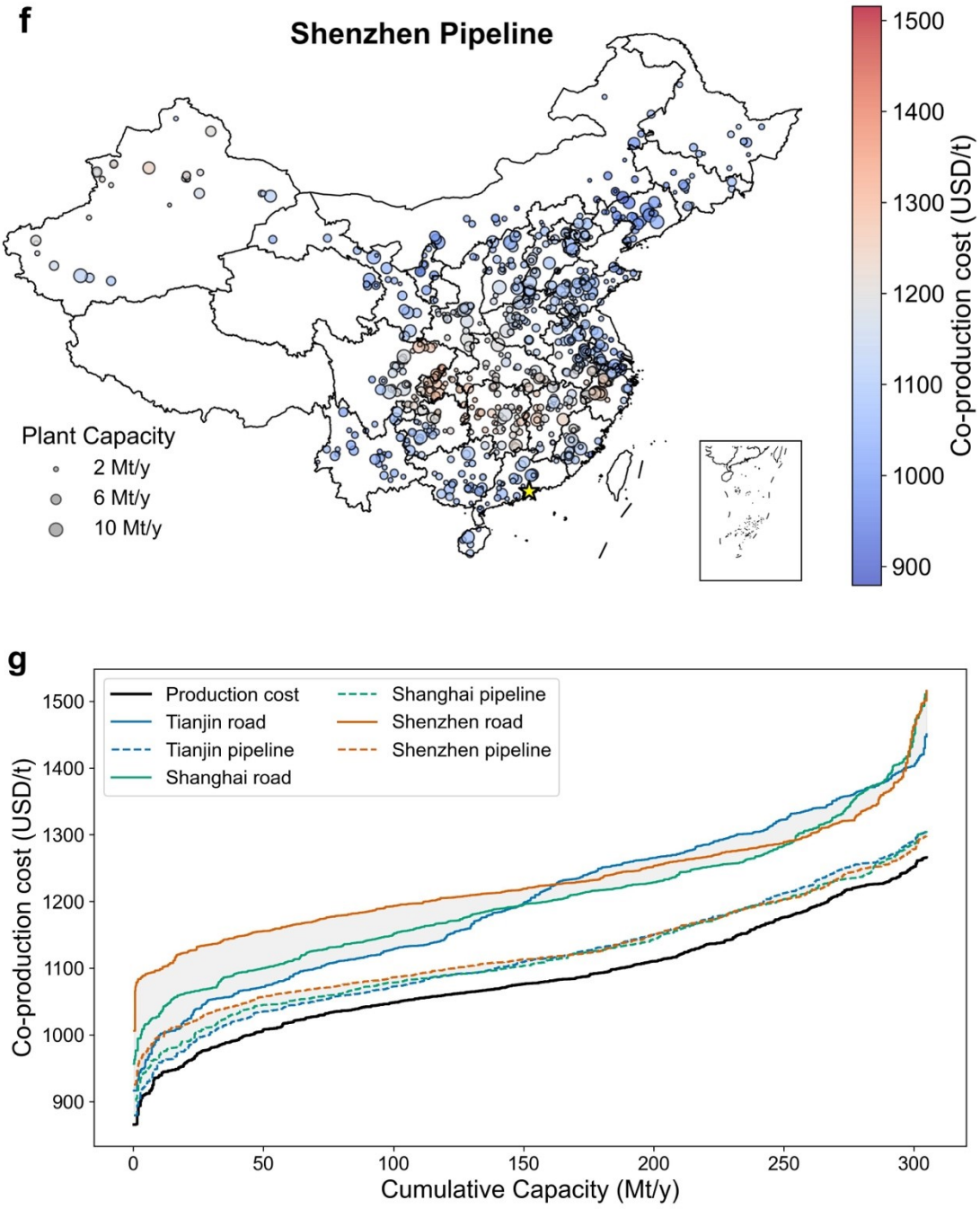

Fig. S40 Combined costs under net-zero methanol production scenarios. Methanol transport costs from production sites to the representative port are incorporated into the co-production cost (excluding CO_2 transport and sequestration). **a-f**, combinations of three ports and two transport modes. The title denotes the port and the methanol transport mode. The yellow star represents the location of the port. **g.** cost–capacity curves sorted in ascending order of abatement cost versus cumulative cement capacity. The co-production cost is based on the 9.76 t cement + 1 t MeOH.

10. Biomass price and substitution-rate sensitivity

The delivered cost of biomass and other alternative fuels can vary widely across locations due to availability, cross-sector competition, logistics, and sustainability constraints, and because achievable substitution levels are often constrained by kiln operability and product-quality requirements, we therefore conduct sensitivity analyses on both alternative-fuel price and the thermal substitution rate. These cases are designed to test the robustness of the techno-economic and emissions conclusions beyond the optimistic full-substitution benchmark.

For alternative-fuel price sensitivity, the baseline alternative-fuel price is scaled by four multipliers (0.8×, 1.2×, 1.5× and 2.0× the baseline) with all other assumptions kept unchanged, as shown in **Fig. S41**.

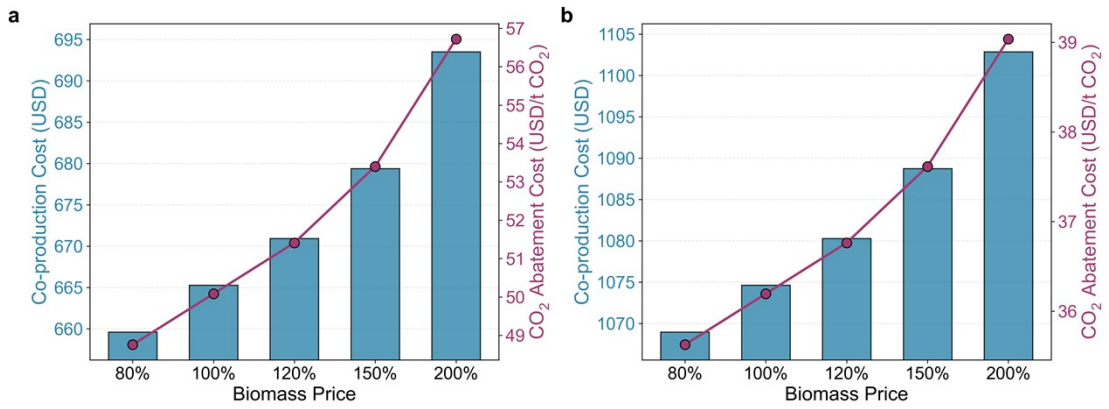

Fig. S41 Sensitivity of co-production cost and CO_2 abatement cost to biomass price under different cement–methanol production ratios. a, under No-CO_2 Sequestration scenario. **b**, under Net-Zero Cement & Methanol scenario. Bars show the total co-production cost, while the line indicates the corresponding CO_2 abatement cost.

Because biomass is modeled as a time-invariant thermal input to the cement kiln, changes in biomass price translate linearly into total system cost. Across the tested range, doubling the biomass price increases the CO_2 abatement cost by only about 3–7 USD/t CO_2, depending on the cement–methanol output ratio. This indicates that biomass price is not a dominant driver of overall system economics in the co-production configuration. Moderate uncertainty in biomass price does not materially alter the competitiveness of the system. For comparison, renewable profiles across different regions could lead to a CO_2 abatement cost difference of 40 USD/t CO_2, as shown in **Fig. 5a**.

The baseline case assumes full biomass substitution for kiln thermal input. To reflect practical multi-fuel operation, we add cases in which biomass supplies only a fraction of kiln thermal input and the remainder is provided by coal. Specifically, we consider five biomass share scenarios: 0% (100% coal), 25%, 50%, 75% and 100% (baseline).

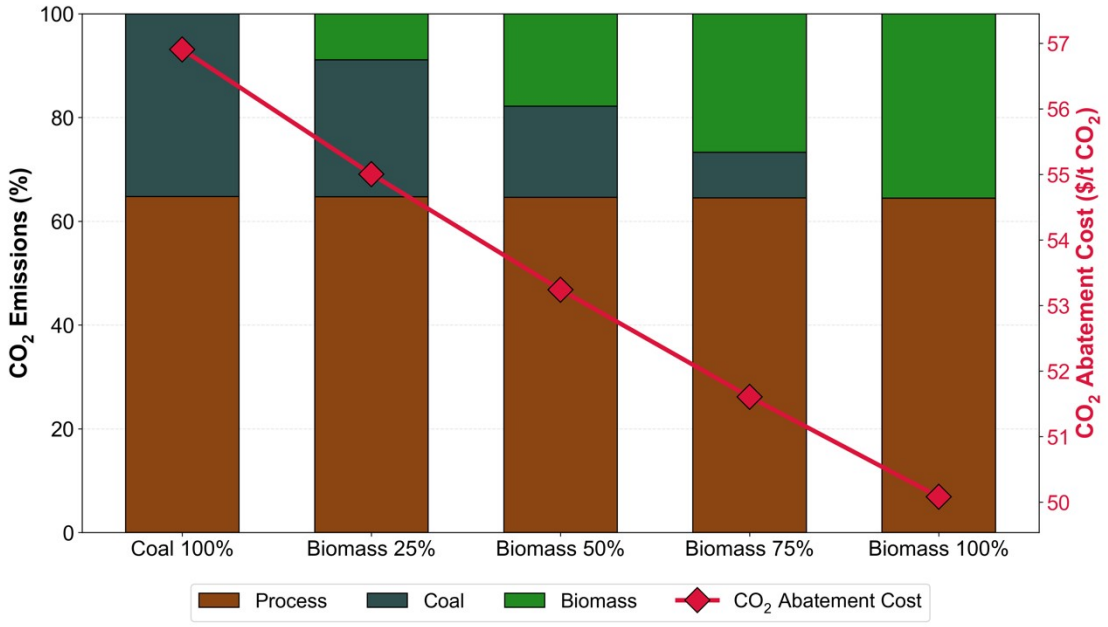

Fig. S42 Sensitivity of CO_2 emissions composition and CO_2 abatement cost to kiln fuel mix under the no CO_2 sequestration scenario. Bars show the contribution of process emissions and fuel-related emissions to total CO_2 emissions across different thermal substitution rates, while the line indicates the corresponding CO_2 abatement cost. CO_2 from biomass is assumed as carbon-neutral.

Fig. S42 illustrates how the kiln fuel mix affects emissions composition and the implied CO_2 abatement cost under the no-CO_2-sequestration scenario. Increasing the biomass share reduces fuel-related emissions and lowers the abatement cost, but the marginal difference between partial and full biomass substitution remains modest. Notably, even in the 100% coal case, the integrated co-production system achieves a relatively low abatement cost, only about 7 USD/t CO_2 higher than the full-biomass benchmark. These results show that the co-production framework remains economically relevant and informative across a wide range of biomass substitution levels. Higher biomass substitution is therefore most valuable in contexts where stricter requirements are imposed on the carbon origin of methanol.

11. References

1. Cheng, M., Verma, P., Yang, Z. & Axelbaum, R. L. Flexible cryogenic air separation unit—An application for low-carbon fossil-fuel plants. *Separation and Purification Technology* **302**, 122086 (2022).
2. Domenichini, R., Mancuso, L., Ferrari, N. & Davison, J. Operating Flexibility of Power Plants with Carbon Capture and Storage (CCS). *Energy Procedia* **37**, 2727–2737 (2013).
3. Fasihi, M. & Breyer, C. Global production potential of green methanol based on variable renewable electricity. *Energy Environ. Sci.* **17**, 3503–3522 (2024).
4. Langholtz, M. 2023 Billion-Ton Report. Oak Ridge National Laboratory (ORNL), Oak Ridge, TN (United States), Bioenergy Knowledge Discovery Framework (BEKDF); Oak Ridge National Laboratory (ORNL), Oak Ridge, TN (United States), Bioenergy Knowledge Discovery Framework (BEKDF) https://doi.org/10.23720/BT2023/2316165 (2024).
5. Tao, M., Azzolini, J. A., Stechel, E. B., Ayers, K. E. & Valdez, T. I. Review—Engineering Challenges in Green Hydrogen Production Systems. *J. Electrochem. Soc.* **169**, 054503 (2022).
6. European Industrial Gases Association (EIGA). *Indirect CO_2 Emissions Compensation: Benchmark Proposal for Air Separation Plants (EIGA PP 33/19)*. https://puritygas.ca/wp-content/uploads/2023/04/EIGA-PP33.pdf (2019).
7. Li, K., Leigh, W., Feron, P., Yu, H. & Tade, M. Systematic study of aqueous monoethanolamine (MEA)-based CO2 capture process: Techno-economic assessment of the MEA process and its improvements. *Applied Energy* **165**, 648–659 (2016).
8. Assunção, R., Eckl, F., Ramos, C. P., Correia, C. B. & Neto, R. C. Oxygen liquefaction economical value in the development of the hydrogen economy. *International Journal of Hydrogen Energy* **62**, 109–118 (2024).
9. IEAGHG. *Deployment of CCS in the Cement Industry*. https://ieaghg.org/publications/deployment-of-ccs-in-the-cement-industry/ (2013).
10. Hunan Provincial Department of Industry and Information Technology. Analysis of Cement Industry Carbon Emission Status and Key Reduction Pathways. http://gxt.hunan.gov.cn/xxgk_71033/gzdt/rdjj/202106/t20210610_19468113.html (2021).
11. Carrasco-Maldonado, F. *et al.* Oxy-fuel combustion technology for cement production – State of the art research and technology development. *International Journal of Greenhouse Gas Control* **45**, 189–199 (2016).
12. National Development and Reform Commission. Benchmarking Levels for Energy Efficiency in Industry Key Areas (2023 Edition). (2023).
13. Gaur, S. & Reed, T. B. *Thermal Data for Natural and Synthetic Fuels*. (CRC Press, Boca Raton, 2020). doi:10.1201/9781003064633.
14. Zhuo, Z. *et al.* Cost increase in the electricity supply to achieve carbon neutrality in China. *Nat Commun* **13**, 3172 (2022).
15. Energy Transition Commisson, RMI. *China 2050 A Fully Developed Rich Zero-Carbon Economy*. https://rmi.org/insight/china-2050-a-fully-developed-rich-zero-carbon-economy/ (2019).
16. Shin, H. K. & Ha, S. K. A Review on the Cost Analysis of Hydrogen Gas Storage Tanks for Fuel Cell Vehicles. *Energies* **16**, 5233 (2023).

17. Thunder Said Energy. Costs of cryogenic air separation. *Thunder Said Energy* https://thundersaidenergy.com/downloads/cryogenic-air-separation-the-economics/.
18. Vogl, V., Åhman, M. & Nilsson, L. J. Assessment of hydrogen direct reduction for fossil-free steelmaking. *Journal of Cleaner Production* **203**, 736–745 (2018).
19. Moore, J. J., Pryor, O., Cormier, I. & Fetvedt, J. Oxygen Storage Incorporated Into Net Power and the Allam-Fetvedt Oxy-Fuel sCO2 Power Cycle – Technoeconomic Analysis. in doi:10.1115/GT2022-82060.
20. Xu, J.-H., Yi, B.-W. & Fan, Y. A bottom-up optimization model for long-term CO 2 emissions reduction pathway in the cement industry: A case study of China. *International Journal of Greenhouse Gas Control* **44**, 199–216 (2016).
21. AGICO CEMENT. How Much Dose It Cost To Start A Cement Grinding Plant? https://cement-plants.com/cement-grinding-unit-cost/ (2024).
22. Global CCS Institute. China begins operations at the world's largest oxy-fuel combustion CCUS project in cement sector. *Global CCS Institute* https://www.globalccsinstitute.com/news-media/insights/china-begins-operations-at-the-worlds-largest-oxy-fuel-combustion-ccus-project-in-cement-sector/ (2024).
23. Pratschner, S., Radosits, F., Ajanovic, A. & Winter, F. Techno-economic assessment of a power-to-green methanol plant. *Journal of CO2 Utilization* **75**, 102563 (2023).
24. Schmidt, O., Melchior, S., Hawkes, A. & Staffell, I. Projecting the Future Levelized Cost of Electricity Storage Technologies. *Joule* **3**, 81–100 (2019).
25. Haendel, M., Hirzel, S. & Süß, M. Economic optima for buffers in direct reduction steelmaking under increasing shares of renewable hydrogen. *Renewable Energy* **190**, 1100–1111 (2022).
26. State-owned Assets Supervision and Administration Commission of the State Council. c. *State-owned Assets Supervision and Administration Commission of the State Council* http://www.sasac.gov.cn/n16582853/n16582883/c17715327/content.html (2021).
27. Wang, Qingyi. *2021 Energy Data*. https://www.igdp.cn/wp-content/uploads/2022/07/2021%E8%83%BD%E6%BA%90%E6%95%B0%E6%8D%AE-%E5%8F%91%E5%B8%83%E7%89%88.pdf (2022).
28. Cai, B., Zhao, L., Zhang, Z. & Lu, X. *China regional power grids carbon dioxide emission factors (2023)*. http://www.caep.org.cn/sy/tdftzhyjzx/zxdt/202310/t20231027_1044179.shtml (2023).
29. Sievert, K., Schmidt, T. S. & Steffen, B. Considering technology characteristics to project future costs of direct air capture. *Joule* **8**, 979–999 (2024).
30. Young, J. *et al.* The cost of direct air capture and storage can be reduced via strategic deployment but is unlikely to fall below stated cost targets. *One Earth* **6**, 899–917 (2023).
31. Mohammed Al-Juaied & Adam Whitmore. *Prospects for Direct Air Carbon Capture and Storage: Costs, Scale, and Funding*. https://www.belfercenter.org/publication/prospects-direct-air-carbon-capture-and-storage-costs-scale-and-funding (2023).
32. IEAGHG. *Global Assessment of Direct Air Capture Costs*. https://ieaghg.org/publications/global-assessment-of-direct-air-capture-costs/ (2021).

33. Wang, R. *et al.* A high spatial resolution dataset of China's biomass resource potential. *Sci Data* **10**, 384 (2023).
34. Luo, H., Cheng, F., Barckholtz, T. A., Greig, C. & Larson, E. D. Biopower with molten carbonate fuel cell carbon dioxide capture: Performance, cost, and grid-integration evaluations. *Energy Conversion and Management* **322**, 119167 (2024).
35. Chen, L., Jiang, Q., Song, Z. & Posarac, D. Optimization of Methanol Yield from a Lurgi Reactor. *Chemical Engineering & Technology* **34**, 817–822 (2011).
36. International Energy Agency. *An Energy Sector Roadmap to Carbon Neutrality in China*. https://www.iea.org/reports/an-energy-sector-roadmap-to-carbon-neutrality-in-china (2021).
37. American Bureau of Shipping. *Carbon Neutral Fuel Pathways and Tranformational Technologies*. https://ww2.eagle.org/content/dam/eagle/publications/whitepapers/2024-sustainability-outlook-web.pdf?utm_source=chatgpt.com (2024).
38. He, Y., Li, Z. & Liu, P. A Co-production system of cement and methanol: Unveiling its advancements and potential. *Journal of Cleaner Production* **473**, 143523 (2024).
39. Pisciotta, M. *et al.* Current state of industrial heating and opportunities for decarbonization. *Prog. Energy Combust. Sci.* **91**, 100982 (2022).
40. IEA bioenergy. *Deployment of Bio-CCS in the Cement Sector: An Overview of Technology Options and Policy Tools | Bioenergy*. https://www.ieabioenergy.com/blog/publications/deployment-of-bio-ccs-in-the-cement-sector-an-overview-of-technology-options-and-policy-tools/ (2022).
41. Ditaranto, M. & Bakken, J. Study of a full scale oxy-fuel cement rotary kiln. *Int. J. Greenhouse Gas Control* **83**, 166–175 (2019).